THE EPIGENETIC REGULATION OF MICRORNA395 EXPRESSION UNDER SULFATE DEPRIVATION IN ARABIDOPSIS THALIANA

By

PEI JIA NG

Bachelor of Science in Biochemistry

Oklahoma State University

Stillwater, Oklahoma

2018

Submitted to the Faculty of the
Graduate College of the
Oklahoma State University
in partial fulfillment of
the requirements for
the Degree of
MASTER OF SCIENCE
May, 2021

THE EPIGENETIC REGULATION OF

MICRORNA395 EXPRESSION UNDER SULFATE

DEPRIVATION IN ARABIDOPSIS THALIANA

Thesis Approved:

Dr. Ramanjulu Sunkar

Thesis Adviser

Dr. Donald Dean Ruhl

Dr. Charles Chen

Dr. Vijaya Gopal Kakani

ACKNOWLEDGEMENTS

Life will be hard without the help of someone. I am extremely blessed to have everyone beside me being physically and mentally supportive to help me finish my Master thesis. First and foremost, I would like to express my sincere gratitude to my advisor, Dr. Ramanjulu Sunkar for the professional advice, useful instructions and unlimited support during my research and thesis writing.

I would like to thank the lab members, Dr. Yongfang Li, Dr. Ganesan Govindan and Dr. Asha Srinivasan for teaching me various techniques and offering professional suggestions patiently. Without their passionate help, I would not be able to solve the technical problems that I encountered during in my research.

Importantly, I would like to thank my committee members, Dr. Donald Ruhl, Dr. Charles Chen and Dr. Gopal Kakani, for their insightful comments and brainstorming questions leading me to improve my research skills.

Last but not least, I would like to thank my parents, Hock Chee Ng and Bee Yean Ong, for their unconditional affection and making me into who I am today.

Name: PEI JIA NG

Date of Degree: MAY, 2021

Title of Study: THE EPIGENETIC REGULATION OF MICRORNA395 EXPRESSION UNDER SULFATE DEPRIVATION IN ARABIDOPSIS THALIANA

Major Field: BIOCHEMISTRY AND MOLECULAR BIOLOGY

Abstract:

MicroRNAs fine-tune target gene expression at post-transcriptional level in organ-, cell-, developmental stage- and stress-specific manner. MicroRNA395 (miR395) targets transcripts encoding two different classes of proteins, i.e., a sulfate transporter (AST68) and ATP sulfurylases (APS1, APS3 and APS4) in *Arabidopsis*. Previous studies have shown that sulfate deprivation (S deprivation) induces miR395 expression in *Arabidopsis*. This induced expression is transcriptionally controlled by SULFUR LIMITATION 1, a transcription factor. However, the epigenetic processes that are associated with miR395 induction under S deprivation are unknown. Histone methylation and histone variants play an essential role in regulating gene expression by altering the chromatin state. In this study, the role of H3K4me3 (ATX1), H3K4me2 (ATX2) and H3K27me3 (SWN3) as well as the role of H2A.Z variant (HTA9 and HTA11) in regulating miR395 induction was assessed in mutants that are defective in depositing these epigenetic marks.

The analysis of all six pri-*MIR395* transcripts (miR395a, b, c, d, e and f) revealed all of these loci are strongly up-regulated in shoots, however in roots, four of the six loci exhibited up-regulation under S deprivation. However, in mutants lacking H3K4me3 and H3K4me2 and their combination (*atx1-2*, *atx2-1* and *atx1-2*/*atx2-1*), the expression levels were significantly different; 5 and 4 loci in shoots and roots, respectively, were more strongly up-regulated in mutants compared to Col-0. Similarly, in mutants lacking H3K27me3 (*swn3*), 3 (shoots) and 4 (roots) loci in shoots and roots, respectively, showed more up-regulation compared to Col-0. Compared to the Col-0 responses, the pri-*MIR395* levels also showed differences both in shoots and roots of *hta* single mutants, and the differences were more pronounced in *hta9-1*/*hta11-2* double mutants.

Overall, some of the results indicated that these epigenetic marks are important for regulating some of the miR395 loci while some other loci did not agree with the expectations but showed contradictory results. It is possible that the *ATX1*, *ATX2*, *SWN3*, *HTA9* and *HTA11* genes that are analyzed in the present study is only targeting sub-set of miR395 loci in *Arabidopsis*.

TABLE OF CONTENTS

Chapter Page

LIST OF TABLES

LIST OF FIGURES

Figure Page

CHAPTER I

INTRODUCTION

1.1 Importance of Sulfur

Throughout their life cycle, plants require sulfur, an essential macronutrient for normal growth and development. Sulfur (S) is a constituent of several biomolecules such as amino acids, proteins, enzymes such as aconitase and protein-like Fe-S clusters, vitamins and most importantly antioxidants such as glutathione (Leustek, 1999). In many parts of the world, the soil concentration of the element is too low, resulting in S deficiency. The sulfur requirement will fluctuate during different developmental stages (vegetative growth and seed production) of the plant and may vary between plant species. Thus, the uptake of sulfate by the roots, its reduction and further assimilation in the shoots under normal conditions highly regulated on "a whole plant level", which will be in tune with the actual sulfur requirement of a plant species (De Kok et al. 2002; Durenkamp and De Kok, 2004). At optimal growth conditions the daily sulfur requirement of different crop species ranges between 2 - 10µmol g^{-1} plant fresh weight day^{-1}. Due to intensification of agriculture coupled with long cropping periods can cause severe nutrient depletion including S depletion in soil (Durán et al., 2011). S-deprivation in plants result in decreased plant tissue sulfur content and this results in decreased cysteine and glutathione; increased amounts of serine, O-acetylserine, and tryptophan; reduced amounts of chlorophyll,

RNA and total protein; increased photorespiration; decreased lipids; and nitrogen imbalance. Overall, these changes lead to to a reduced rate of metabolism and growth coupled with a range of developmental defects including yellowing of young leaves and even plant death, thus limiting crop productivity (Leustek, 1999; Baramidze et al., 2015, Schachtman and Shin, 2007, Carciochi et al., 2019).

1.2 Importance of Sulfate Uptake and Assimilation Under Stress

Sulfate transporters (SULTR) in plant root hairs absorb inorganic sulfate from the soil. Sulfate transporters are also essential in loading the absorbed sulfate into the xylem and transport to leaves (Awazuhara et al., 2005). The metabolism of sulfate occurs in the chloroplasts (Leustek, 2002), where it is first activated into adenosine 5'-phosphosulfate (APS) by ATP sulfurylases (ATPS). Once APS is formed, sulfate assimilation reaches a diverging point where APS can either reduced to sulfite by the APS reductase (APR) or phosphorylated to form 3′-phosphoadenosine 5′-phosphosulfate (PAPS) catalyzed by APS kinase (APK) (Kopriva et al., 2006). PAPS is catalyzed by sulfotransferases (SOT) and converted into o-sulfated metabolites such as the glucosinolates (GS), which are important defense metabolites against pathogens such as fungi and bacteria (Frerigmann et al., 2012).

After the reduction of APS to sulfite by APR, sulfite reductase (SiR) catalyzes sulfite to further reduce into sulfide. Sulfide is associated with O-acetylserine (OAS) to produce the amino acid residue, cysteine (Leustek *et al.* 2000). Cysteine provides a metabolic precursor for all cellular components containing reduced sulfur, including methionine, S-adenosylmethionine, glutathione (GSH), iron-sulfur clusters, vitamin cofactors like biotin and thiamin (Rausch and Wachter 2005; Koprivova et al., 2014). The thiol groups of the cysteine residues in proteins can

be oxidized resulting in disulfide bridges, which contribute to the structure of proteins. The thiol groups are also of great importance in substrate binding of enzymes, in metal-sulfur clusters in proteins (e.g., ferredoxins) and in regulatory proteins (e.g., thioredoxins). GSH, a major non-protein thiol, accounts for 1-2 % of the total sulfur in plant cells. Its concentration differs between the cellular compartments, i.e., ranging between 0.1-1.5mM in leaves and up to 20mM in chloroplasts (Mullineaux and Rausch, 2005; Klapheck et al., 1987). GSH accumulation appears to provide protection against oxidative and environmental stress conditions (Criessen et al., 1996). GSH is a major redox regulator, which occurs *via* thiol (GSH-reduced)/disulfide (GSSG-oxidized) states of the molecule. GSH oxidation is determined by reactive oxygen species and other oxidants, whereas GSSG reduction is mediated by glutathione reductase. Glutathione is also the precursor for the synthesis of phytochelatins, which are important for heavy metal sequestration and detoxification (Freeman et al., 2004; Blum et al., 2007; Couto et al., 2013).

The assimilation of sulfate is important for the adaptation of plants to adverse environmental conditions (Koprivova et al. 2008). More precisely, the S assimilation-based plant stress tolerance is closely associated with GSH-mediated ROS detoxification. Consistently, the transcripts of APS reductase, a key enzyme in sulfate metabolism, are induced under high salinity or other abiotic stresses (Koprivova et al. 2008). Furthermore, *Brassica* species contain secondary sulfur compounds such as glucosinolates (Falk et al., 2007) and altering glucosinolate levels could modulate disease resistance in plants (Brader et al., 2006).

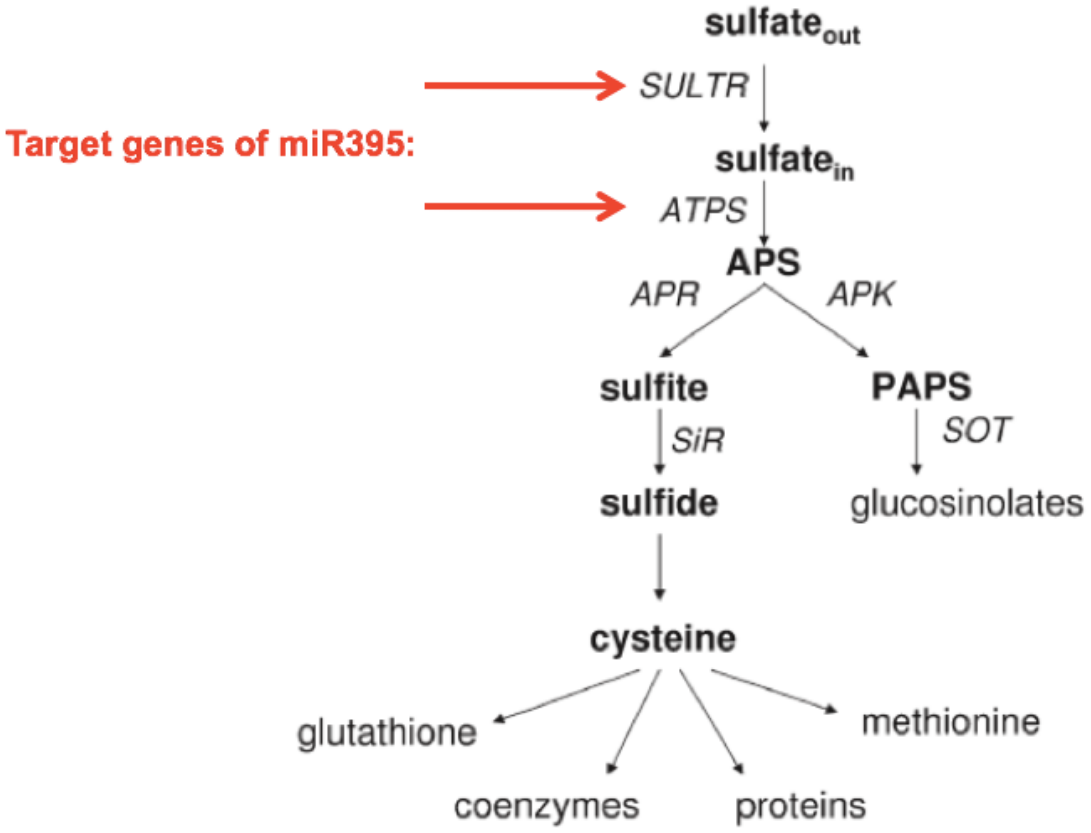

Figure 1. Sulfate assimilation pathway in plants. Modified from: Koprivova, A., & Kopriva, S. (2014). Molecular mechanisms of regulation of sulfate assimilation: first steps on a long road. *Frontiers in Plant Science, 5*, 589–589.

1.3 Plant MicroRNAs

Plant microRNAs (miRNAs) are usually 21 nucleotides long non-coding RNAs that fine-tunes the target gene expression at post-transcriptional level. This miRNA-mediated target gene regulation is an integral part of gene regulatory networks associated with almost all of the biological processes of plant growth and development, adaptation to biotic or abiotic stresses including nutrient deprivation (Sunkar et al., 2012).

Plant canonical miRNA biogenesis pathway is shown in Figure 2. In the plant nucleus, miRNA gene is transcribed by RNA polymerase II (Pol II) and the resulting primary microRNA (pri-miRNA) transcripts can form a hairpin-like structures. The dicing complex containing Dicer-like1 (DCL1) protein along with several other proteins such as double-strand RNA binding protein 1 (DRB1), Serrate (SE) and HYPONASTIC LEAVES 1 (HYL1) recognizes the hairpin-like structure and processes the release of 21-nucleotide long miRNA/miRNA* duplex with 2 nucleotide overhangs at their 3'ends. The RNA methyl transferase HEN1, methylates the 3'ends of the miRNA/miRNA* duplex. The duplex is then exported to cytoplasm through HASTY, a nuclear membrane-localized protein forming a pore like structure. In the cytoplasm, the guide miRNA (miRNA) from the miRNA/miRNA* duplex is loaded onto an Argonaute 1 (AGO1) protein. Heat shock cognate protein 70/ heat shock protein 90 (Hsc70/Hsp90) chaperones and Adenosine triphosphate (ATP) appears to assist in miRNA loading onto AGO1 to form the RNA-induced silencing complex (RISC) (Iwasaki et al., 2010; Nakanishi, 2016; Liu, 2017). The miRNA with in the AGO1 guides the RISC to specific mRNA targets on the basis of complementary to the miRNA and causes a precise cleavage between 10th and 11th nucleotide at the complementary site on the mRNA target or inhibits the translation from the target mRNA.

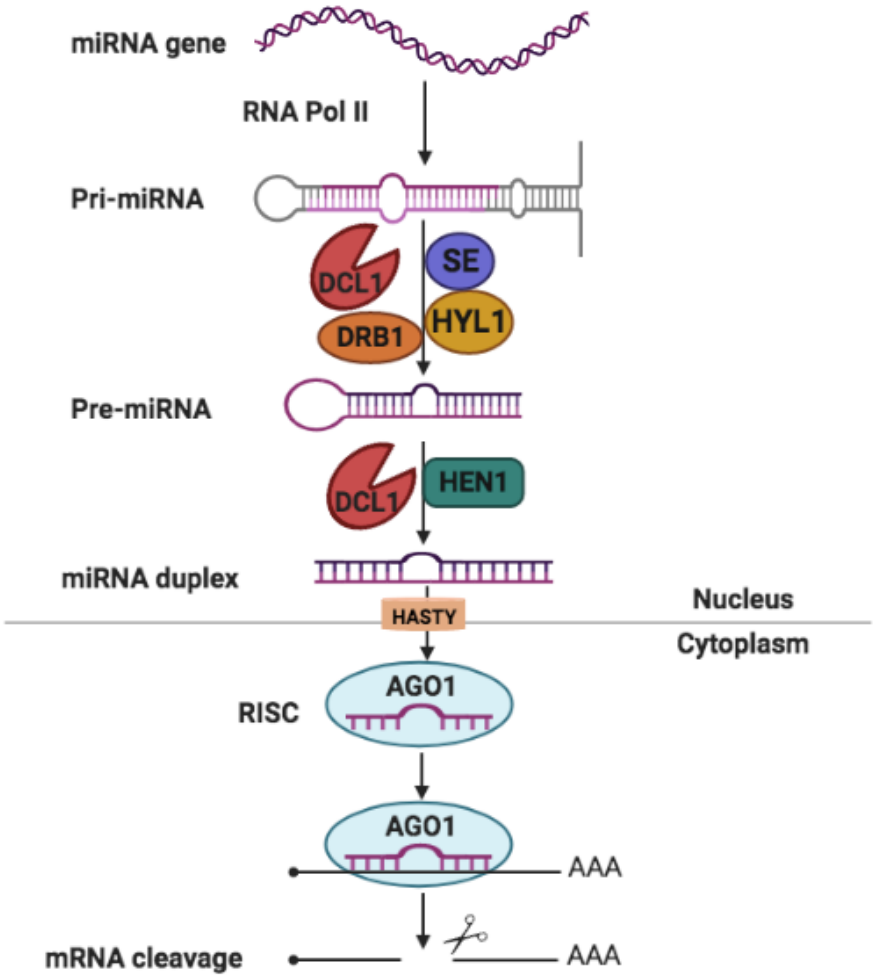

Figure 2. MicroRNA biogenesis pathway in plants. Modified from: Liu, S., Zhou, J., Hu, C., Wei, C., & Zhang, J. (2017). MicroRNA-Mediated Gene Silencing in Plant Defense and Viral Counter-Defense. *Frontiers in Microbiology, 8*, 1801–1801.

CHAPTER II

REVIEW OF LITERATURE

2.1 MicroRNA395

MiR395 is one of the conserved miRNAs in higher plants including *Arabidopsis* (Sunkar and Jagadeeswaran, 2008). MiR395 is encoded by six different loci miR395a, miR395b, miR395c, miR395d, miR395e and miR395f in the *Arabidopsis* genome. Under normal conditions, small RNA blot analysis cannot detect *MIR395* levels but can be amplified and quantified using quantitative Real-Time Polymerase Chain Reaction (qRT-PCR) assays. It was shown that each of the six loci shows varying levels of expression in different tissues including shoots and roots (Jagadeeswaran et al., 2014). Previous reports have shown that miR395 levels are induced in response to S deprivation in *Arabidopsis* (Jones-Rhoades and Bartel, 2004; Kawashima et al., 2009; Jagadeeswaran et al., 2014). Interestingly, miR395 is targeting two different families of genes that coordinately functions in the (1) sulfur translocation by targeting a low-affinity sulfate transporter, *AST68*; *SULTR2;1*, which is expressed in pericycle and xylem parenchyma to function in loading sulfate into root xylem for translocation to shoots, specifically to control how much of S needs to be translocated to shoots (Takahashi et al., 1997; 2000), and, (2) S assimilation by targeting 3 *APS* genes (*APS1*, *APS3* and *APS4*) that code for enzymes critical for S assimilation (Figure 1). A high-level conservation of miR395 and its target genes

coupled with its inducible expression under S deprivation in different plant species (Li et al., 2011; Jagadeeswaran et al., 2009; 2014) suggests that miR395 is an important component of the overall gene regulatory networks critical for S homeostasis under S deprivation in plants. More precisely, the importance of S deprivation-induced miR395 was appeared to coordinate dual functions in roots and shoots: (1) in roots, the induced miR395 is thought to enhance translocation of S from roots to shoots (Maruyama-Nakashita et al., 2006; Kawashima et al., 2011; Takahashi, 2019), and (2) in shoots, the induced miR395 decreases the levels of *APS1*, *APS3* and *APS4* transcripts due to decreased demand for these enzymes under S deprivation.

2.2 Epigenetic Regulation

Being anchored to the soil, plants cannot avoid but has to endure biotic or abiotic stressful environments. The sustained efforts over last three decades has certainly offered several molecular insights on how plants cope with stress. Nevertheless, we still lack a complete understanding of the molecular mechanisms because these complicated but highly coordinated multi-tiered regulations of stress-responsive gene expression operates at many different levels, i.e., transcriptional, post-transcriptional and even post-translational levels. Prior to transcriptional regulation, epigenetic regulation determines the activation or repression of gene expression (Ashapkin et al., 2020). Epigenetic regulation includes modifications to the DNA and modifications to the histones that alters chromatin organization.

The basic unit of chromatin is the nucleosome. Nucleosomes consist of approximately 146 base pairs of DNA wrapped around a histone octamer which composed of core histone proteins, canonical H2A, H2B, H3 and H4 (Zlatanova, 1998). The assembly of two copies of each H2A, H2B, H3 and H4 forms histone octamer. Histone 1 (H1) plays a role as a linker to maintain

the interaction between DNA and nucelosomes. The interaction between nucleosomes produces chromatin fibers (Luger et al., 2012). Chromatin can be organized in two different states which is heterochromatin or euchromatin. Heterochromatin, also called "closed chromatin" state is inactive or because of its condensed chromatin structure, transcription factors are not accessible for driving the transcription. On the other hand, euchromatin is an "open chromatin" state as it has a loosely packed chromatin structure that allows the binding of transcription factors and the RNA polymerase II (Pol II) (To et al., 2014) to bind and initiate transcription.

DNA methylation and histone modifications, commonly known as "epigenetic modifications", regulate gene expression by altering the chromatin state. For instance, 5'-methylation of cytosines is a major epigenetic modification of genomic DNA, which is frequently involved in the silencing of genes. Similarly, methylation/acetylation at specific positions on histones, the so-called "histone-code" determines whether a gene is expressed or silenced (Grunstein, 1997; Sun and Allis, 2002). Apart from histone modifications, histone variants are also often being shown to affect gene regulation and are considered to be part of epigenetic regulation. These epigenetic modifications dictate when and where a gene should be expressed or silenced. In plants, the importance of "epigenetic modifications" that contribute to the gene regulations during stress has been reported (Kim et al., 2015, Agarwal et al., 2020).

2.3 Histone Modifications: H3K4me3, H3K4me2 and H3K27me3

Although all four core histones are known to undergo posttranslational modifications at their N-terminus, H3 undergoes a large number of posttranslational modifications such as methylation, acetylation, phosphorylation, ubiquitination, sumoylation etc., (Agarwal et al., 2020). Histone methylation, specifically mono-, di-, or tri-methylation of lysine (K) residues at

the N-terminus histone H3 is one of the frequently studied epigenetic marks that facilitates changes in the chromatin organization (Liu et al., 2019). Histone 3 lysine (H3K) methylation modification is conferred by a large family of enzymes called histone lysine methyltransferases (HKMT) and S-Adenosyl methionine (SAM) donates its methyl group to methylate lysine residue of histone protein. Most of them contain SET (suppressor of variegation, enhancer of zeste and trithorax) domain which is responsible for the methyltransferase activity. *Arabidopsis* genome encodes 49 SET DOMAIN GROUP (SDG). Based on the activity and domain architecture, SDG proteins are classified into five distinct classes (Dong et al., 2015). The five different classes of histone lysine methyltransferase (HKMT) are class I to V (Pontvianne et al., 2010). Class III HKMT is composed of homologues of Trithorax which is called Arabidopsis Trithorax-like protein 1-5 (ATX1-5). ATX1 and ATX2 sequences are highly similar but the biochemical properties are different (Saleh et al., 2008). ATX1 and ATX2 have different modifications on chromatin organization. ATX1 catalyzes tri-methylation of H3K4 (H3K4me3) that enhances transcriptional activation by the loosening of chromatin structure (euchromatin state) (Binda et al., 2010; Ferrier et al., 2011) (Figure 3). Euchromatin state is active for transcription because of its lightly packed structure, transcription factors are accessible for transcriptional processes.

The presence of H3K4me3 result in increased levels of mRNA production as H3K4me3 act as an activation mark for transcription elongation (Ding et al., 2012). On the other hand, ATX2 catalyzes di-methylation of H3K4 (H3K4me2) (Liu et al., 2018). However, the role of H3K4me2 is debated. For instance, in *Drosophila*, it has been reported that H3K4me2 is associated with heterochromatin which enriched on the promoters (Boros, 2012). By contrast, the enrichment of H3K4me2 is negatively correlated with transcript level of genes in rice (Liu et al., 2019). These discrepancies could be due to positional differences of these marks on the genes. For example, it was found that H3K4me3 is enriched in the promoter regions particularly at the 200bp upstream of transcription start sites (TSS) (Zhang et al., 2009; Foroozani et al., 2021). In

contrast, H3K4me2 is enriched in 5' end of transcribing regions (~200bp – 400bp upstream of TSS) (Zhang et al., 2009; Hyun et al., 2017). This suggest that H3K4me2 is distributed slightly downstream of H3K4me3 (Zhang et al., 2009) and suggests non-overlapping patterns of deposition of these epigenetic marks, which can have opposing consequences. Interestingly, in plants, the overlapping level of H3K4me2 with the genes marked with H3K27me3 is high, suggesting the possibility that H2K4me2 could suppress the gene expression in plants (Liu et al., 2019).

Trimethylation of H3K27 (H3K27me3) is another most important histone modification, a repressive mark that is often studied in plants. Enhancer of zeste homolog E(Z) is class I HKMT, which catalyze histone 3 lysine 27 (H3K27) methyltransferase activity (Pontvianne et al., 2010). *Arabidopsis* Polycomb Repressive Complex 2 (PRC2) complexes consist of Enhancer of zeste homolog (EZH), which causes trimethylation of H3K27 and alters the chromatin state into facultative heterochromatin leading to gene silencing (Wiles et al., 2017) (Figure 3). SWINGER (SWN) is a E(Z)-like protein that composed by two E(Z) domains, a SET domain, a cysteine-rich region (CXC) and SANT DNA-binding domain that consists of SWITCH/SUCROSE NONFERMENTING 3 (SWI3), transcriptional adaptor 2 (ADA2), nuclear receptor co-repressor (N-CoR) and transcription factor (TFIIIB) (Peterson et al., 2004; Tomasz et al., 2005; Hark et al., 2009; Pontvianne et al., 2010). SWN encodes a Polycomb Group Protein (PcG) which form *Arabidopsis* Polycomb Repressive Complex 2 (PRC2) (Shu et al., 2019). PRC2 is a transcriptional repressor that catalyzes tri-methylation of H3K27 (H3K27me3) for gene silencing (Liu et al., 2018; Yan et al., 2020). A well-known example of H3K27me3 function includes repressing the expression of *FLOWERING LOCUS C* (*FLC*) in *Arabidopsis* (Tamada et al., 2009).

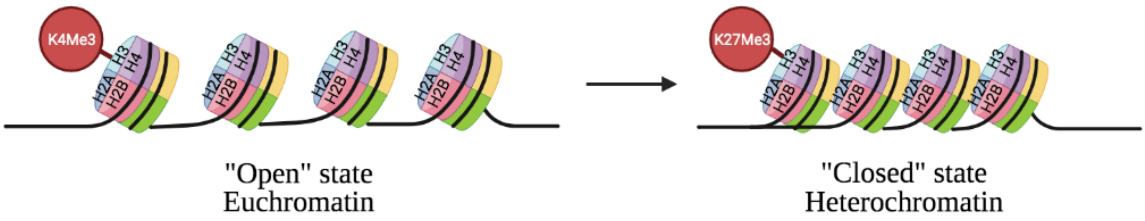

Figure 3. Histone methylations alter the chromatin organization. Designed by using the application from (https://biorender.com/). Modified from: Huang, Y., Nayak, S., Jankowitz, R., Davidson, N. E., & Oesterreich, S. (2011). Epigenetics in breast cancer: what's new?. *Breast cancer research: BCR*, *13*(6), 225.

2.4 Histone Variant: H2A.Z

Similar to histone modifications, the occupancy of specific histone variants in place of canonical histones, can also affect chromatin organization, thus influences gene expression. Among four histones, majority of histone variants are represented by H2A, i.e., H2A.Z, H2A.X and H2A.W in *Arabidopsis* (Bönisch et al., 2012; Jiang et al., 2017). Of these, H2A.Z deposition in nucleosomes affects the chromatin organization (Bernstein et al, 2006). In *Arabidopsis*, H2A is encoded by 13 HTA genes (HTA1-13). Among these, HTA8, HTA9 and HTA11 are H2A.Z encoding genes. The ATP-dependent chromatin remodeling complex called *Saccharomyces cerevisiae* SWI2/SNF2-Related 1 Chromatin Remodeling 1 (SWR1) replaces the canonical H2A with H2A.Z (Mizuguchi et al., 2012; Aslam et al., 2019). SWR1 complex that includes SWR1 COMPLEX 6 (SWC6), PHOTOPERIOD-INDEPENDENT EARLY FLOWERING1 (PIE1) and ACTIN-RELATED PROTEIN 6 (ARP6) replaces the canonical H2A–H2B histone dimers with H2A.Z–H2B histone dimers in nucleosome (Kobor et al., 2004; Mizuguchi et al., 2004; Berriri et al., 2016; Aslam et al., 2019). PIE1 specifically binds with H2A.Z variants, HTA8, HTA9 or HTA11 to deposit into nucleosomes (March-Díaz et al., 2009) (Figure 4).

The function of H2A.Z on gene expression is rather ambiguous. For instance, H2A.Z enrichment along the gene body, specifically under stress conditions such as heat (Kumar and Wigge, 2010; Cortijo et al., 2017), drought (Sura et al., 2017) and phosphorus (P) deprivation (Smith et al., 2010) appears to have a repressive role. On the other hand, H2A.Z was implicated in positive regulation of gene regulation at the FLC locus in *Arabidopsis* (Deal et al., 2007). Similarly, H2A.Z facilitates juvenile vegetative identity by up-regulating the gene expression of *MIR156A* and *MIR156C* (Xu et al., 2018). Additionally, depending on where on a gene H2A.Z is deposited, the gene expression appears to be regulated differently. The deposition of H2A.Z in gene body repressed the expression of genes whereas the deposition of H2A.Z in +1 nucleosomes of a gene activates the transcription activity (Gómez-Zambrano et al., 2019). In rice, Zahraeifard et al., 2018 have shown that H2A.Z enrichment on the gene body was negatively correlated with the expression of inorganic phosphate (Pi) deprivation-responsive genes. On the other hand, enhanced H2A.Z deposition at the TSS has affected differently; repressed some of the stress responsive genes but activated some of the house keeping genes (Zahraeifard et al., 2018).

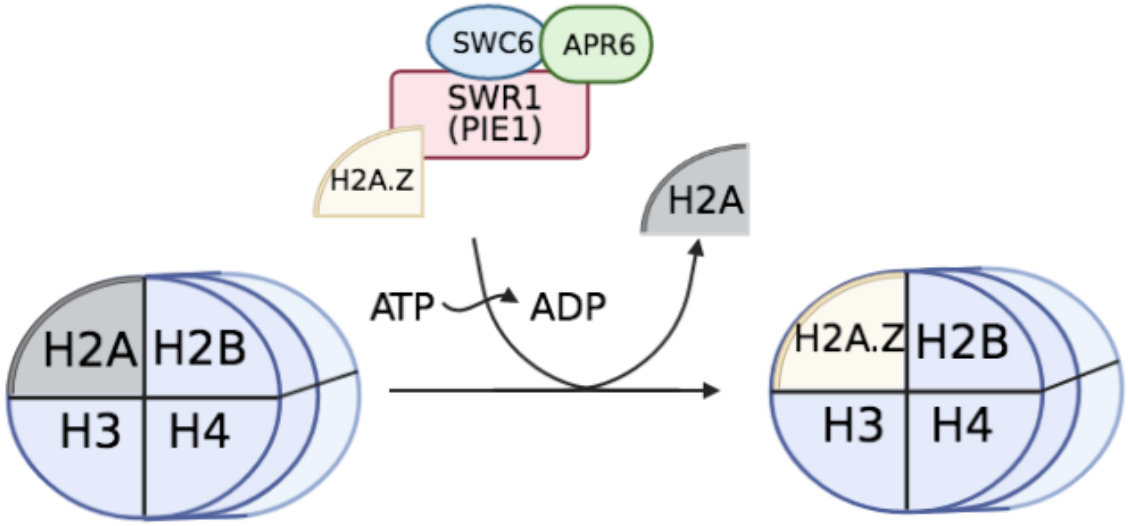

Figure 4. Deposition of histone variant H2A.Z. Designed by using the application from (https://biorender.com/). Modified from: Berriri, S., Gangappa, S. N., & Kumar, S. V. (2016).

SWR1 chromatin-remodeling complex subunits and H2A.Z have non-overlapping functions in immunity and gene regulation in *Arabidopsis*. Molecular plant, *9(7)*, 1051–1065.

2.5 Objectives

At the transcriptional level, the epigenetic processes play critical roles in inducing or silencing genes by altering the chromatin state to 'open' or 'closed' configuration. In response to S deprivation, miR395 is known to be induced in *Arabidopsis* (Jagadeeswaran *et al*., 2014). Furthermore, it's induction is transcriptionally controlled by SULFUR LIMITATION 1 (SLIM1), a transcription factor (Kawashima et al., 2011). However, the epigenetic processes that are associated with miR395 induction at the transcriptional level are unknown. Histone 3 lysine 4 trimethylation (H3K4me3) and histone 3 lysine 27 trimethylation (H3K27me3) serve as positive and negative markers of gene expression, respectively. Likewise, the occupancy of specific histone variants such as H2A.Z in place of canonical H2A, can also affect chromatin organization, thus influencing gene expression. Consequently, the importance of H3K4me3 (ATX1), H3K4me2 (ATX2) and H3K27me3 (SWN3) as well as the role of H2A.Z variant (HTA9 and HTA11) in miR395 regulation can be assessed in *atx*, *swn* and *hta* mutants that cannot deposit these epigenetic marks. The expression levels of target genes in wild type and mutants under S deprivation could establish potential correlations between miR395 and target genes. Understanding the epigenetic regulation of miR395 expression under S deprivation could also offer insights into the contributions of epigenetic processes, which are associated with stress-inducible miRNAs in plants.

CHAPTER III

METHODOLOGY

3.1 PCR for Homozygosity Identification

The following transfer DNA (T-DNA) mutants were used: *atx1-2* (SALK_149002), *atx2-1* (SALK_074806), *swn3* (SALK_050195), *hta9-1* (SALK_054814C) and *hta11-2* (SALK_031471) for investigating the role of epigenetic regulation. The seeds of single mutant lines were obtained from Arabidopsis Biological Resource Center (ABRC). The *atx1-2/atx2-1* and *hta9-1/hta11-2* double mutant seeds were obtained from Dr. Scott Poethig, University of Pennsylvania. By comparing the expression level of miR395 between wild type and mutant plants, the link between epigenetic processes (histone methylation and histone variants) and miR395 was determined.

The wild type and mutant seeds were planted on potting soil (MetroMix 360) at 16 h/8 h light/dark cycle at 22°C in a growth chamber maintained at 200μmol m^{-2} sec^{-1} light intensity for 3 weeks. The DNA was isolated using modified CTAB method (Doyle et al., 1987). To extract DNA, 0.3g of leaf tissue (one to two leaves) was ground to fine powder in presence of liquid nitrogen. DNA samples were extracted in cetyltrimethylammonium bromide (CTAB) extraction buffer (300μl) containing 100mM Tris pH 8.0, 1.4 M sodium chloride (NaCl), 20mM of EDTA

pH 8.0 and 2% of CTAB. After the addition of buffer, samples were incubated in water bath at 55°C for 30-60 minutes. DNA samples were added with 300µl of chloroform and vortexed to mix well. Then, the samples were centrifuged at 14,000 rpm for 10 minutes. The aqueous phase of the samples containing DNA was transferred to a new fresh tube and 300µl cold isopropanol was added to the aqueous phase and mixed gently. The samples were incubated in the freezer (-20℃) for 1 hour. Then, the samples were centrifuged for 10 minutes at 14,000 rpm. The supernatant was discarded carefully and retained the DNA pellet. For further precipitation, 70% of ethanol (700µl) was added to the pellet and centrifuged for 1 minute at 14,000 rpm. The supernatant was removed and the DNA pellets were air dried under room temperature and dissolved in nuclease free water (20µl).

The isolated DNA samples are used for screening the homozygous T-DNA mutants using PCR reaction. Gene-specific primers were designed for the screening of mutant lines. There are two combinations of primers needed for mutants screening. Left primer (LP) and right primer (RP) represents the gene-specific forward and reverse primers. Whereas the left border primer (LB) anchors the T-DNA, which is often used as forward primer. The homozygosity of *atx*, *swn* and *hta* mutant lines were confirmed by polymerase chain reaction (PCR) analysis. The following conditions were used for PCR amplification: (Step 1) 95°C – 5 minutes; (Step 2) 95°C – 30 seconds; (Step 3) 55°C – 30 seconds; (Step 4) 72°C – 1 minute; (Step 5) Repeat Step 2 – 4 for 34 cycles; (Step 6) 72°C – 5 minutes; (Step 7) 4°C – ∞. The gene-specific primers (LP and RP primer pair) are anticipated to amplify PCR products from wild-type and heterozygous mutants, whereas LB (T-DNA left border primer) and RP primer (anchoring the gene) pair could amplify the product from homozygous mutants. After the confirmation of mutant lines, seeds from homozygous mutants were collected for further use.

3.2 Hydroponic Cultures for S Deprivation Treatments

For analyzing miR395 expression, wild type and homozygous mutant seeds were surface sterilized using 20% bleach plus 5µL SDS by soaking for 5 minutes and then washed thoroughly. The seeds were again soaked for 5 minutes in 20% bleach alone for the second wash and then the seeds were rinsed for 5-10 times with autoclaved, distilled water. The sterilized seeds plated on the surface of agar (0.8% plant culture agar, pH 5.7), which was filled in the wells of PCR plates whose bottom have been trimmed off. The plates were sealed with paraffin plastic film and kept at 4°C for 2 days for vernalization. After 2 days, the paraffin plastic film was completely removed and the plates were transferred to the growth chamber maintained at 22°C with a 16/8 hours of light/dark cycle and light intensity of 200µmol m^{-2} sec^{-1}. After germination, the agar plates were transferred into Hoagland medium (pH 5.7) (Hoagland et al., 1950).

Experimental Setup for *Arabidopsis* Hydroponics:

A 96-well PCR plate in which the bottoms were slightly cropped off and sealed the holes at the bottom with a paraffin plastic film was used as a platform for hydroponics. Then, the holes in the PCR plate were filled with the Hoagland-agar medium and allowed it to solidify. The seeds were then placed on top of the solidified agar and the tops were also sealed with a paraffin plastic film to avoid drying of the agar. The plates were kept at 4°C for 2 days and then transferred to growth chamber and allowed the seeds to germinate. Once the seeds were germinated, both the top and bottom paraffin plastic films were discarded and the PCR plates were allowed to float in a pipette tip box, which is filled with the Hoagland solution. For imposing sulfate deficiency, Yoshida solution (Yoshida et al., 1976) was prepared with or without S (+S or -S). S deprivation solutions were prepared by replacing sulfate salts in the medium with equivalent amounts of chloride salts. The control plants remained grown on Yoshida medium containing 0.3mM sulfate.

The nutrient solutions were replaced on alternate days. The roots and shoots were harvested for analyses after growing plants for 10 days under S sufficient and S deprivation.

For tissue-specific expression analysis of genes *ATX1*, *ATX2*, *SWN3*, *HTA9* and *HTA11* in wild type plants, root tissues were collected from Col-0 plants cultured on the hydroponic medium for 4 weeks. The cauline leaves, rosette leaves, shoots and flower/inflorescence were collected from the Col-0 plants grown on potting mix.

3.3 RNA Isolation

The total RNA was isolated using Trizol protocol. Different tissues (cauline leaves, rosette leaves, shoots, flowers and root) (0.5 g) was ground to fine powder in the presence of liquid nitrogen. To the powdered tissue, 500µl TRIzol reagent was added and incubated the samples for 5 minutes at room temperature and then 600µl of chloroform was added and vortexed to mix well. The samples were incubated at room temperature for 5 minutes, and then centrifuged at 12,000 rpm for 15 minutes. The aqueous phase of the sample containing RNA was carefully pipetted out and transferred to a fresh tube. Cold isopropanol (1500µl) was added to the extracted aqueous phase and mixed gently. The samples were incubated on ice for 10 - 20 minutes and then centrifuged at 12,000 rpm for 10 minutes at 4°C. The supernatant was carefully discarded, and the pellet was suspended in 75% of ethanol (700µl) and centrifuged for 5 minutes at 4°C, 7,500 rpm. The supernatant was discarded by using a micropipette. The RNA pellets were air dried under room temperature for 5 - 10 minutes and dissolved with 20µl of 0.1% diethylpyrocarbonate (DEPC) water.

3.4 cDNA Synthesis

For determining gene expression (*ATX1*, *ATX2*, *SWN3*, *HTA9* and *HTA11*) and *miR395* levels, 2 µg of total RNA was converted into cDNA. Initially, the total RNA (2 µg) was treated with DNase I and incubated at 37°*C* for 15 minutes; 70℃ for 10 minutes. The treated RNA was reverse transcribed by using oligo-dT primer, deoxynucleoside triphosphates (dNTPs), reverse transcriptase, and RNaseOUT™ Recombinant Ribonuclease Inhibitor (Thermofisher, (https://www.thermofisher.com/order/catalog/product/10777019#/10777019) by incubating at 25°C for 10 minutes; 42℃ for 1 hour; 72℃ for 10 minutes.

3.5 Real-Time Polymerase Chain Reaction (RT-PCR)

Real time-PCR analysis was executed to determine the expression levels of *ATX1*, *ATX2*, *SWN3*, *HTA9* and *HTA11*, pri-*MIR395a, b, c, d, e* and *f* transcripts and miR395 target genes (*AST68*, *APS1*, *APS3* and *APS4*) in different tissues of Col-0. Real time-PCR was conducted using 5µL of the Maxima™ SYBR Green PCR Master Mix (http://www.thermoscientificbio.com/qpcr-master-mixes-and-assays/maxima-sybr-green-qpcr-master-mixes/), 2µL of cDNA and 0.25µL of 10µM gene-specific primers. The RT-PCR analysis was operated in the 7500 Real-time PCR System. The standard program of RT-PCR was performed. (Preincubation for 1 cycle: 50°C – 120 seconds; Preincubation for 1 cycle: 95°C - 180 seconds; 3-steps amplification for 45 cycles: 95°C – 20 seconds, 55°C - 20 seconds, 72°C - 1 minute with single acquisition mode; Melting for 1 cycle: 95°C – 10 seconds, 65°C - 60 seconds, 97°C - 1 second; Cooling for one cycle: 37°C – 30 seconds). Three technical and two biological replicate PCR reactions conducted for each gene.

3.6 Schematic Diagrams

The schematic diagrams of genomic structure for mutant loci (*atx, swn* and *hta*) were designed using the website (http://wormweb.org/exonintron).

CHAPTER IV

RESULTS

4.1 Characterization of Homozygous Histone Methylation (H3K4me3, H3K4me2, and H3K27me3) and Histone Variant (H2A.Z) Mutants

Arabidopsis thaliana Columbia (Col-0) (Passardi et al., 2007) was used as the wild type. To assess the contribution of H3K4me3 (ATX1 - H3K4 tri-methyltransferase) and H3K4me2 (ATX2 - H3K4 di-methyltransferase) and their combination in regulating miR395 levels, *atx1-2* and *atx2-1* single mutants as well as *atx1-2/atx2-1* double mutants were used. On the other hand, to examine the contribution of H3K27me3 (SWN3 - H3K27 tri-methyltransferase), *swn3* mutant was used. Also, to assess the importance of H2A.Z variant in regulating miR395 induction, *hta9-1* and *hta11-2* single mutants (both encode H2A.Z variants) as well as *hta9-1*/*hta11-2* double mutant was used. The PCR analysis was used to identify homozygous mutants of *atx1-2, atx2-1, swn3, hta9-1 and hta11-2.* Likewise, *atx1-2/atx2-1*, and *hta9-1/hta11-2* double mutants were also confirmed using PCR analysis (Figure 5).

A.

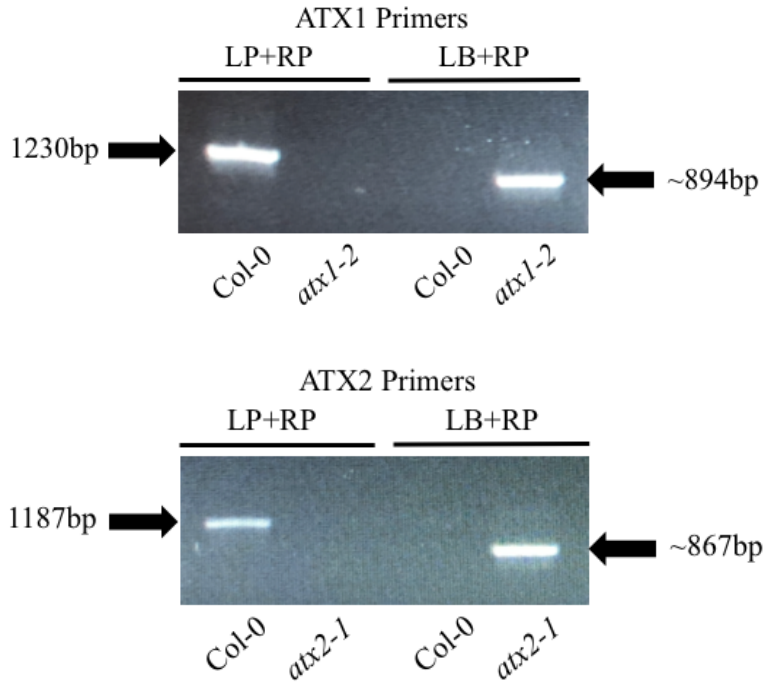
ATX1 Primers
LP+RP
LB+RP
1230bp
~894bp
Col-0
atx1-2
Col-0
atx1-2
ATX2 Primers
LP+RP
LB+RP
1187bp
~867bp
Col-0
atx2-1
Col-0
atx2-1

B.

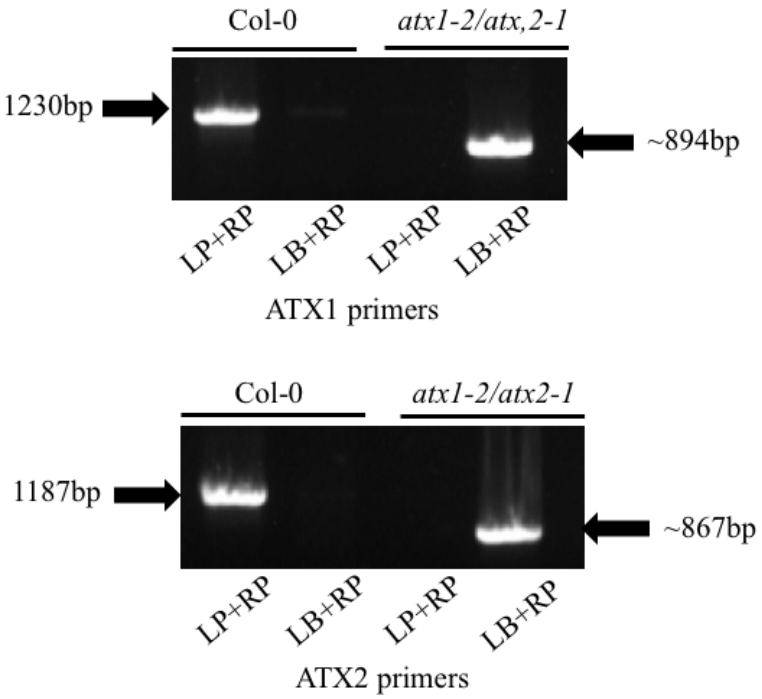
Col-0
atx1-2/atx,2-1
1230bp
~894bp
LP+RP
LB+RP
LP+RP
LB+RP
ATX1 primers
Col-0
atx1-2/atx2-1
1187bp
~867bp
LP+RP
LB+RP
LP+RP
LB+RP
ATX2 primers

C.

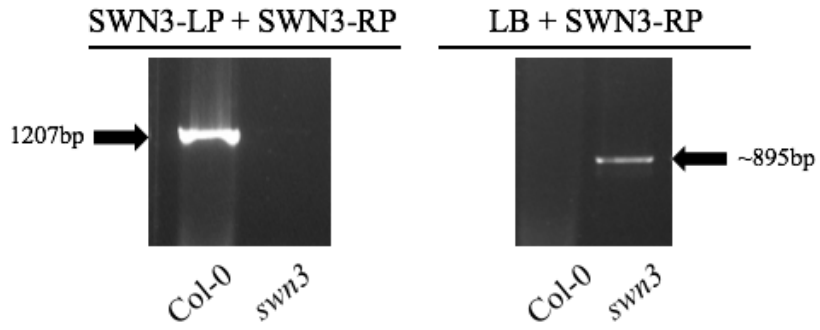

D.

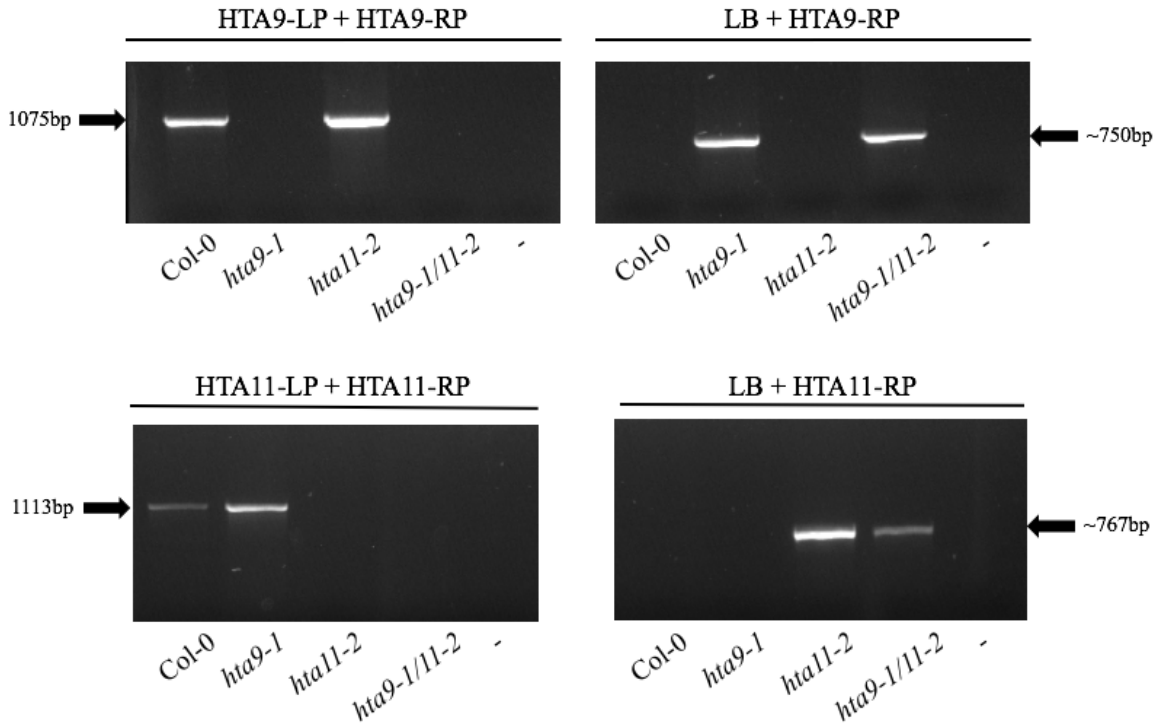

Figure 5. Characterization of *atx1-2*, *atx2-1*, *atx1-2/atx2-1, swn3, hta9-1, hta11-2* and *hta9-1/hta11-2* mutants.

A. Confirmation of homozygous lines of *atx1-2* and *atx2-1* single mutants. LP and RP indicate the gene specific forward and reverse primers of ATX1 or ATX2. LB indicates

the T-DNA insertion forward primer while RP indicates the gene-specific reverse primer of ATX1 or ATX2.

B. Confirmation of homozygous lines of *atx1-2/atx2-1* double mutant. LP and RP indicate the gene specific forward and reverse primers of ATX1 or ATX2. LB indicates the T-DNA insertion forward primer while RP indicates the gene-specific reverse primer of ATX1 or ATX2.

C. Confirmation of homozygous line of *swn3* mutant. LP and RP indicate the SWN3 gene specific forward and reverse primers. LB indicates the T-DNA insertion forward primer while RP indicates the SWN3 gene-specific reverse primer.

D. Confirmation of homozygous lines of *hta9-1* and *hta11-2* single and *hta9-1/hta11-2* double mutants. HTA9-LP and HTA9-RP; HTA11-LP and HTA11-RP indicate the gene specific primers. LB and HTA9-RP; LB and HTA11-RP indicate the T-DNA insertion forward primers and gene specific-reverse primers, respectively. Homozygous lines are validated by the amplification of PCR product with T-DNA specific primers.

4.2 Tissue-Specific Profiles of *ATX1*, *ATX2*, *SWN3, HTA9* and *HTA11* Transcripts in Col-0

The gene expression profiles often vary in different tissues and different phases of life cycle of a plant system. Prior to assessing the function of *ATX1, ATX2, SWN3, HTA9* and *HTA11* genes in regulation of miR395 expression, the expression levels of these genes was determined in roots, flowers, shoots, rosette leaves and cauline leaves (Figure 6).

In roots, *ATX1*, *ATX2* and *SWN3* levels were almost similar but *HTA9* was barely detected and displayed the lowest expression levels. In flowers, both *ATX1* and *ATX2* transcripts

showed highest abundances, followed by *SWN3*. In contrast, *HTA9* and *HTA11* showed least abundances in flower tissue. In shoots, *ATX2* followed by *SWN3* showed greatest expression levels but *HTA11* showed least abundances. The *SWN3* levels were relatively higher than *ATX1* but lower than *ATX2* in shoots. In rosette leaves, a high level of expression was detected for *ATX1*, followed by *SWN3* and *ATX2*. In rosette leaves, the expression level of *ATX1* was high, whereas *HTA11* levels were least. In cauline leaves, *HTA9* levels showed greatest abundances whereas *SWN3* showed least abundances. The expression level of *ATX2* in cauline tissues was lower to some degree as compared to the abundance of *ATX1* (Figure 6).

In general, the *ATX1* and *ATX2* transcript levels were most abundant in flower tissue. The expression level of *ATX2* in shoot and flower tissues was comparatively higher than in other tissues. Given the higher abundance of *ATX1* in the flower tissues suggests that *ATX1* plays an important role in the regulation of floral development (Alvarez-Venegas *et al.,* 2003). The expression levels of *SWN3* in shoot and rosette leaves were approximately similar.

The expression level of *HTA9* was the highest in cauline leaves, followed by rosette leaves, shoots and least in flowers and roots. The *HTA11* levels in flowers, stem and rosette leaves were extremely low. Taken together, *HTA9* and *HTA11* have low abundances in several tissues except for *HTA9* in cauline leaves, and *HTA11* in roots, in which these were expressed at relatively higher levels. The overall differential profiles in different tissues for these genes suggests a role in tissue-specific functions.

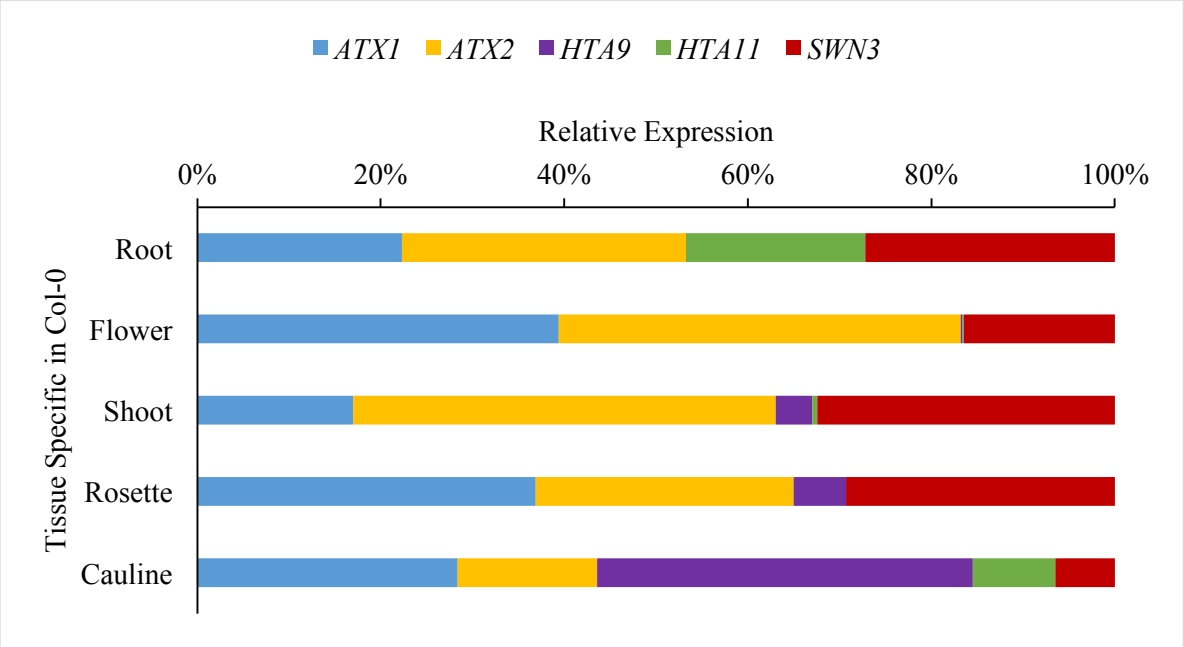

Figure 6. Tissue-specific expression profiles of *ATX1*, *ATX2*, *SWN3*, *HTA9* and *HTA11* in Col-0. The qRT-PCR of *ATX1*, *ATX2*, *SWN3*, *HTA9* and *HTA11* expression levels in different tissues of wild type, Col-0. The expression level was normalized to that of SERINE/THREONINE PROTEIN PHOSPHATASE 2A (PP2A). Result shown is the average of three technical replicates.

4.3 Expression Profiles of *ATX1*, *ATX2*, *SWN3*, *HTA9* and *HTA11* in Col-0 Under S Deprivation

Other than developmental cues, gene expression is also responsive to environmental factors. To determine whether the *ATX1*, *ATX2, SWN3, HTA9* and *HTA11* transcripts are responding to S deprivation, their expression profiles were analyzed both in roots and shoots of *Arabidopsis*. Interestingly, in shoot tissues, the transcript levels of *ATX1*, *ATX2* and *HTA9* were mildly down-regulated but *SWN3* levels were unaffected while *HTA11* levels were slightly up-

regulated under S deprivation (Figure 7). Conversely, in root tissues, the transcript levels of *ATX1*, *ATX2, SWN3, HTA9* and *HTA11* levels were up-regulated, although *ATX1* and *ATX2* levels were more strongly up-regulated under S deprivation (Figure 8).

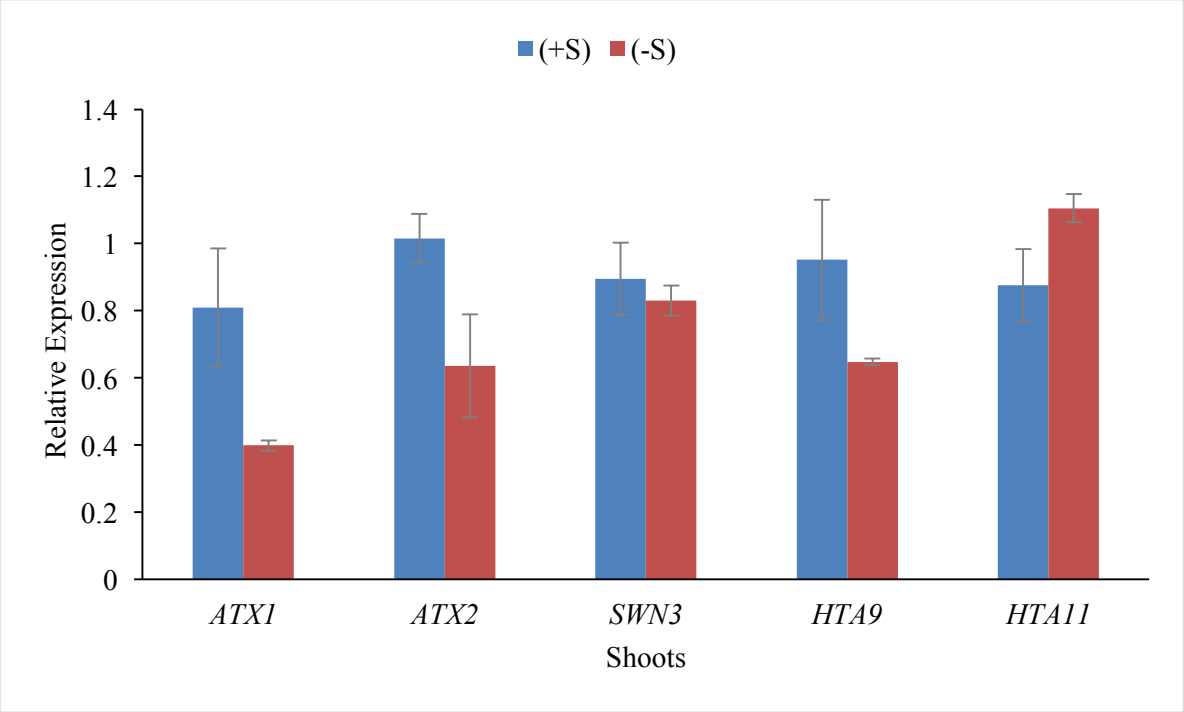

Figure 7. Expression profiles of *ATX1*, *ATX2*, *SWN3*, *HTA9* and *HTA11* genes under S deprivation in shoots of Col-0. The qRT-PCR of *ATX1*, *ATX2*, *SWN3*, *HTA9* and *HTA11* levels in the shoots of wild type, Col-0 under control (+S) and sulfate deprivation (-S) conditions. The *PP2A* transcript levels were used to normalize the expression levels. Error bars indicates the standard deviation. Result shown is the average of three technical replicates.

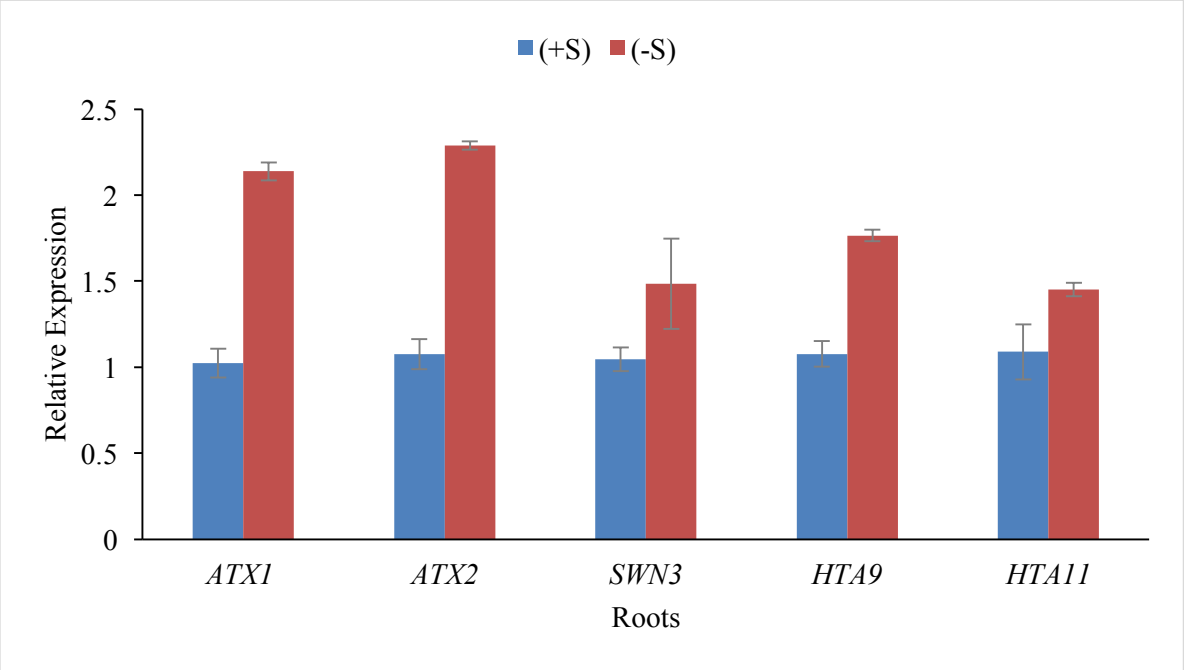

Figure 8. Expression profiles of *ATX1*, *ATX2*, *SWN3*, *HTA9* and *HTA11* genes under S deprivation in roots of Col-0. The qRT-PCR of *ATX1*, *ATX2*, *SWN3*, *HTA9* and *HTA11* levels in the roots of wild type, Col-0 under control (+S) and sulfate deprivation (-S) conditions. The *PP2A* transcript levels were used to normalize the expression levels. Error bars denotes the standard deviation. Result shown is the average of three technical replicates.

4.4 Expression Profiles of pri-*MIR395* Transcripts in Mutants Defective in H3K4 and H3K27 Methylation Under S Deprivation

To address the role of H3K4 and H3K27 methylation in miR395 regulation, knockout mutants in genes encoding H3K4 methyltransferases (ATX1 and ATX2) and H3K27 methyltransferases (SWN3) in *Arabidopsis* were analyzed (Figure 9). MiR395 is encoded by six different loci (miR395a, b, c, d, e and f) in the *Arabidopsis* genome. The expression profiles of

these loci in *atx1*-2, *atx2-1* and *swn3* mutants could offer insights into the importance of histone methylation in inducing miR395 expression under S deprivation.

A.

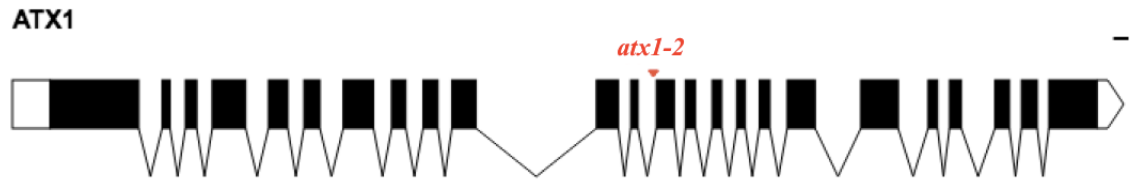

B.

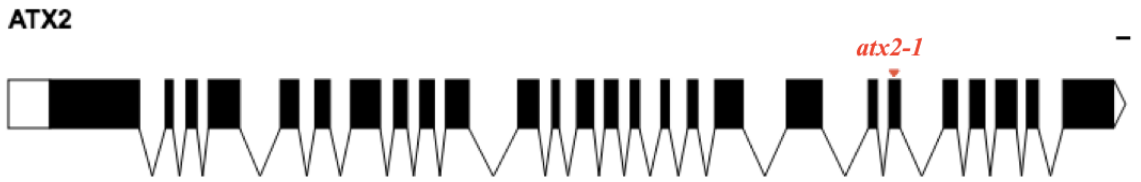

C.

Figure 9. Schematic diagram of T-DNA insertion site on *ATX1, ATX2* and *SWN3* genes.

A. Schematic diagram of genomic structure for *ATX1* locus (AT2G31650). ATX1 consists of 7160 base pairs of genomic DNA and 3615 base pairs of cDNA. Black boxes represent exons. The unfilled white portions represent introns. There are a total of 24 exons and 23 introns. The triangle (*atx1-2*) represents the position of T-DNA insertion. T-DNA is inserted at the intron of *ATX1* to disrupt the function of gene.

B. Schematic diagram of genomic structure for *ATX2* locus (AT1G05830). *ATX2* consists of 7750 base pairs of genomic DNA and 3983 base pairs of cDNA. Black boxes represent exons. The unfilled white portions represent introns. There are a total of 26 exons and 25 introns. The triangle (*atx2-1*) represents the position of T-DNA insertion. T-DNA is inserted at the exon of ATX2 to disrupt the function of gene.

C. Schematic diagram of genomic structure for *SWN3* locus (AT4G02020). *SWN3* consists of 5408 base pairs of genomic DNA and 2928 base pairs of cDNA. Black boxes represent exons. The unfilled white portions represent introns. There are a total of 17 exons and 16 introns. The triangle (*swn3*) represents the position of T-DNA insertion. T-DNA is inserted at the exon of SWN3 to disrupt the function of gene.

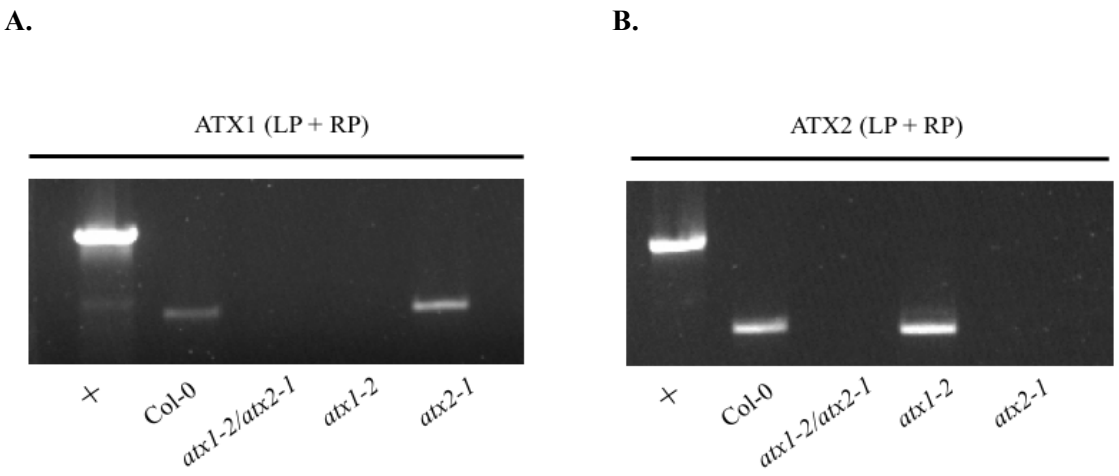

Figure 10. Expression analysis of *ATX1* and *ATX2* transcripts in *atx* single and double mutants. The cDNA was used as a template to assess the transcripts of *ATX1* and *ATX2* in *atx* single and double mutants.

A. LP and RP indicate *ATX1* gene-specific primers. Only Col-0 and *atx2-1* were amplified because both genes are not disrupted by T-DNA insertion. "+" is the Col-0 DNA which act as a positive control.

B. LP and RP indicate *ATX2* gene-specific primers. Only Col-0 and *atx1-2* were amplified because both genes are not disrupted by T-DNA insertion. "+" is the Col-0 DNA which act as a positive control.

To analyze the expression of pri-*MIR395* transcripts in wild type (WT) and mutants, plants were grown on control (0.3mM sulfate) and sulfate-deprived (0mM sulfate) hydroponic cultures for 10 days. QRT–PCR assays revealed the up-regulation of pri-*MIR395a, b, c, d,* and *f* levels in shoots of Col-0 as well as the mutants, i.e., *atx1-2, atx2-1*, *atx1-2/atx2-1* and *swn3* under S deprivation although the up-regulation was stronger in case of mutants. Pri-*MIR395e* was the only exception to this trend as its' levels were differed even under control condition, i.e., levels were remarkably low in *swn3* but greater in *atx1-2/ax2-1* double mutant (Figure 11). On the other hand, under S deprivation, pri-*MIR395e* levels were down-regulated in mutants compared to WT (Figure 11).

Interestingly, in roots, pri-*MIR395a, b, c* and *f* levels exhibited up-regulation both in WT and the mutants. Although this trend is similar in both WT and mutants, the up-regulation was far greater in mutants compared to WT. By contrast, pri-*MIR395d* and *e* transcript profiles differed greatly between WT and mutants under control conditions, i.e., in all four mutants, their levels were clearly low. Under S deprivation, pri-*MIR395d* and *e* levels were unaltered in WT but their levels were decreased in the mutants. These results imply that the pri-*MIR395* levels were differentially regulated in roots of mutants compared to WT under S deprivation (Figure 12).

A.

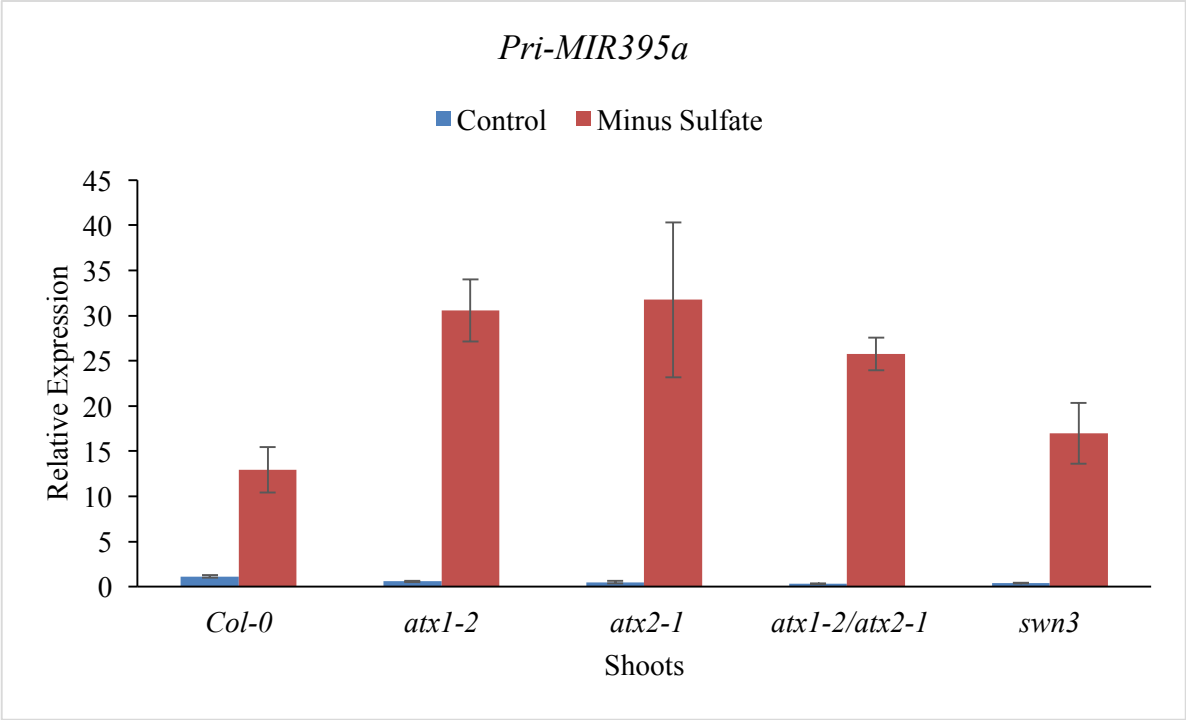
Pri-MIR395a
Control
Minus Sulfate
Relative Expression
45
40
35
30
25
20
15
10
5
0
Col-0
atx1-2
atx2-1
atx1-2/atx2-1
swn3
Shoots

B.

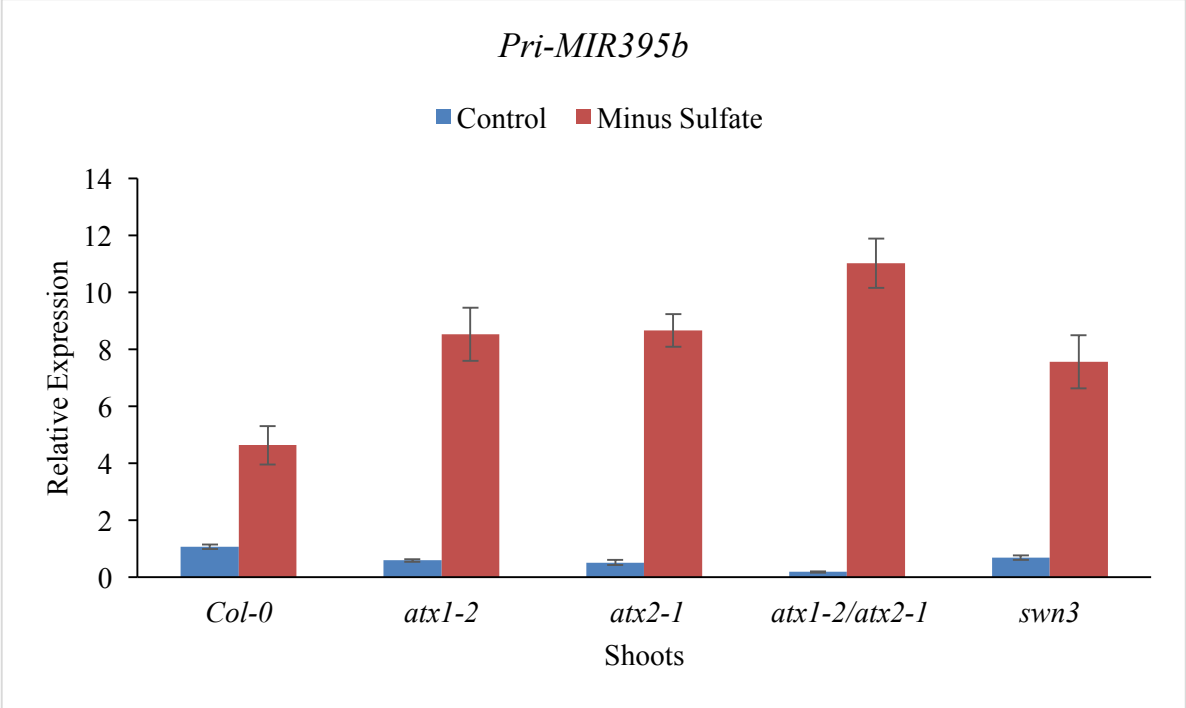
Pri-MIR395b
Control
Minus Sulfate
Relative Expression
14
12
10
8
6
4
2
0
Col-0
atx1-2
atx2-1
atx1-2/atx2-1
swn3
Shoots

C.

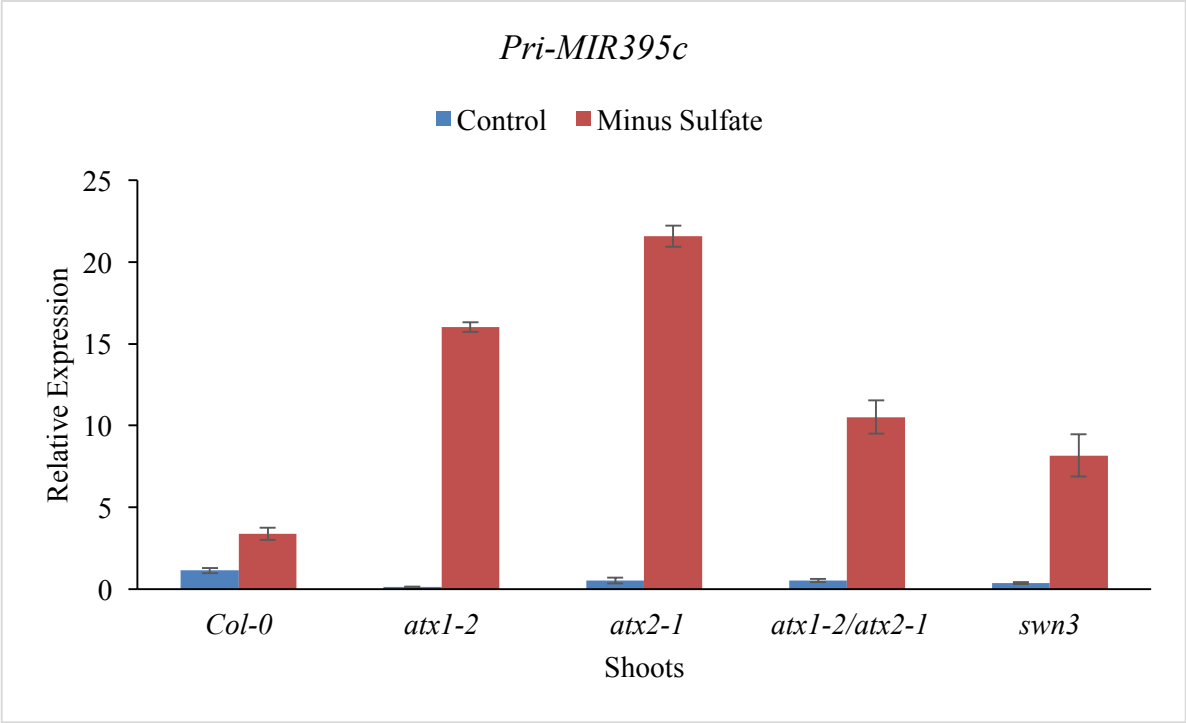
Pri-MIR395c
Control
Minus Sulfate
Relative Expression
25
20
15
10
5
0
Col-0
atx1-2
atx2-1
atx1-2/atx2-1
swn3
Shoots

D.

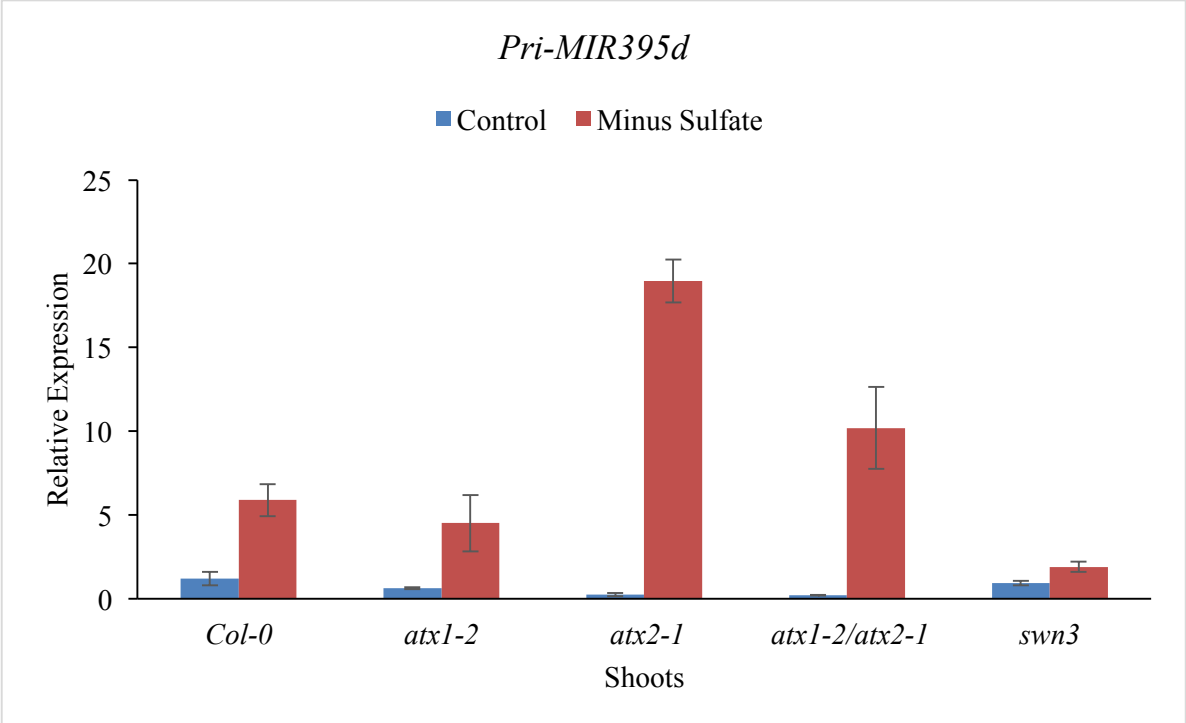
Pri-MIR395d
Control
Minus Sulfate
Relative Expression
25
20
15
10
5
0
Col-0
atx1-2
atx2-1
atx1-2/atx2-1
swn3
Shoots

E.

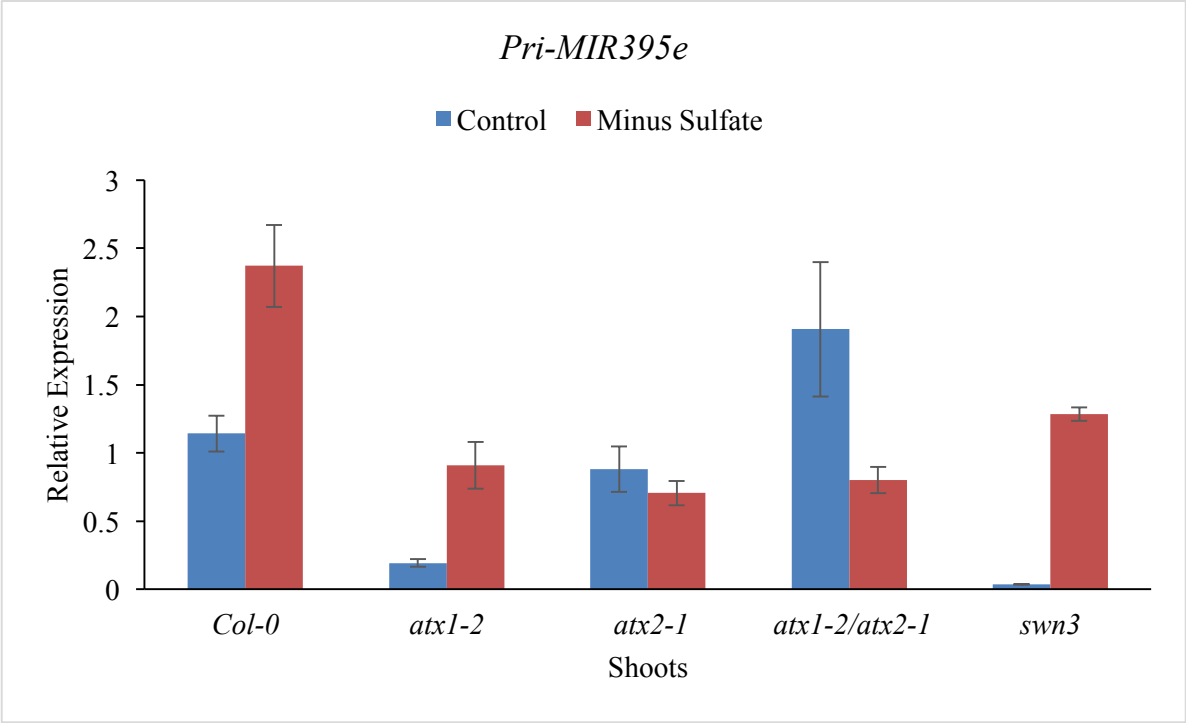
Pri-MIR395e
Control
Minus Sulfate
Relative Expression
3
2.5
2
1.5
1
0.5
0
Col-0
atx1-2
atx2-1
atx1-2/atx2-1
swn3
Shoots

F.

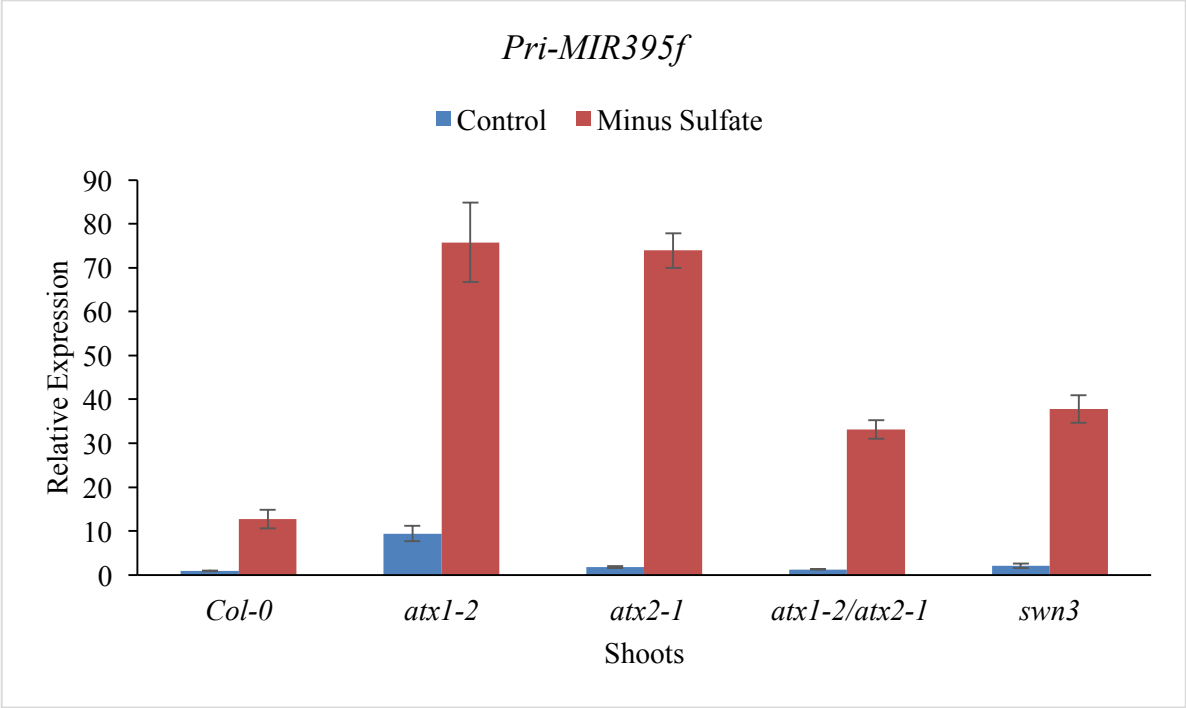
Pri-MIR395f
Control
Minus Sulfate
Relative Expression
90
80
70
60
50
40
30
20
10
0
Col-0
atx1-2
atx2-1
atx1-2/atx2-1
swn3
Shoots

Figure 11. Expression profiles of pri-*MIR395* transcripts under S deprivation in shoots of WT, *atx* and *swn3* mutants.

A - F. The qRT-PCR of pri-*MIR395a-f* expression levels in shoot tissue of *atx1-2, atx2-1*, *atx1-2/atx2-1* and *swn3* mutants under control and S deprivation conditions. The *PP2A* transcript levels were used to normalize the expression levels. Error bars denotes the standard deviation. Result shown is the average of three technical replicates.

A.

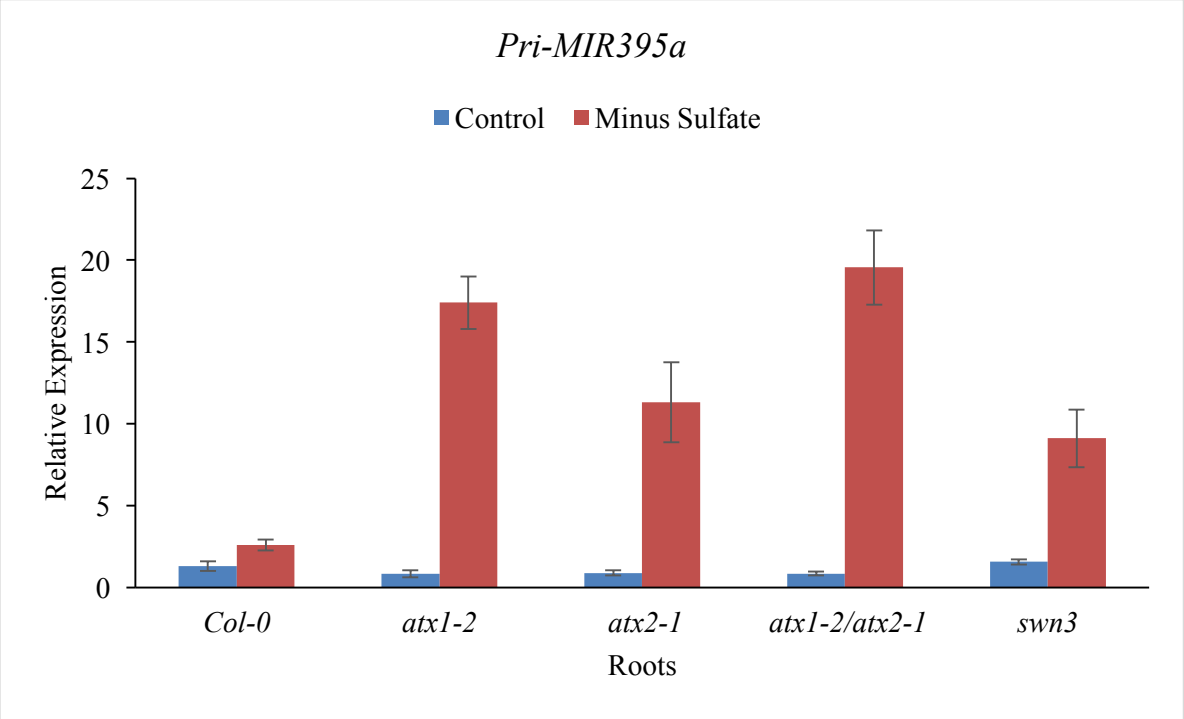

B.

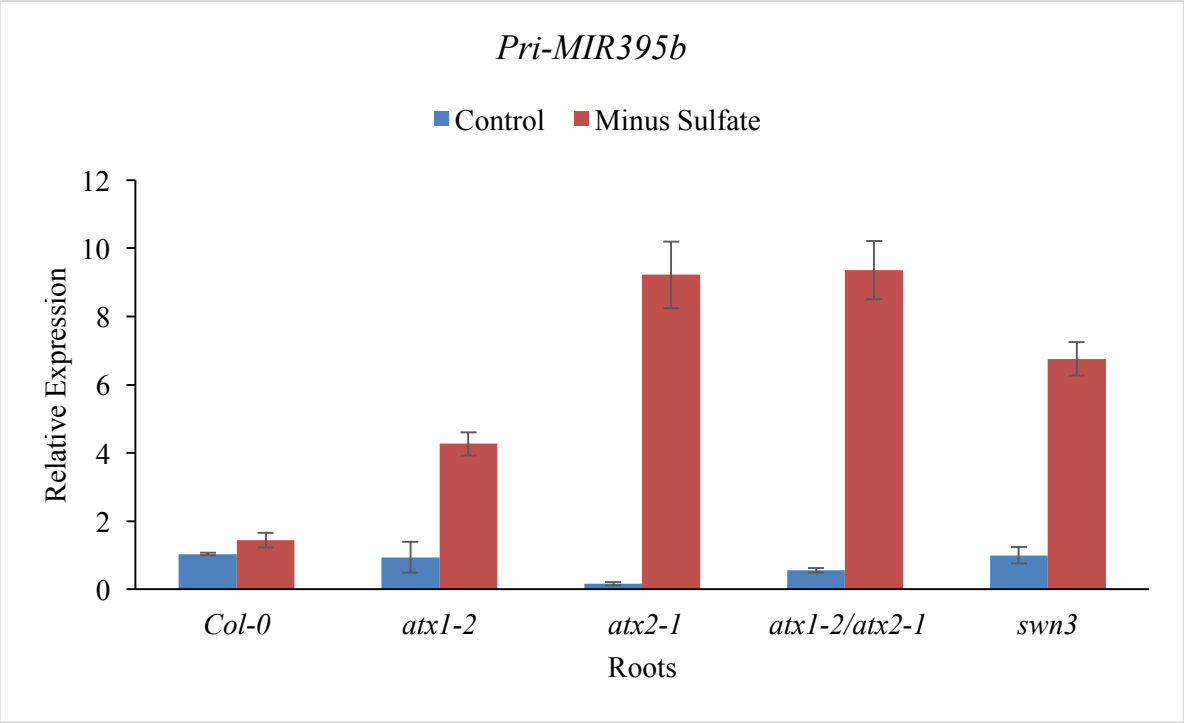
Pri-MIR395b
Control
Minus Sulfate
Relative Expression
12
10
8
6
4
2
0
Col-0
atx1-2
atx2-1
atx1-2/atx2-1
swn3
Roots

C.

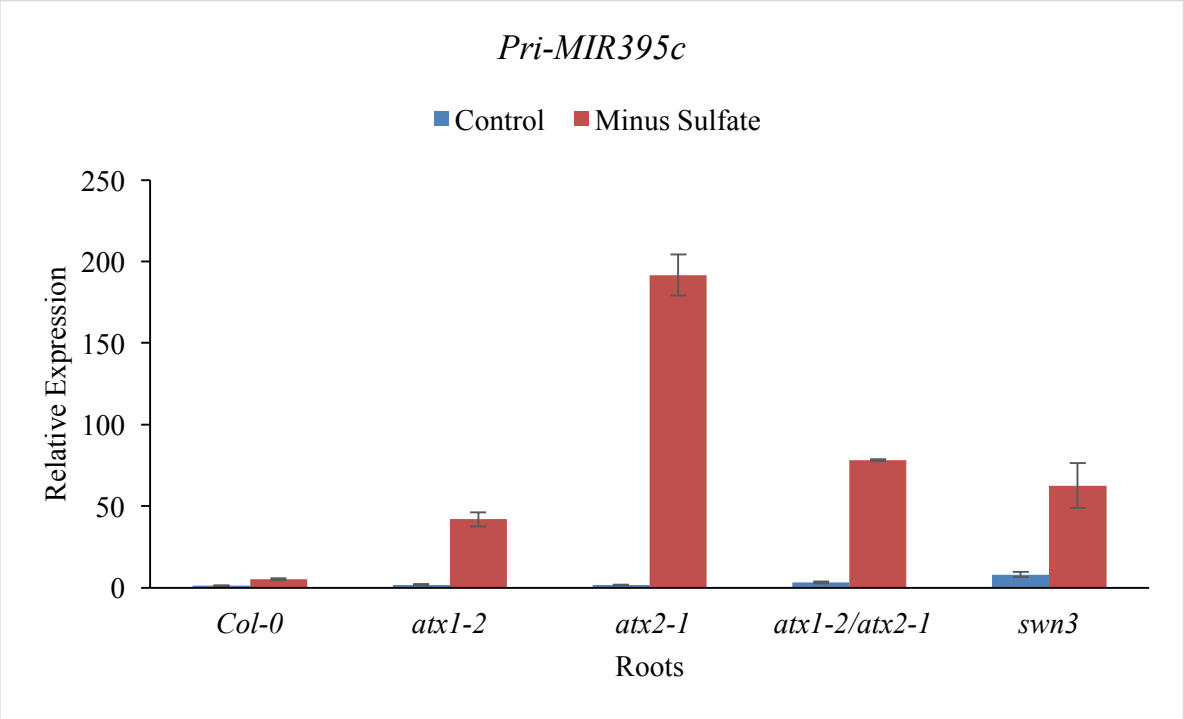
Pri-MIR395c
Control
Minus Sulfate
Relative Expression
250
200
150
100
50
0
Col-0
atx1-2
atx2-1
atx1-2/atx2-1
swn3
Roots

D.

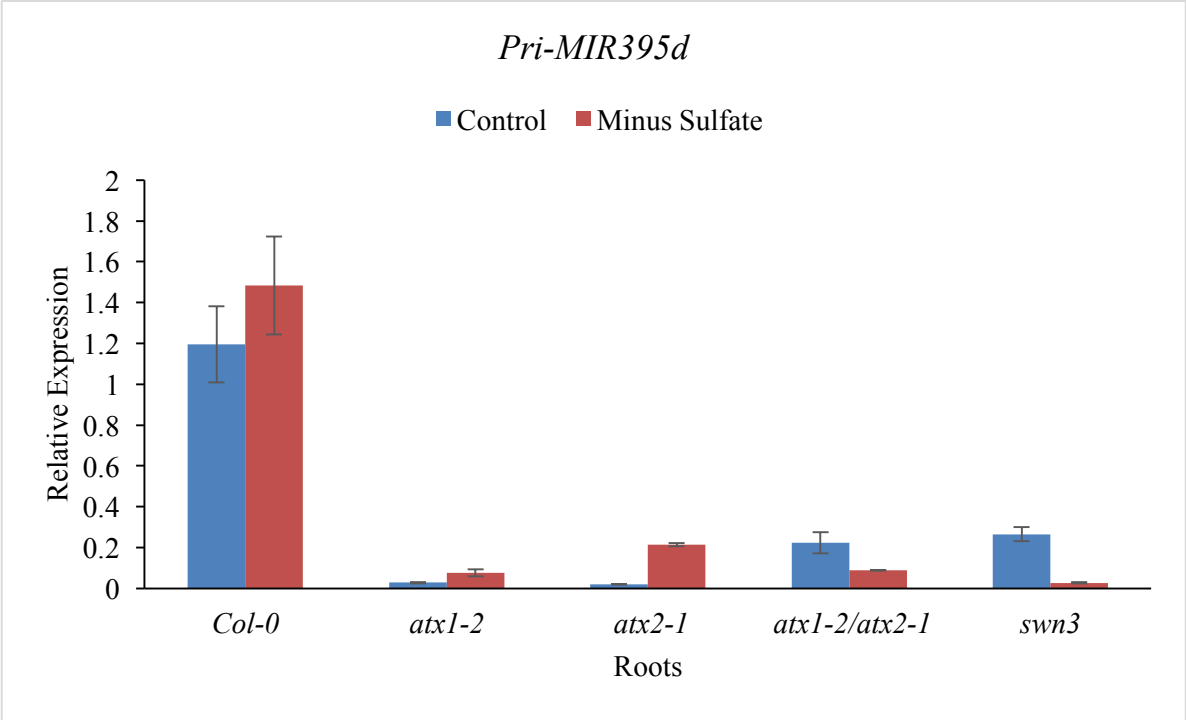
Pri-MIR395d
Control
Minus Sulfate
Relative Expression
2
1.8
1.6
1.4
1.2
1
0.8
0.6
0.4
0.2
0
Col-0
atx1-2
atx2-1
atx1-2/atx2-1
swn3
Roots

E.

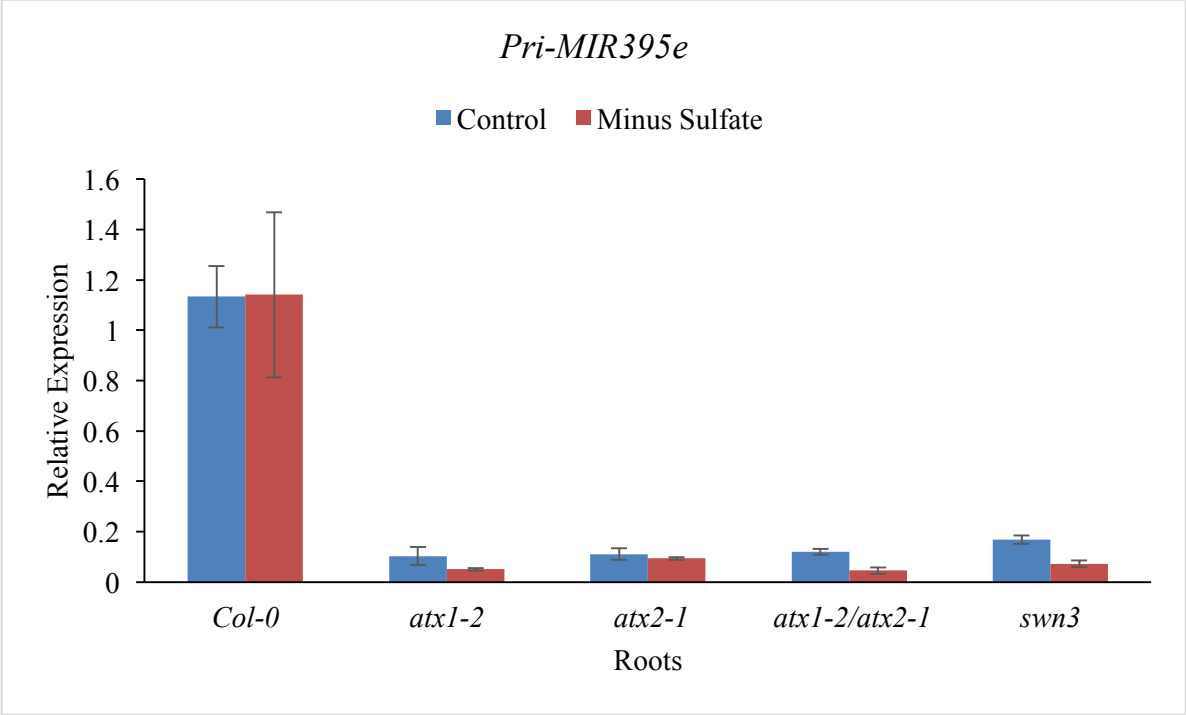
Pri-MIR395e
Control
Minus Sulfate
Relative Expression
1.6
1.4
1.2
1
0.8
0.6
0.4
0.2
0
Col-0
atx1-2
atx2-1
atx1-2/atx2-1
swn3
Roots

F.

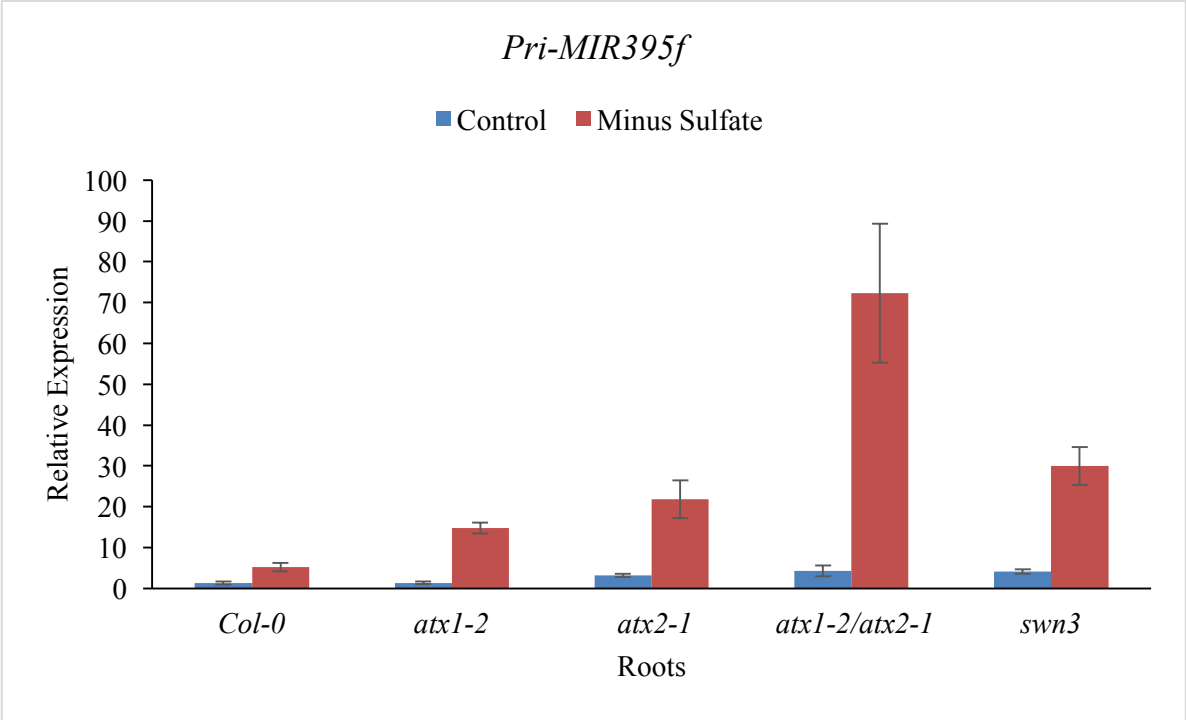

Figure 12. Expression profiles of pri-*MIR395* transcripts under S deprivation in roots of WT, *atx* and *swn3* mutants.

A - F. The qRT-PCR of pri-*MIR395a-f* expression levels in roots of *atx1-2, atx2-1*, *atx1-2/atx2-1* and *swn3* mutants under control and S deprivation conditions. The *PP2A* transcript levels were used to normalize the expression levels. Error bars indicates the standard deviation. Result shown are the average of three technical replicates.

4.5 Expression Profiles of genes targeted by miR395 in Mutants Defective in H3K4 and H3K27 Methylation Under S Deprivation

MiR395 is targeting a low-affinity sulfate transporter (*AST68* also called *SULTR2;1*) that transport sulfate into xylem for translocation into shoots and three *APS* genes (*APS1*, *APS3* and *APS4*) that are involved in assimilating sulfate (Liang et al, 2010; Liang and Yu, 2010). Previous studies have shown that the abundances of miR395 and target genes were negatively correlated in shoots and roots under S deprivation and the only exception was *AST68* levels in roots, whose levels were also elevated when miR395 levels were elevated (Jagadeeswaran et al., 2014). To assess the impact of altered miR395 levels on their target gene expression in mutants, the *AST68, APS1*, *APS3* and *APS4* levels were analyzed. This analysis measures the transcript abundances, which are not only affected by miR395-guided transcript degradation but translational repression also into account. It should be noted that the target genes could also be undergoing transcriptional regulation in the histone methylation and histone variant mutants.

Under sulfate deprivation, the transcript levels of all four targets (*AST68, APS1, APS3* and *APS4*) in shoots of Col-0 were down-regulated (Figure 13), which could largely be attributed to the induced miR395 levels. These results are in agreement with a previous study (Jagadeeswaran et al., 2014). However, *AST68* transcript levels were markedly up-regulated in *atx1-2*, *atx1-2/atx2-1* and *swn3* mutants under control conditions. Similarly, under S deprivation, the *AST68* levels were highly up-regulated in all four mutants (*atx1-2, atx2-1*, *atx1-2/atx2-1* and *swn3*) compared to the WT (Figure 13). Under normal conditions, in shoots, *APS1* transcript levels in *atx1-2* were similar to the WT but their levels were low in the remaining 3 mutants (*atx2-1*, *atx1-2/atx2-1* and *swn3*). Under S deprivation, the *APS1* levels were down-regulated in *atx1-2*, *atx2-1* and *atx1-2/atx2-1* mutants but unaltered in *swn3* mutant. To a certain degree, both

APS3 and *APS4* levels displayed similar responses both in control and S deprivation conditions. The *APS3* levels were almost similar in all four mutants (*atx1-2, atx2-1*, *atx1-2/atx2-1* and *swn3*) under control conditions. Under S deprivation, *APS3* levels were strongly down-regulated in WT but unaltered in *atx1-2, atx2-1* and *atx1-2/atx2-1* mutants, i.e., showing similar levels as found in control conditions. However, these levels in mutants were elevated when compared to the response of WT under S deprivation. In *swn3* mutant, the *APS3* levels were strongly up-regulated under S deprivation compared to the other 3 mutants and WT. Compared to *APS3* in shoots, *APS4* levels were only slightly up-regulated in *swn3* under S deprivation.

Contrasting to the responses observed in the shoots of Col-0 (WT), *AST68*, *APS1*, *APS3* and *APS4* transcript levels were up-regulated in the roots under S deprivation (Figure 14). Remarkably, the up-regulation of *AST68* was about 18-fold greater compared to the *APS* genes that are only slightly up-regulated. In the mutants, *AST68* levels in roots were either unaltered (*atx1-2*, *atx2-1* and *atx1-2/atx2-1* mutants) or even down-regulated (*swn3* mutant) under S deprivation. The *APS1* and *APS3* levels showed similar profiles (up-regulated in *atx1-2* but down-regulated in *atx2-1* and *atx1-2/atx2-1*) under S deprivation in the roots of *atx1-2, atx2-1*, *atx1-2/atx2-1* and *swn3*. Unlike in WT in which *APS4* levels in roots were slightly elevated, their levels in roots were down-regulated in all mutants under S deprivation.

A.

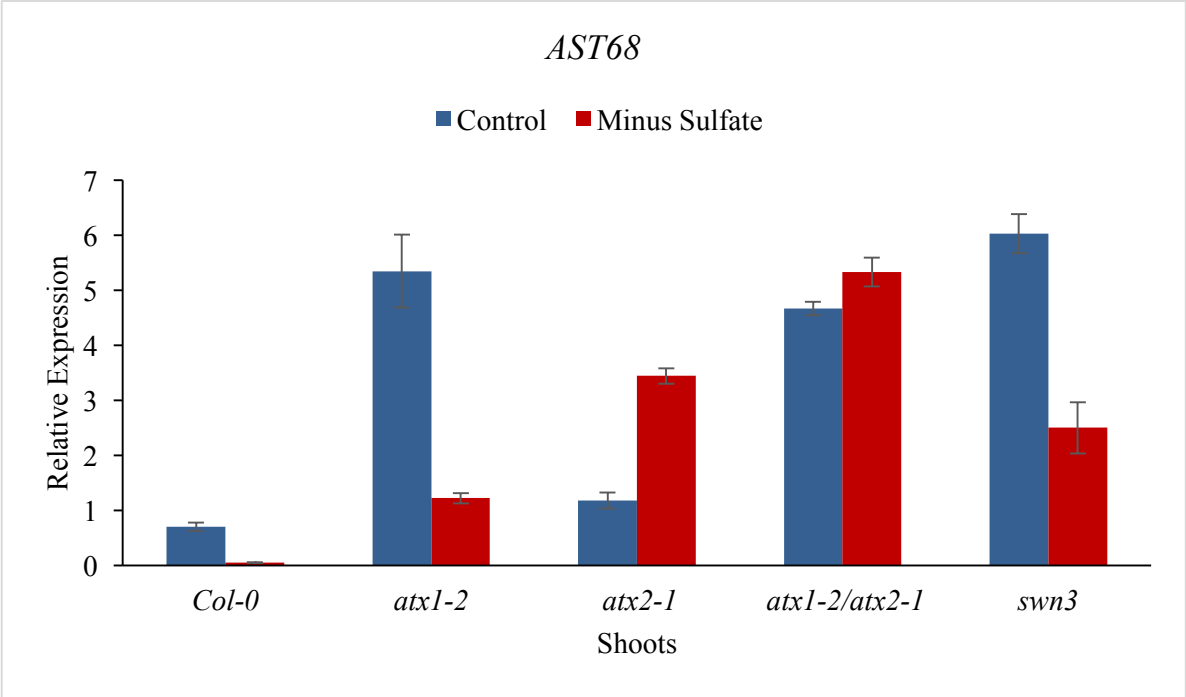
AST68
Control
Minus Sulfate
Relative Expression
7
6
5
4
3
2
1
0
Col-0
atx1-2
atx2-1
atx1-2/atx2-1
swn3
Shoots

B.

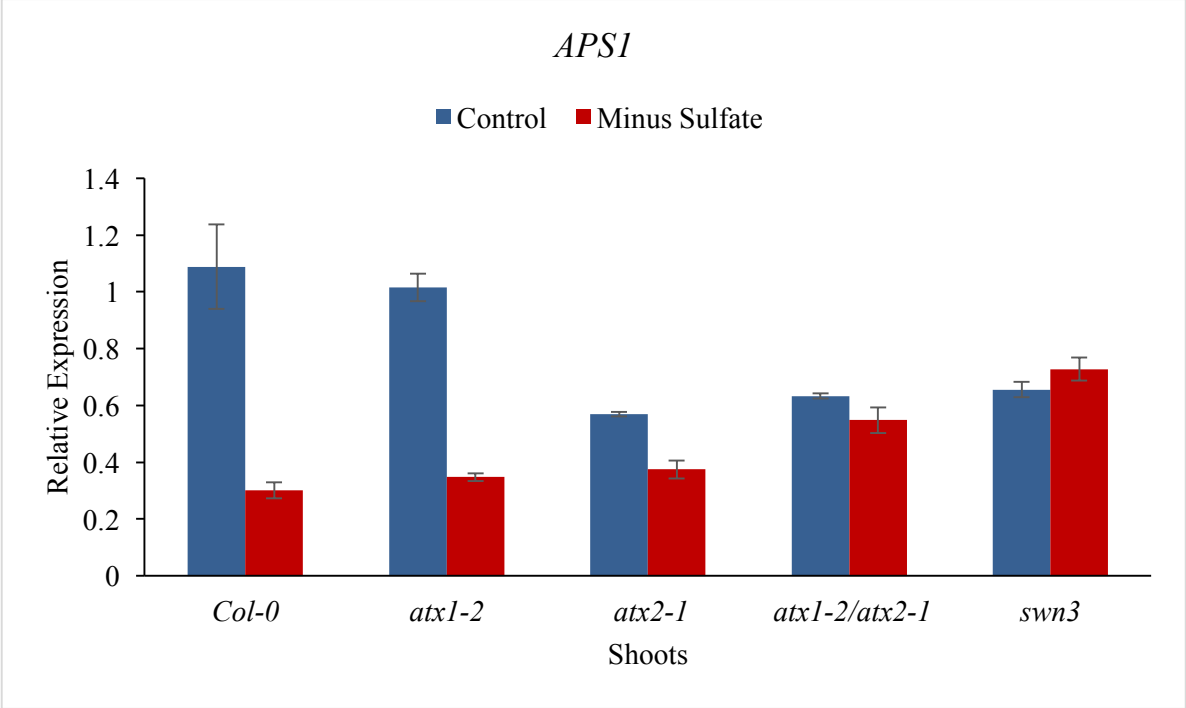
APS1
Control
Minus Sulfate
Relative Expression
1.4
1.2
1
0.8
0.6
0.4
0.2
0
Col-0
atx1-2
atx2-1
atx1-2/atx2-1
swn3
Shoots

C.

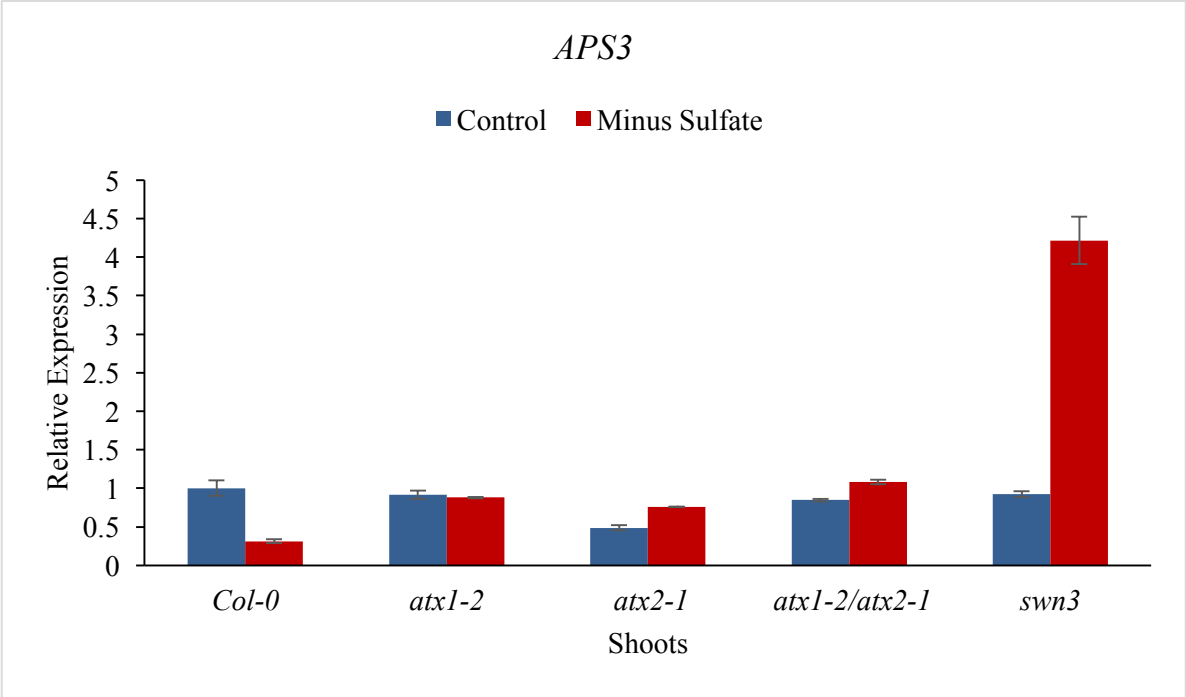
APS3
Control
Minus Sulfate
Relative Expression
5
4.5
4
3.5
3
2.5
2
1.5
1
0.5
0
Col-0
atx1-2
atx2-1
atx1-2/atx2-1
swn3
Shoots

D.

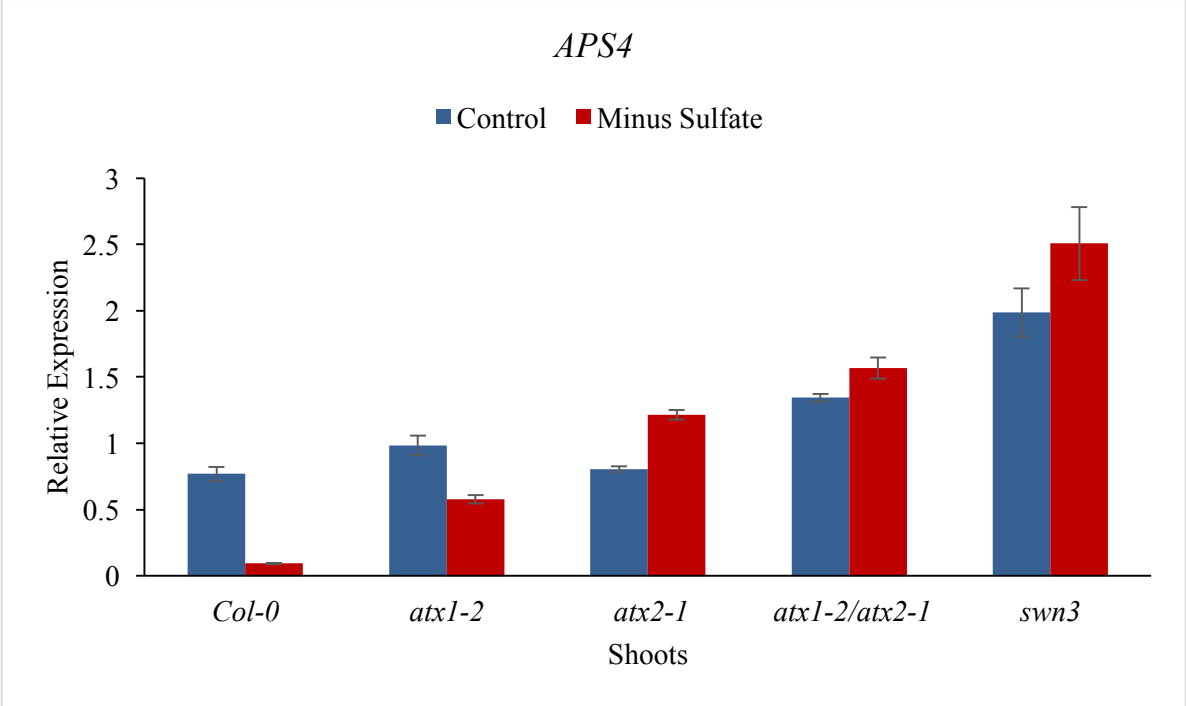
APS4
Control
Minus Sulfate
Relative Expression
3
2.5
2
1.5
1
0.5
0
Col-0
atx1-2
atx2-1
atx1-2/atx2-1
swn3
Shoots

Figure 13. Expression profiles of genes targeted by miR395 in shoots of WT, *atx* and *swn* mutants.

A - D. The qRT-PCR for expression levels of miR395 target genes in shoots tissue under control and sulfate stress conditions. The *PP2A* transcript levels were used to normalize the expression levels. Error bars denotes the standard deviation. Result shown is the average of three technical replicates.

A.

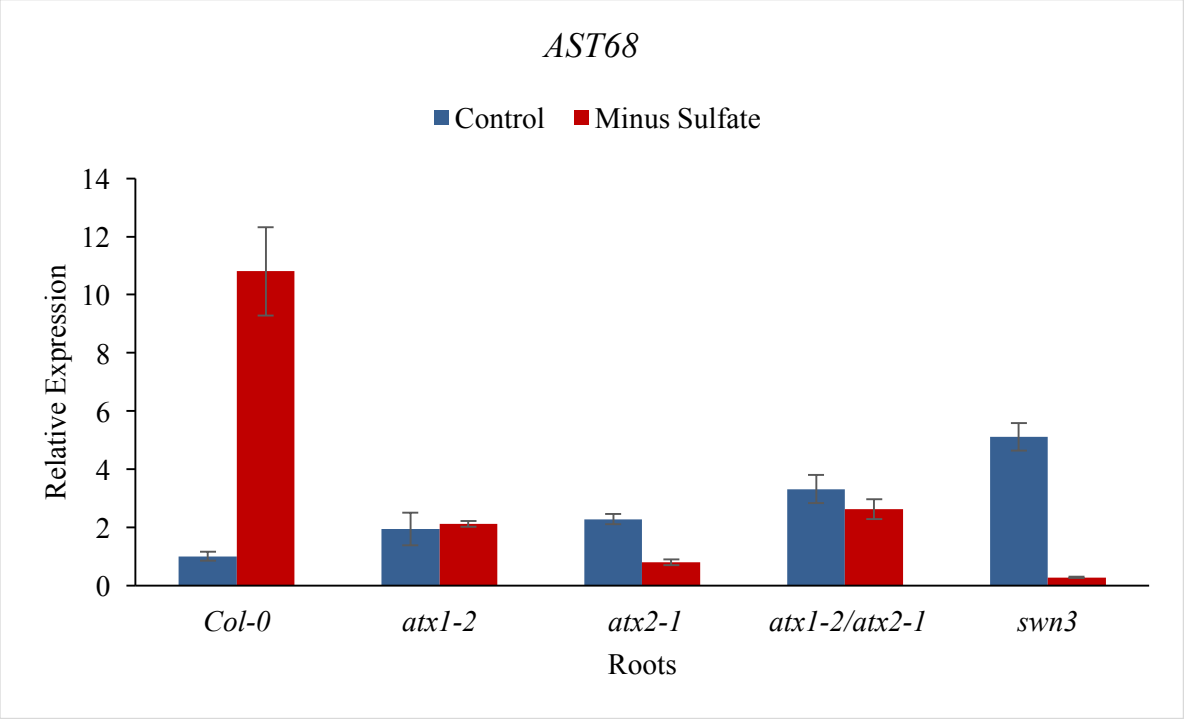

B.

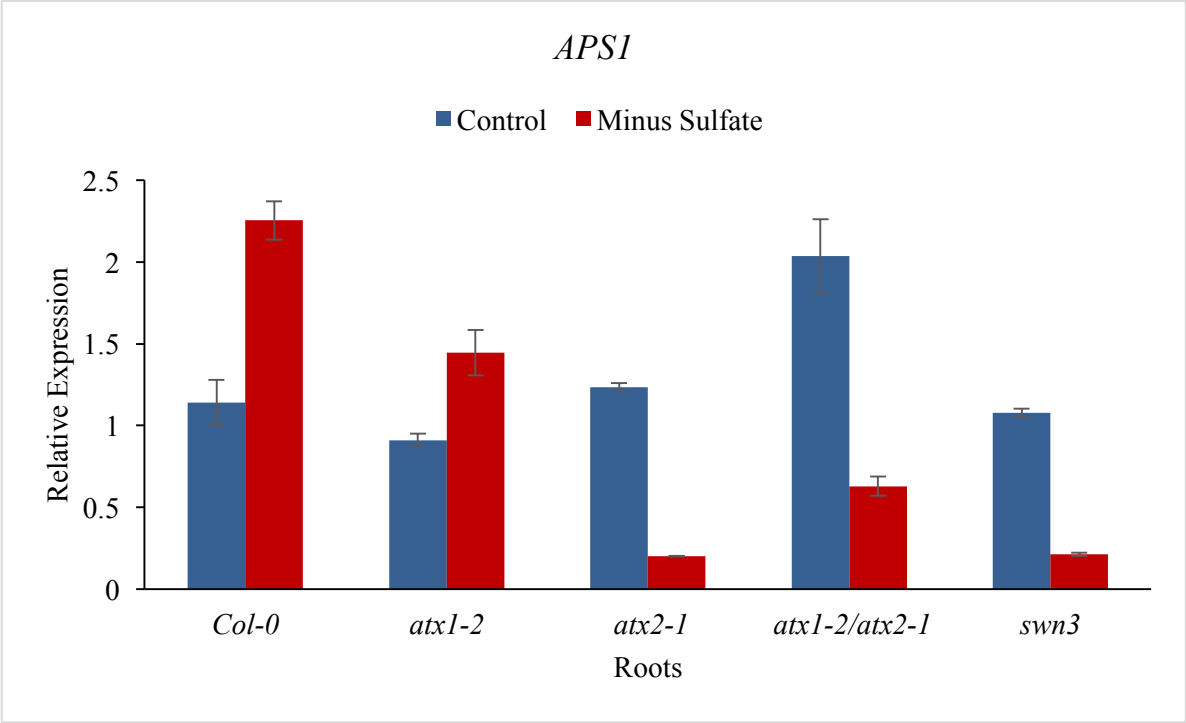
APS1
Control
Minus Sulfate
Relative Expression
2.5
2
1.5
1
0.5
0
Col-0
atx1-2
atx2-1
atx1-2/atx2-1
swn3
Roots

C.

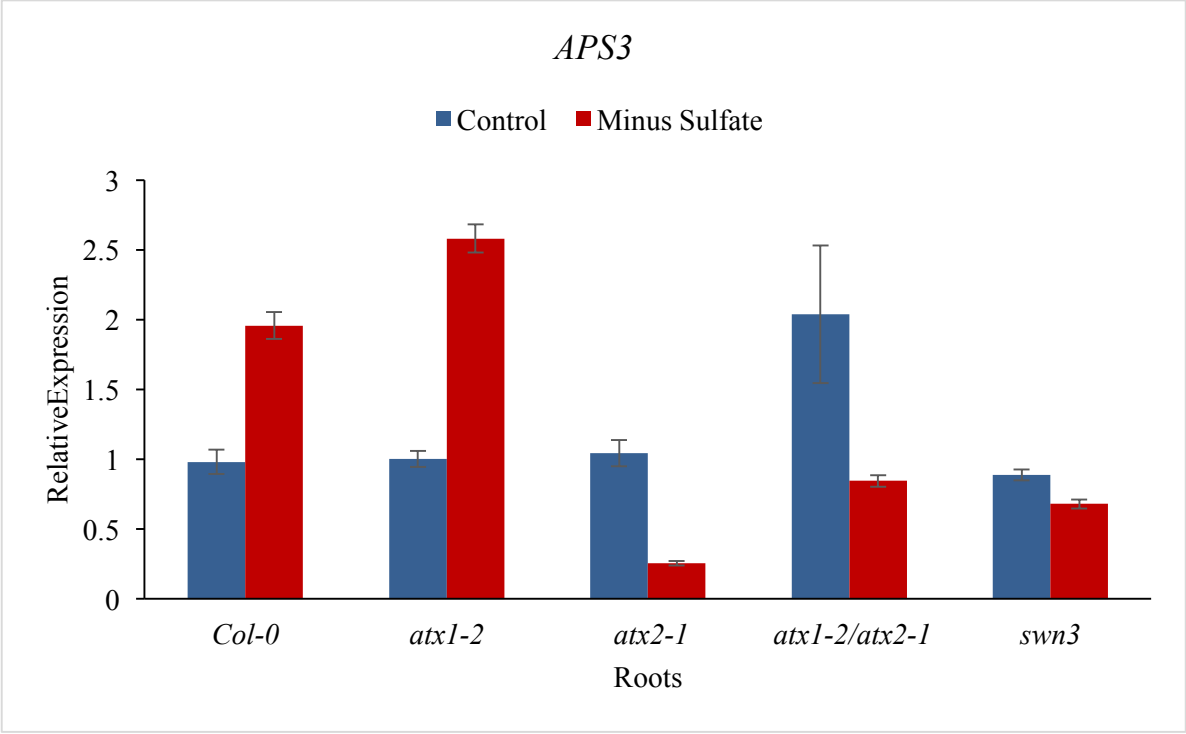
APS3
Control
Minus Sulfate
RelativeExpression
3
2.5
2
1.5
1
0.5
0
Col-0
atx1-2
atx2-1
atx1-2/atx2-1
swn3
Roots

D.

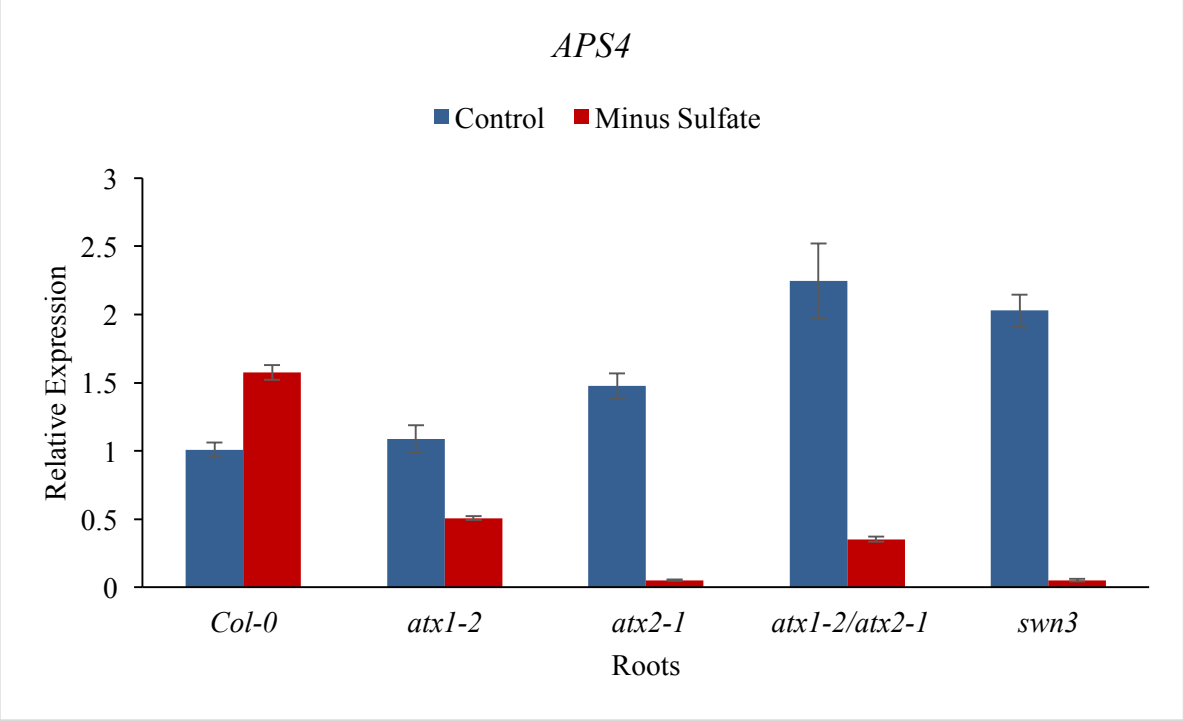

Figure 14. Expression profiles of genes targeted by miR395 in roots of WT, *atx* and *swn* mutant.

A - D. The qRT-PCR for expression levels of target genes in root tissue under control and sulfate stress conditions. The *PP2A* transcript levels were used to normalize the expression levels. Error bars denotes the standard deviation. Result shown is the average of three technical replicates.

4.6 Expression Profiles of Pri-*MIR395* in Mutants Defective in H2A.Z Deposition Under S Deprivation.

To address the role of H2A.Z in miR395 regulation under S deprivation in *Arabidopsis*, *hta9-1* and *hta11-2* mutants that are defective in H2A.Z deposition were exposed to S deprivation and the transcript levels of pri-*MIR395* in single mutants (*hta9-1* and *hta11-2*) and double mutant (*hta9-1/hta11-2*) were analyzed.

The T-DNA was inserted into the intron of *hta9-1*. Using *HTA9* gene-specific primers, the transcripts of *HTA9* could be amplified both in the *hta9-1* and *hta9-1/hta11-2* mutants. This suggests that during transcription, the T-DNA-containing intron was spliced out (Osabe et al., 2017), causes the transcript of *hta9-1* to be identical to the wild type (Zhang et al., 2016). Although the transcript level of *hta9-1* tends to be identical to the wild type, intronic T-DNA insertion in *hta9-1* was advocated to disrupt the function of *HTA9* either by the formation of premature 3'-end mRNA or improper splicing and transcription (Zhang et al., 2016; Osabe et al., 2017). A study has shown that the *HTA9* transcript levels in *hta9-1* mutant represents approximately 0.04% of the wild type levels (Coleman-Derr et al., 2012). On the other hand, using *HTA11* gene specific primers, the transcript levels of *HTA11* were only amplified in WT and *hta9-1* mutant lines but not in the *hta11-2* mutants.

A.

B.

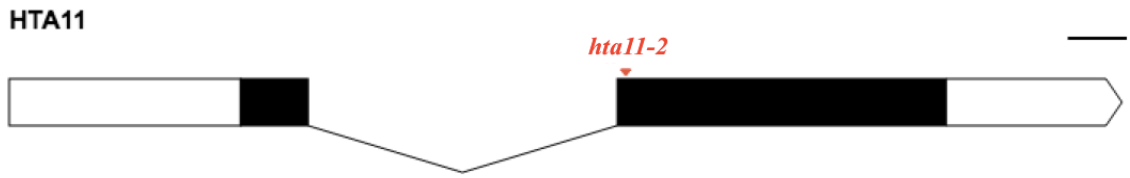

Figure 15. Schematic diagram of T-DNA insertion site on *HTA9* and *HTA11* genes.

A. Schematic diagram of genomic structure for *HTA9* locus (AT1G52740). *HTA9* consists of 1250 base pairs of genomic DNA and 842 base pairs of cDNA. Black boxes represent exons. The unfilled white portions represent introns. There are a total of 2 exons and 2 introns. The triangle (*hta9-1*) represents the position of T-DNA insertion. T-DNA is inserted at the intron of *HTA9* to disrupt the function of gene.

B. Schematic diagram of genomic structure for *HTA11* locus (AT3G54560). *HTA9* consists of 1587 base pairs of genomic DNA and 891 base pairs of cDNA. Black boxes represent exons. The unfilled white portions portions represent introns. There are a total of 2 exons and 2 introns. The triangle (*hta11-2*) represents the position of T-DNA insertion. T-DNA is inserted at the exon of *HTA11* to disrupt the function of gene.

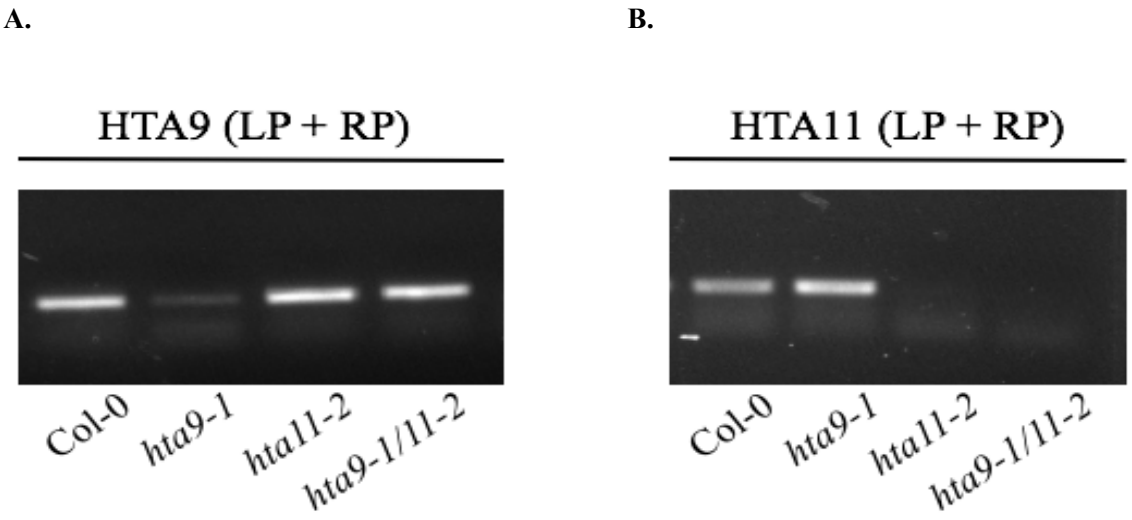

Figure 16. Expression analysis of *HTA9* and *HTA11* transcripts in *hta* single and double mutants.

A. cDNA was used to test *hta* single and double mutants at the transcript level. LP and RP indicate HTA9 gene specific primers. A low level of *HTA9* was expressed in *hta9-1*. "+" is the Col-0 DNA which act as a positive control.

B. cDNA was used to test *hta* single and double mutants at the transcript level. LP and RP indicate HTA11 gene specific primers. Only WT and *hta9-1* were detected because HTA11 gene in *hta11-2* and *hta9-1/hta11-2* is truncated by T-DNA insertion. "+" is the Col-0 DNA which act as a positive control.

The expression profiles of pri-*MIR395* transcript levels in wild type (WT) and H2A.Z mutants grown under control and S deprivation conditions were assessed. The qRT–PCR analysis revealed that the pri-*MIR395a, b, c, d, e* and *f* levels were up-regulated in shoots of WT under S deprivation. All these six loci displayed varying expression profiles in different mutants. For instance, pri-*MIR395a* was strongly up-regulated in *hta9-1* but unaltered in *hta11-2*, whereas the

levels were only slightly up-regulated in *hta9-11/hta11-2* under S deprivation (Figure 17). Pri-*MIR395b* and *f* levels displayed similar pattern of responses in mutants; strong up-regulation in *hta9-1* and intermediate level of up-regulation in *hta11-2* and mild up-regulation in *hta9-11/hta11-2*. Relative to pri-*MIR395b* and *f*, pri-*MIR395c* expression levels displayed opposite patterns; mild up-regulation in *hta9-1* and intermediate level of up-regulation in *hta11-2*, and strong up-regulation in *hta9-11/hta11-2*. Although up-regulated in shoots under S deprivation, pri-*MIR395d* levels did not vary between WT, *hta9-1* and *hta11-2*. Interestingly, in *hta9-11/hta11-2*, pri-*MIR395d* levels were unresponsive to S deprivation. Compared to Col-0, pri-*MIR395e* levels were more up-regulated in *hta11-2* mutant but displayed less up-regulation in *hta9-1* and *hta9-11/hta11-2* mutants (Figure 18).

In roots, compared to the Col-0, pri-*MIR395a* and *c* levels exhibited similar responses although the degree of induction differed between the mutants, i.e., more strongly up-regulated in *hta9-1* and *hta11-2*, but suppressed in *hta9-11/hta11-2*. Interestingly, under control conditions, pri-*MIR395b* levels in roots were low in mutants compared to Col-0. Under S deprivation, pri-*MIR395d* levels were strongly up-regulated in *hta11-2* and *hta9-11/hta11-2 mutants*. Pri-*MIR395e* levels exhibited mild differences between the WT and mutants both under control and S deprivation conditions; under control conditions, the levels were slightly more in the mutants. Interestingly, the pri-*MIR395f* levels were relatively high in mutants compared to Col-0 under control conditions. Under S deprivation, pri-*MIR395f* levels were strongly up-regulated only in *hta9-1*. Taken together, pri-*MIR395a-f* levels showed differential expression profiles in both shoots and roots of *h2a.z* mutants compared to Col-0 (Figure 18).

A.

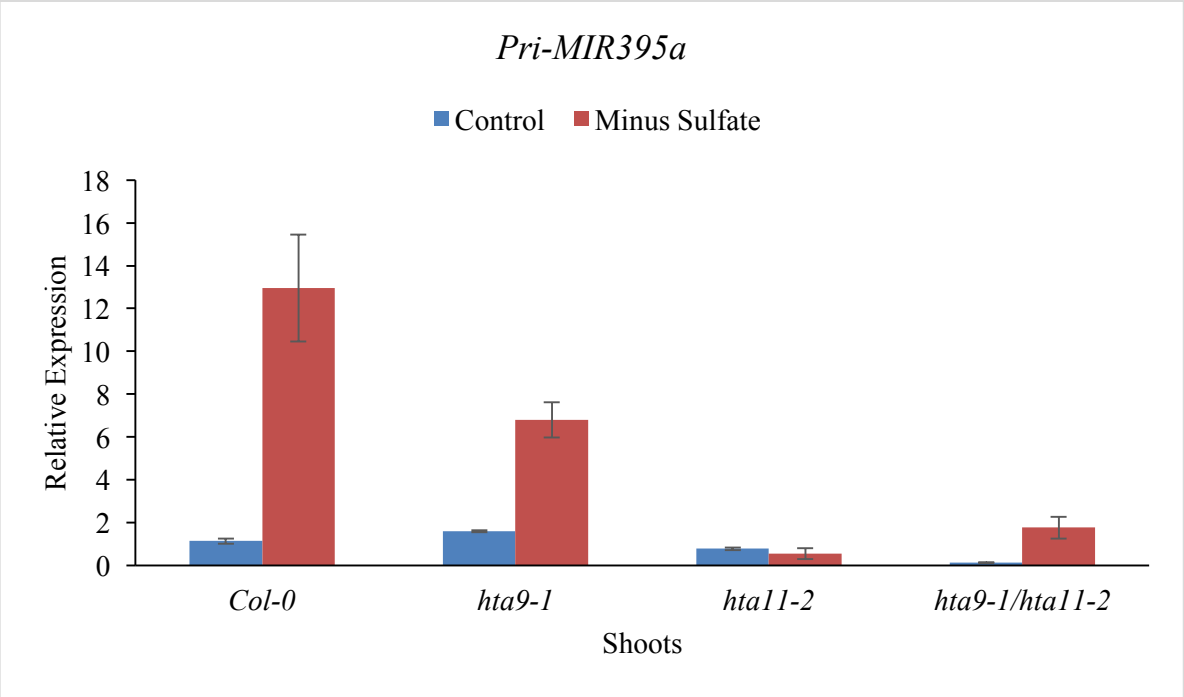
Pri-MIR395a
Control
Minus Sulfate
Relative Expression
18
16
14
12
10
8
6
4
2
0
Col-0
hta9-1
hta11-2
hta9-1/hta11-2
Shoots

B.

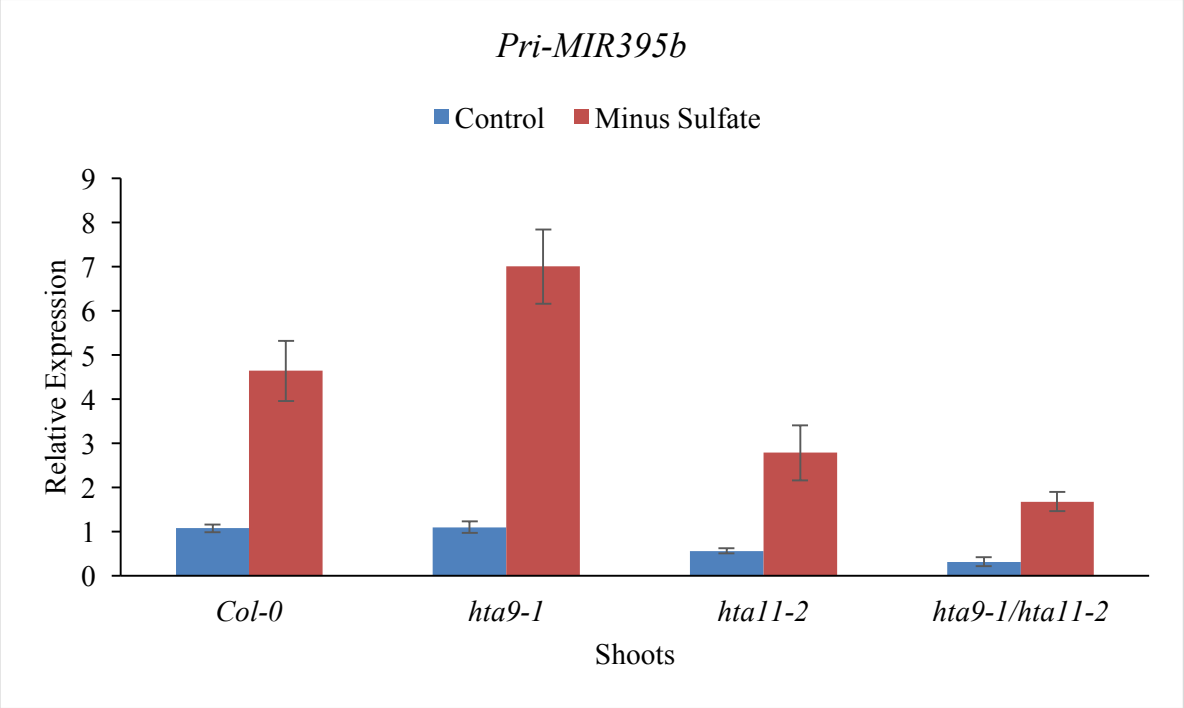
Pri-MIR395b
Control
Minus Sulfate
Relative Expression
9
8
7
6
5
4
3
2
1
0
Col-0
hta9-1
hta11-2
hta9-1/hta11-2
Shoots

C.

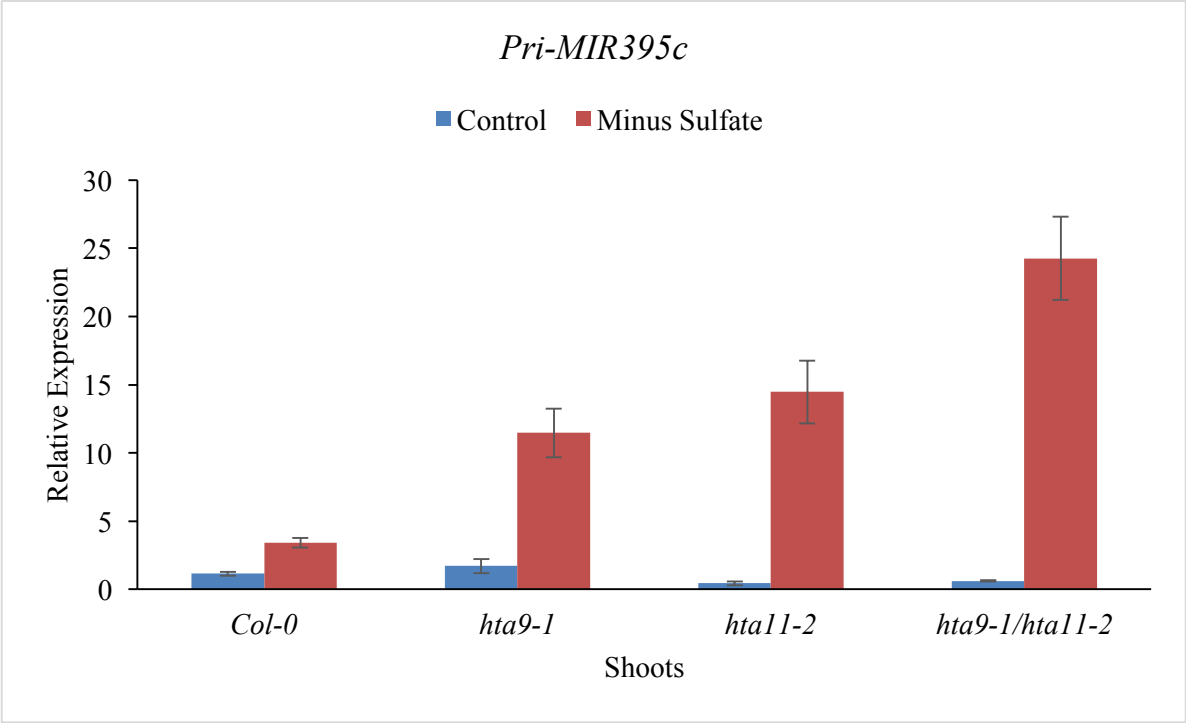
Pri-MIR395c
Control
Minus Sulfate
Relative Expression
30
25
20
15
10
5
0
Col-0
hta9-1
hta11-2
hta9-1/hta11-2
Shoots

D.

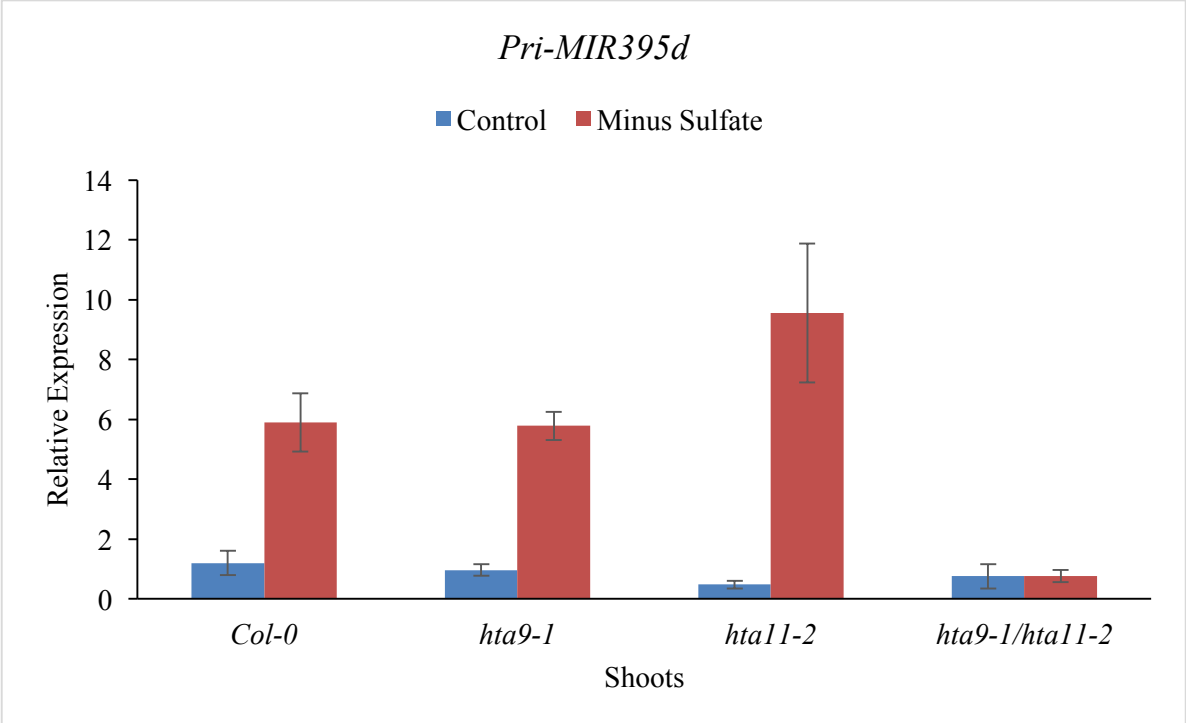
Pri-MIR395d
Control
Minus Sulfate
Relative Expression
14
12
10
8
6
4
2
0
Col-0
hta9-1
hta11-2
hta9-1/hta11-2
Shoots

E.

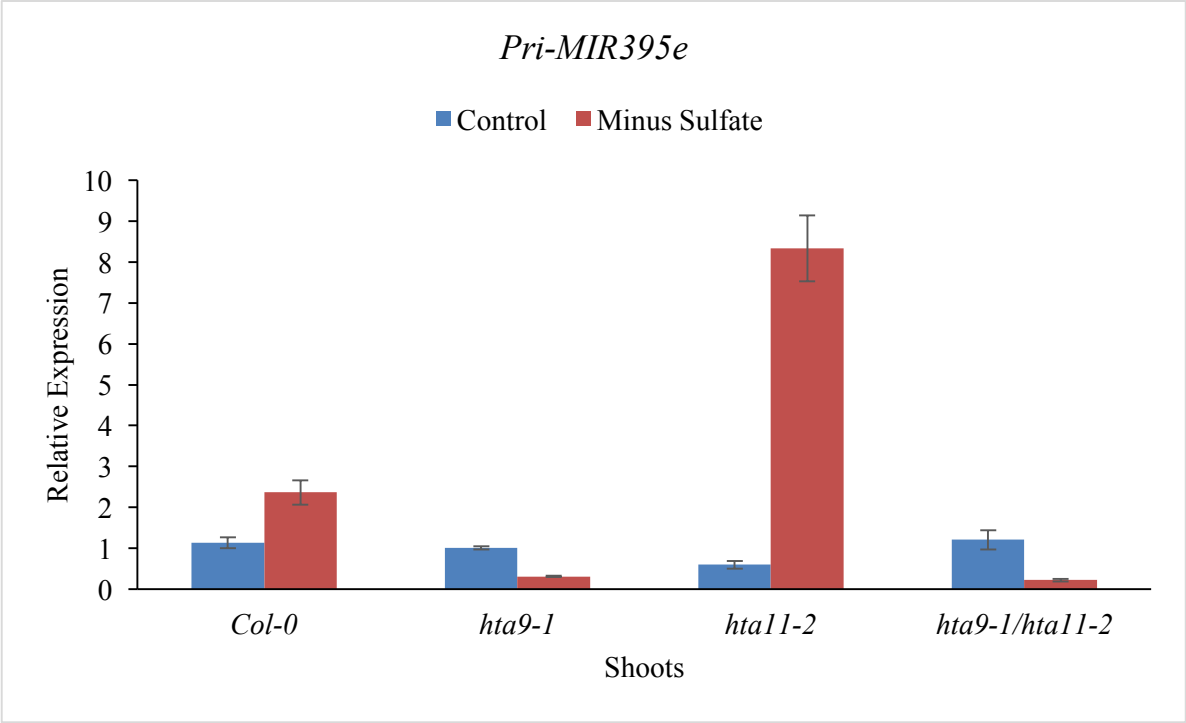
Pri-MIR395e
Control
Minus Sulfate
Relative Expression
10
9
8
7
6
5
4
3
2
1
0
Col-0
hta9-1
hta11-2
hta9-1/hta11-2
Shoots

F.

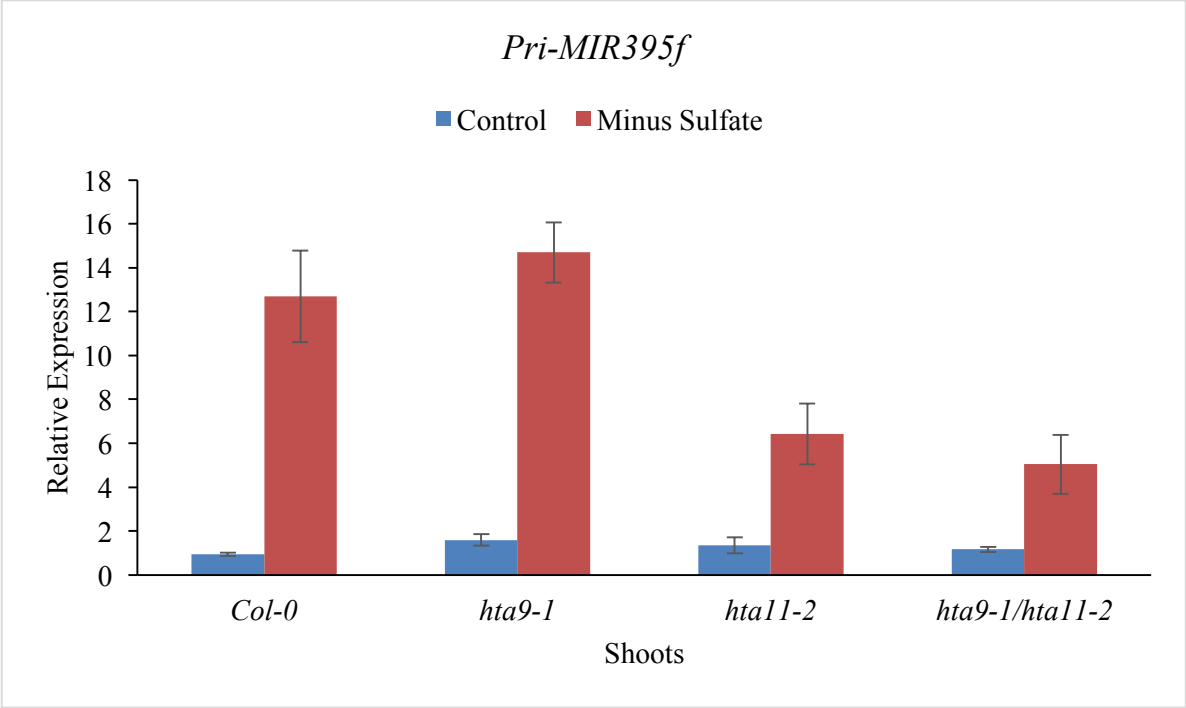
Pri-MIR395f
Control
Minus Sulfate
Relative Expression
18
16
14
12
10
8
6
4
2
0
Col-0
hta9-1
hta11-2
hta9-1/hta11-2
Shoots

Figure 17. Expression profiles of pri-*MIR395* under S deprivation in shoots of WT and *hta* mutants.

A - F. The qRT-PCR of pri-*MIR395a-f* expression levels in shoot tissues of H2A.Z mutants under control and S deprivation conditions. The *PP2A* transcript levels were used to normalize the expression levels. Error bars denotes the standard deviation. Results shown are the average of three technical replicates.

A.

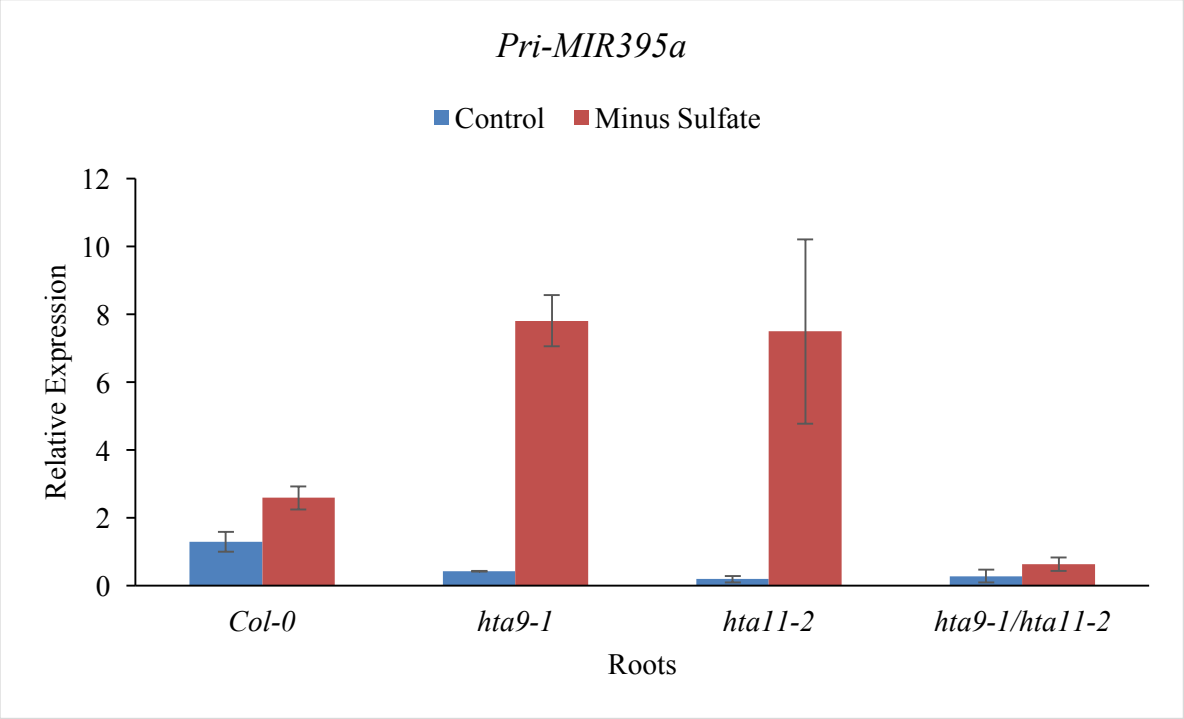

B.

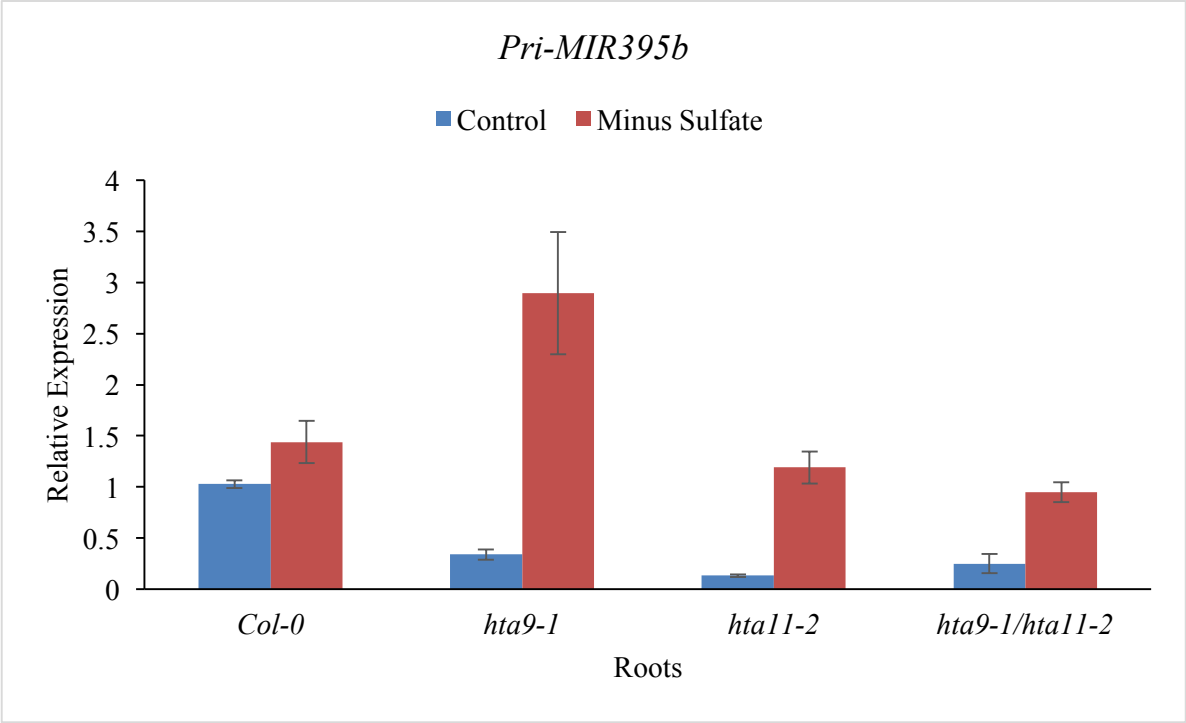
Pri-MIR395b
Control
Minus Sulfate
Relative Expression
4
3.5
3
2.5
2
1.5
1
0.5
0
Col-0
hta9-1
hta11-2
hta9-1/hta11-2
Roots

C.

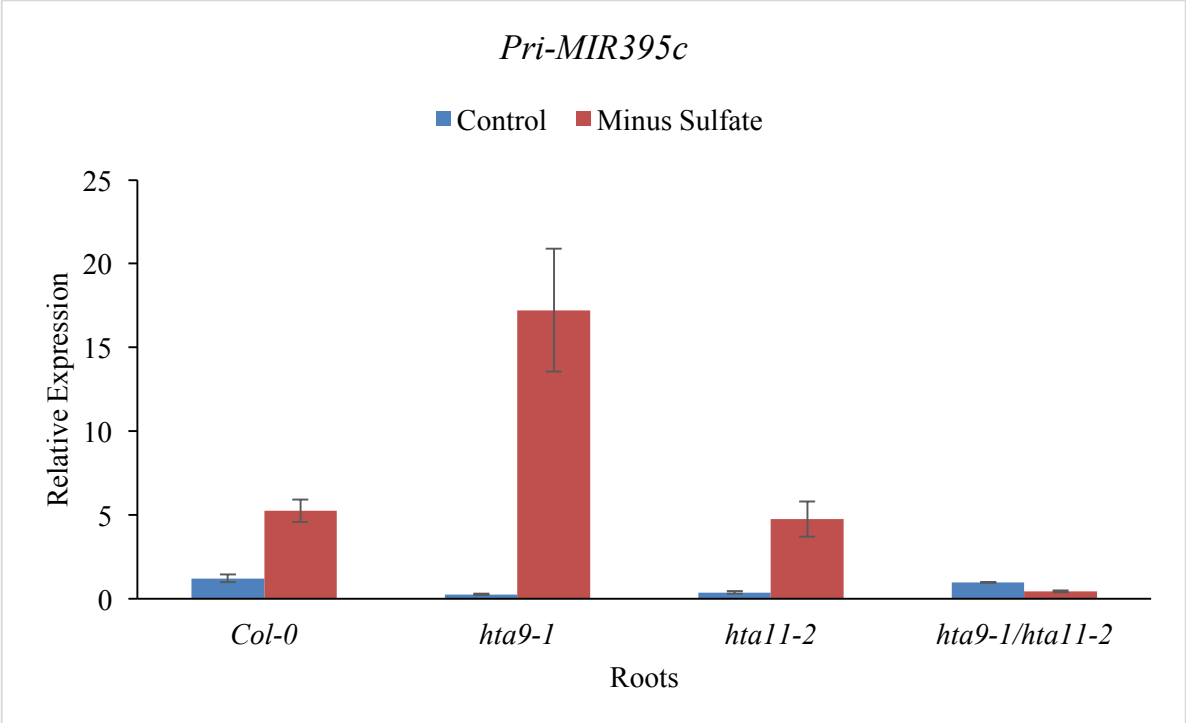
Pri-MIR395c
Control
Minus Sulfate
Relative Expression
25
20
15
10
5
0
Col-0
hta9-1
hta11-2
hta9-1/hta11-2
Roots

D.

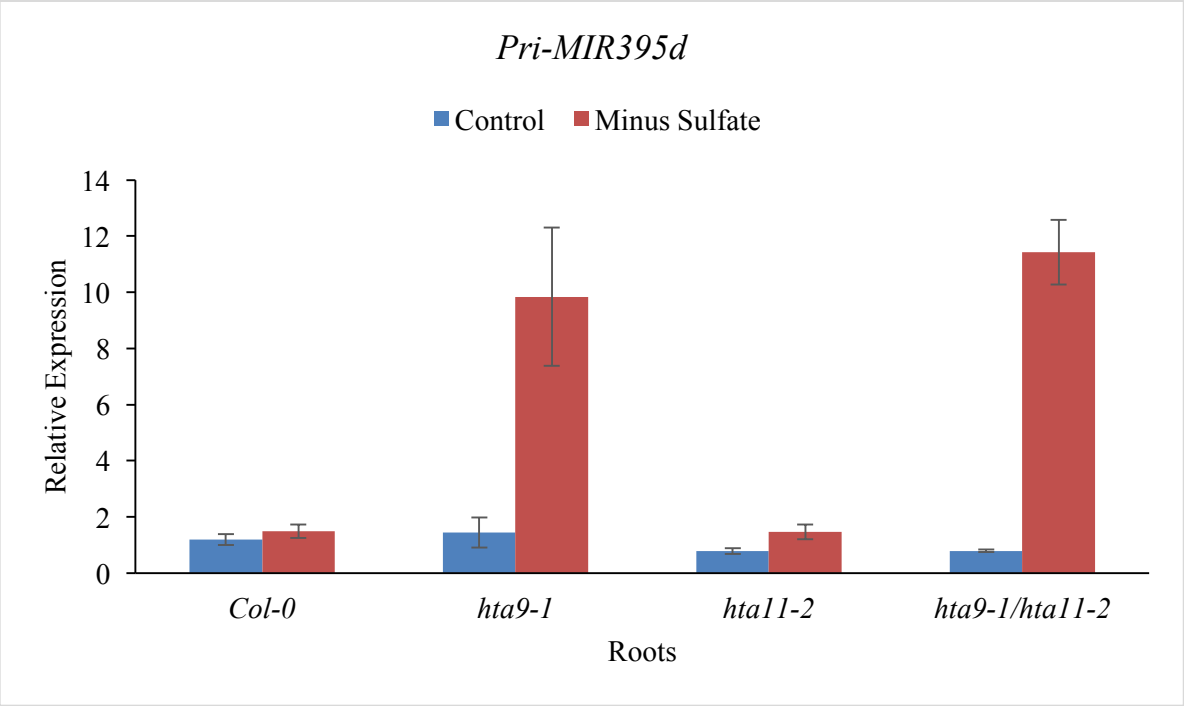
Pri-MIR395d
Control
Minus Sulfate
Relative Expression
14
12
10
8
6
4
2
0
Col-0
hta9-1
hta11-2
hta9-1/hta11-2
Roots

E.

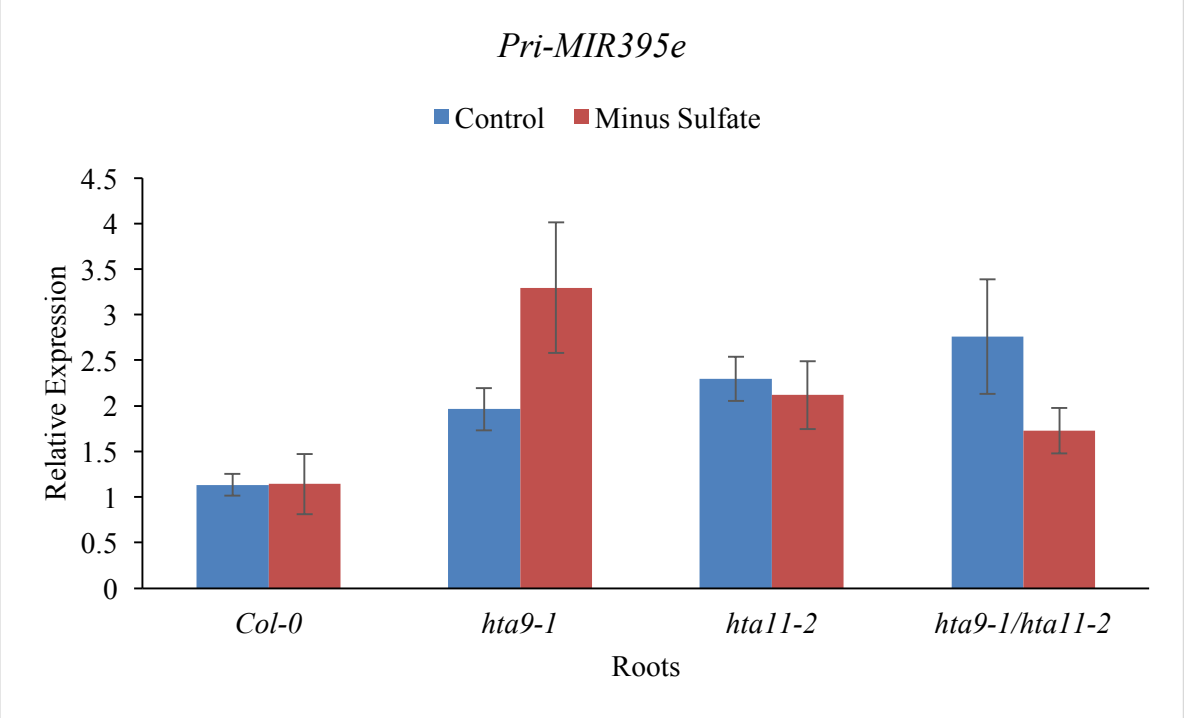
Pri-MIR395e
Control
Minus Sulfate
Relative Expression
4.5
4
3.5
3
2.5
2
1.5
1
0.5
0
Col-0
hta9-1
hta11-2
hta9-1/hta11-2
Roots

F.

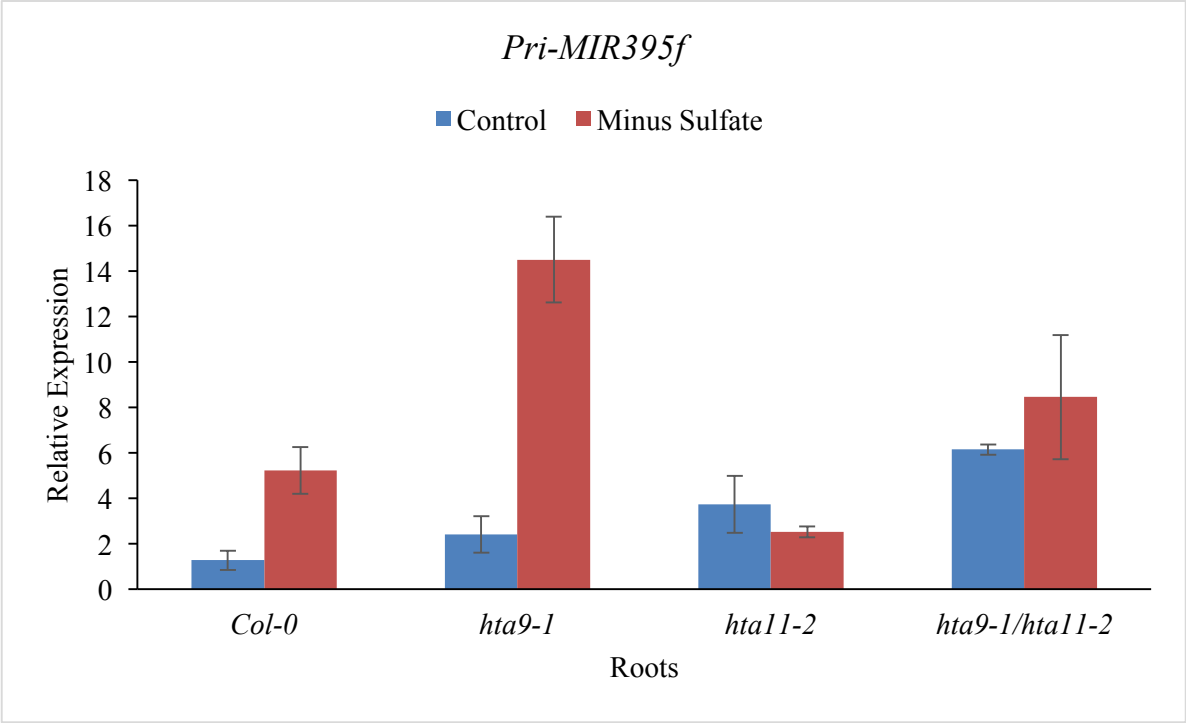

Figure 18. Expression profiles of pri-*MIR395* under S deprivation in roots of WT and *hta* mutants.

A - F. The qRT-PCR of pri-*MIR395a-f* expression levels in root tissues of H2A.z mutants under control and S deprivation conditions. The *PP2A* transcript levels were used to normalize the expression levels. Error bars indicates the standard deviation. Results shown are the average of three technical replicates.

4.7 Expression Profiles of genes targeted by miR395 in Mutants Defective in H2A.Z Deposition Under S Deprivation.

Notably, the transcript levels of *AST68, APS1, APS3* and *APS4* were relatively low in shoots of mutants compared to Col-0 under control conditions. The levels of *AST68, APS1, APS3* and *APS4* were down-regulated in Col-0 under S deprivation (Figure 19). Unlike the down-regulation that was observed in Col-0 under S deprivation, the transcript levels of *AST68*, *APS1* and *APS3* were up-regulated in *hta9-1* but down-regulated in *hta11-2*.

In roots, the *AST68, APS1* and *APS4* levels were relatively high in mutants compared to Col-0 under control conditions. Under S deprivation, in Col-0, the *AST68, APS1, APS3* and *APS4* levels were up-regulated. However, in mutants, these genes were only either mildly altered or did not differ under S deprivation (Figure 20). The transcript levels of *APS4* in root tissues of *hta9-1* and *hta11-2* were strongly up-regulated compared to Col-0 under S deprivation.

A.

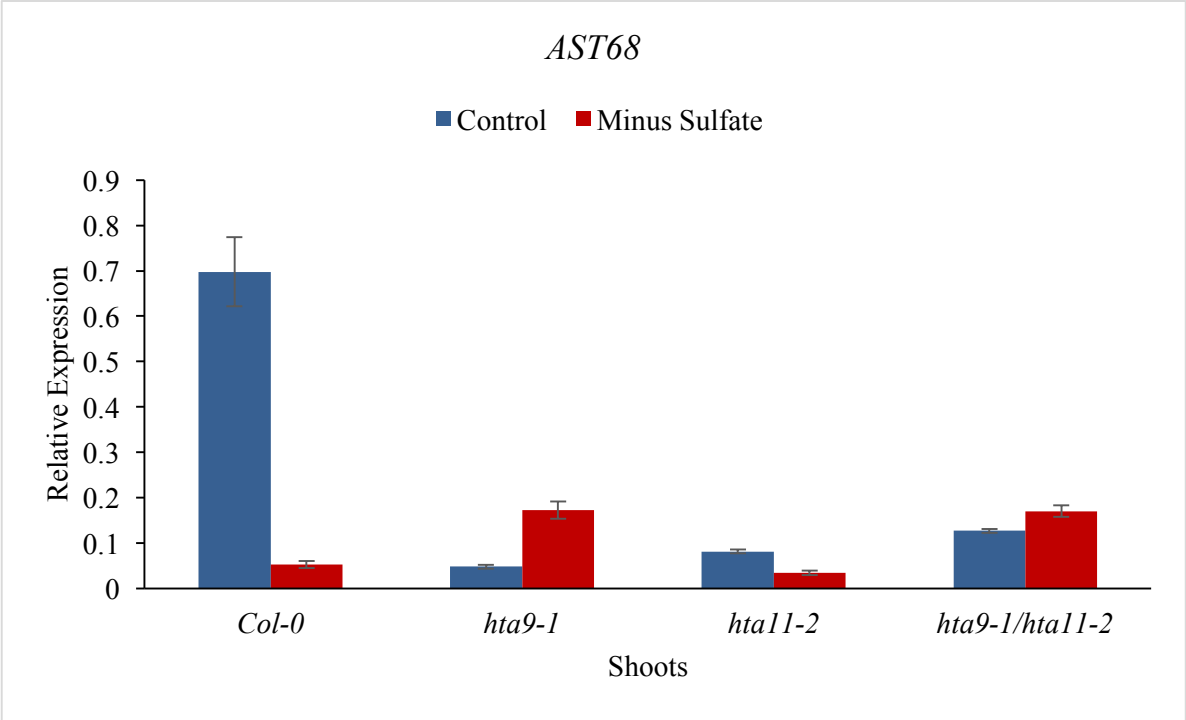
AST68
Control
Minus Sulfate
Relative Expression
0.9
0.8
0.7
0.6
0.5
0.4
0.3
0.2
0.1
0
Col-0
hta9-1
hta11-2
hta9-1/hta11-2
Shoots

B.

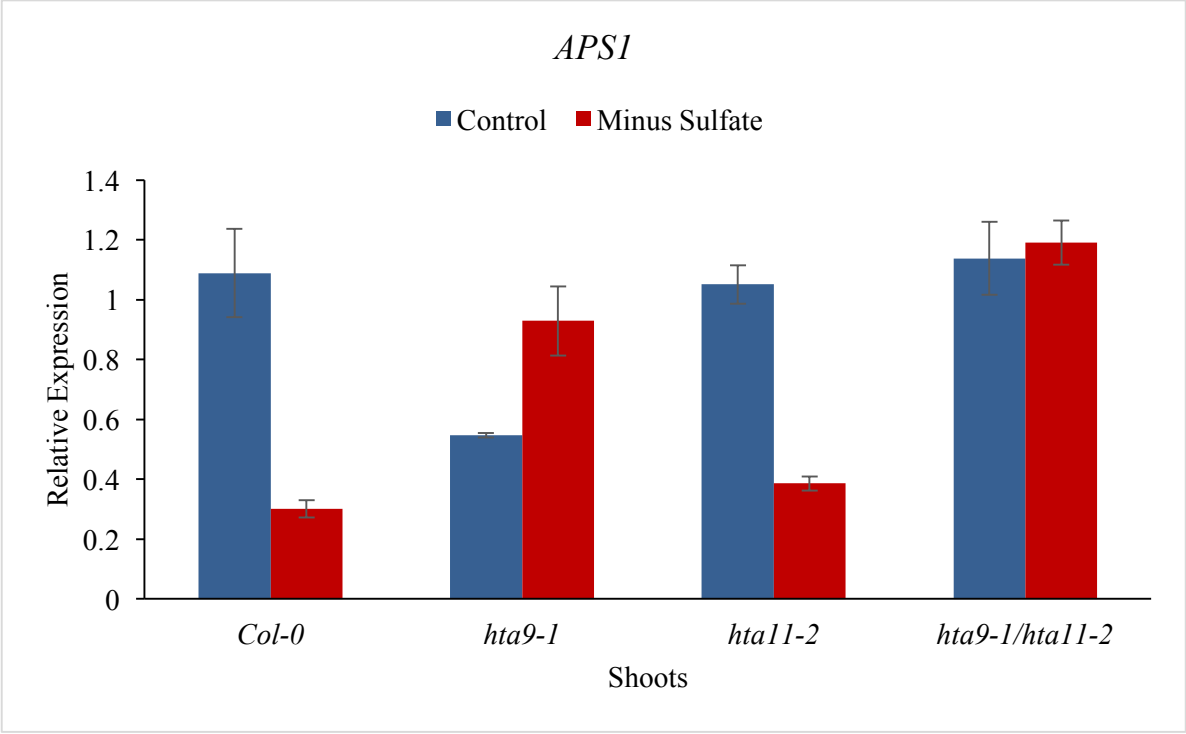
APS1
Control
Minus Sulfate
Relative Expression
1.4
1.2
1
0.8
0.6
0.4
0.2
0
Col-0
hta9-1
hta11-2
hta9-1/hta11-2
Shoots

C.

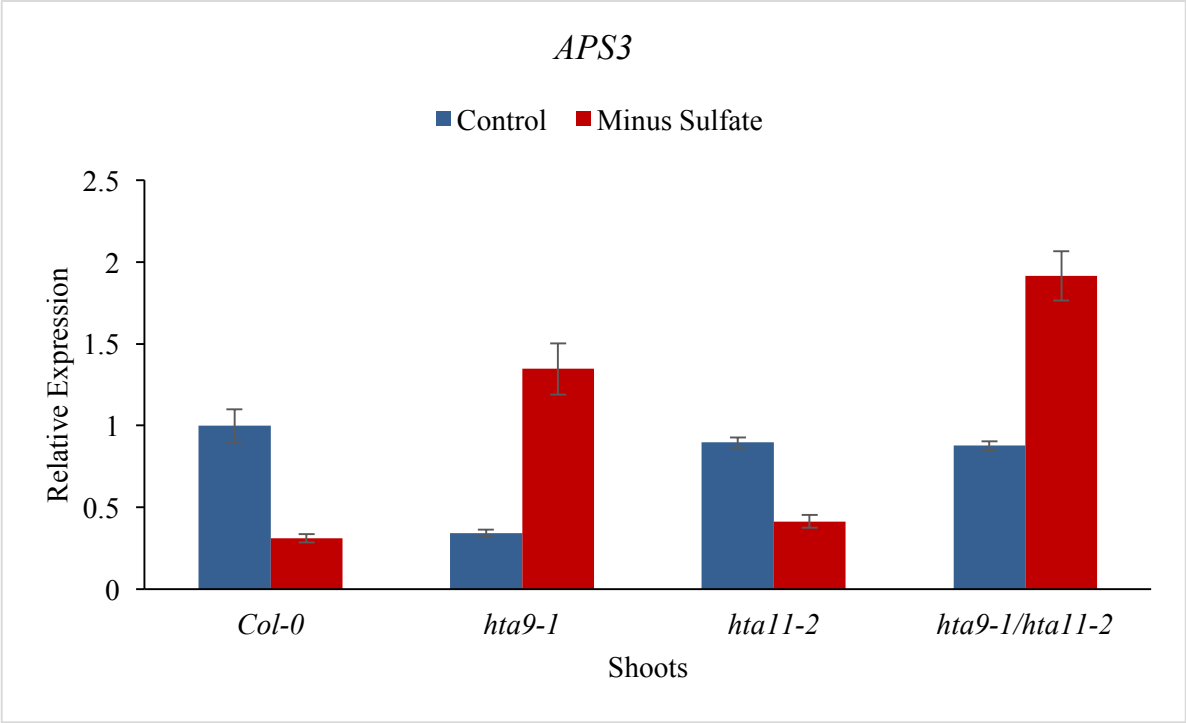
APS3
Control
Minus Sulfate
Relative Expression
2.5
2
1.5
1
0.5
0
Col-0
hta9-1
hta11-2
hta9-1/hta11-2
Shoots

D.

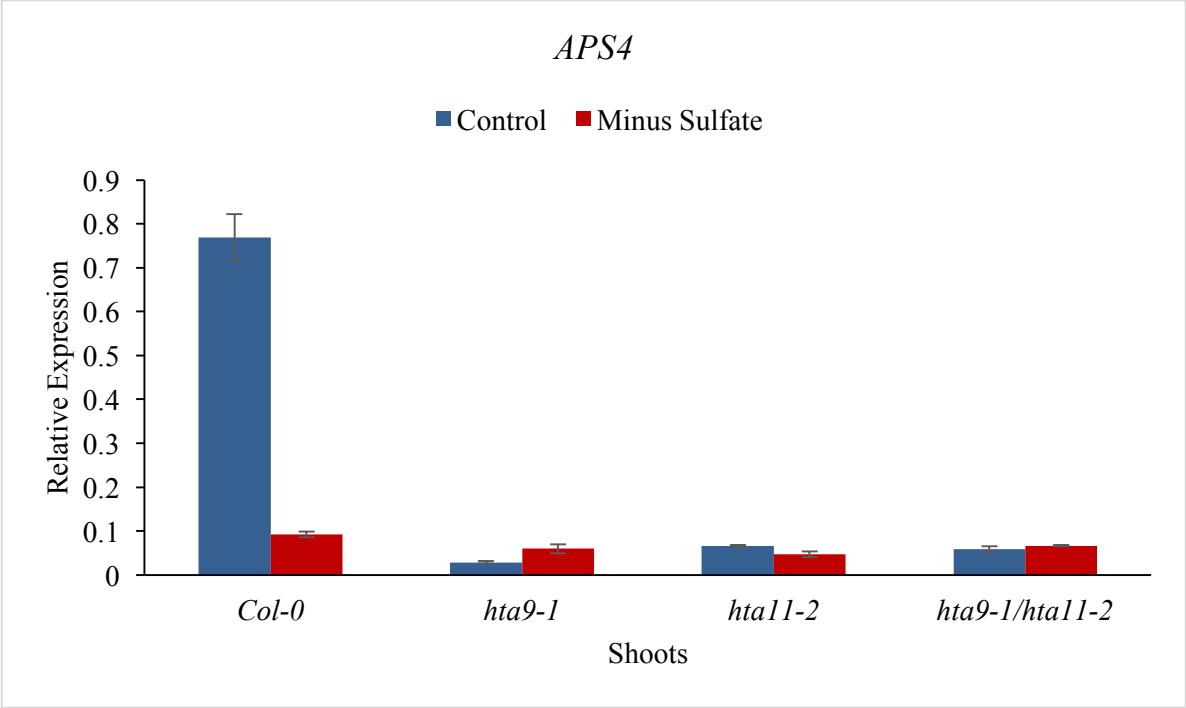
APS4
Control
Minus Sulfate
Relative Expression
0.9
0.8
0.7
0.6
0.5
0.4
0.3
0.2
0.1
0
Col-0
hta9-1
hta11-2
hta9-1/hta11-2
Shoots

Figure 19. Expression profiles of genes targeted by miR395 in shoots of WT and *hta* mutants.

A - D. The qRT-PCR for expression levels of target genes in shoot tissues under control and sulfate stress conditions. The *PP2A* transcript levels were used to normalize the expression levels. Error bars denotes the standard deviation. Results shown are the average of three technical replicates.

A.

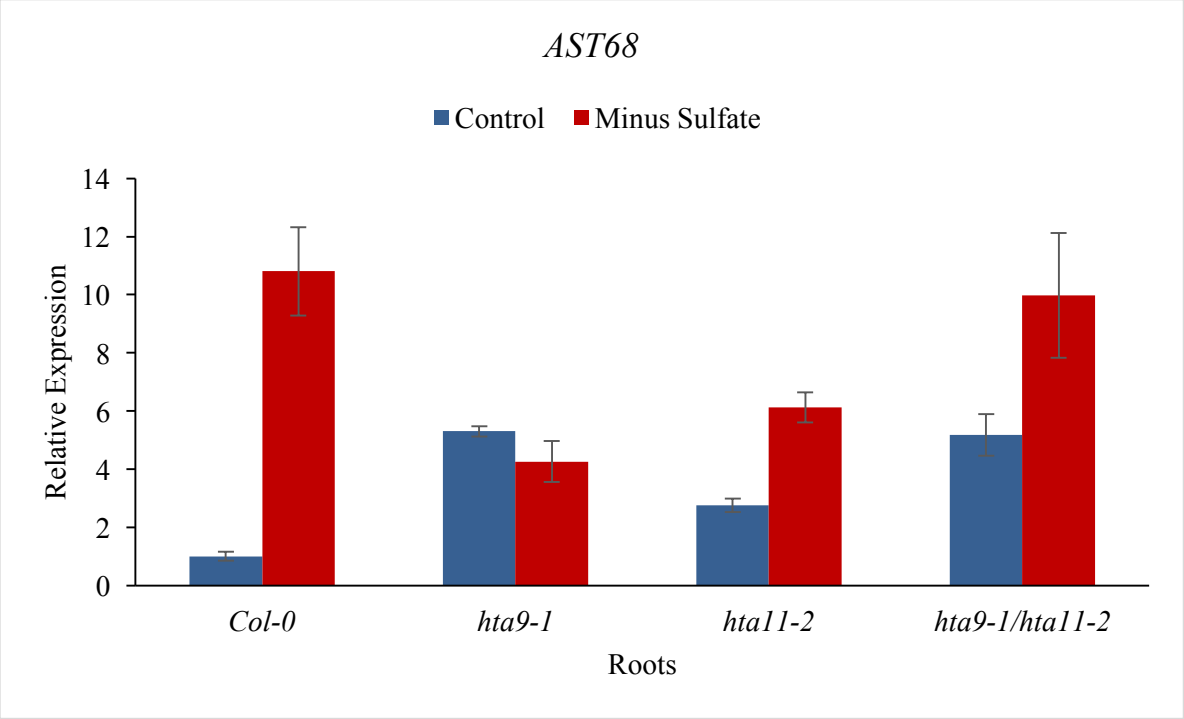

B.

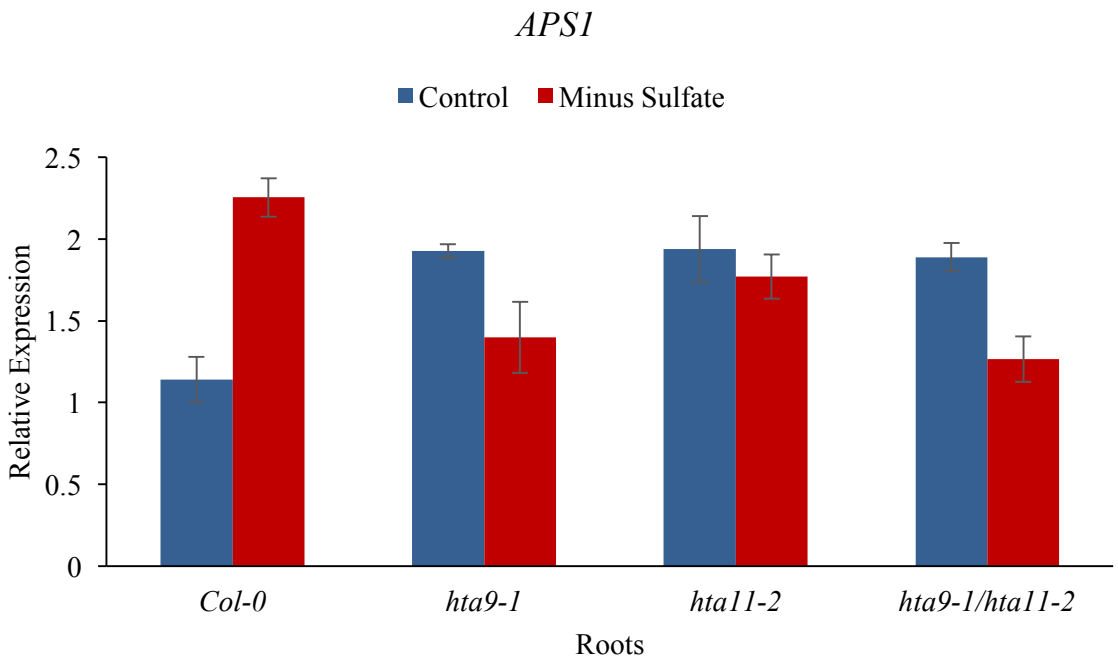
APS1
Control
Minus Sulfate
Relative Expression
2.5
2
1.5
1
0.5
0
Col-0
hta9-1
hta11-2
hta9-1/hta11-2
Roots

C.

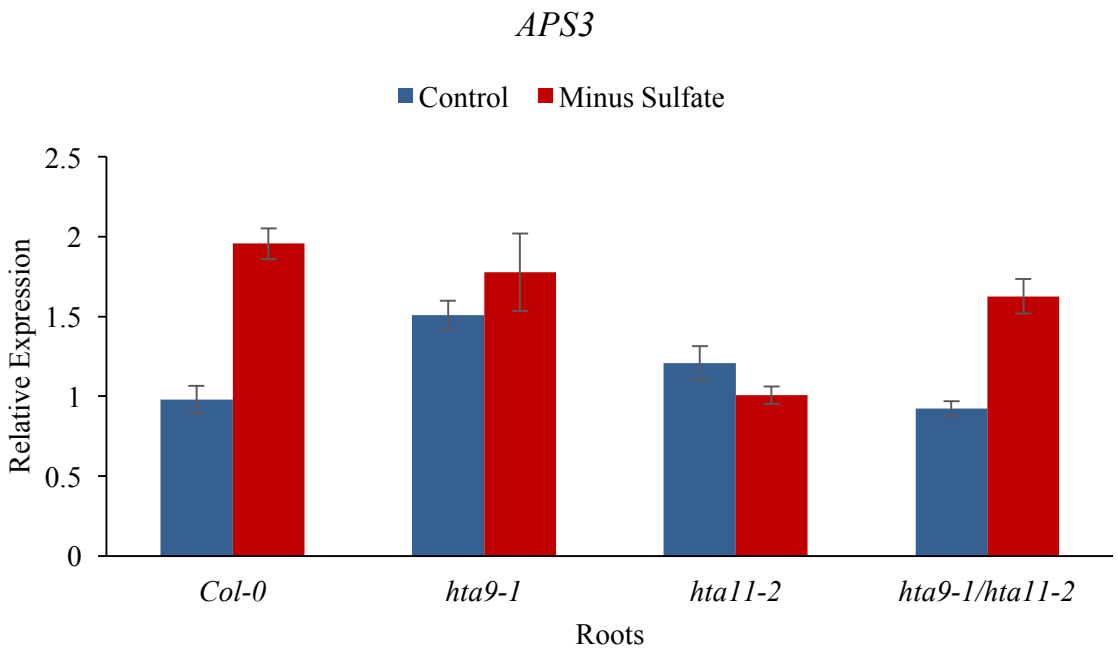
APS3
Control
Minus Sulfate
Relative Expression
2.5
2
1.5
1
0.5
0
Col-0
hta9-1
hta11-2
hta9-1/hta11-2
Roots

D.

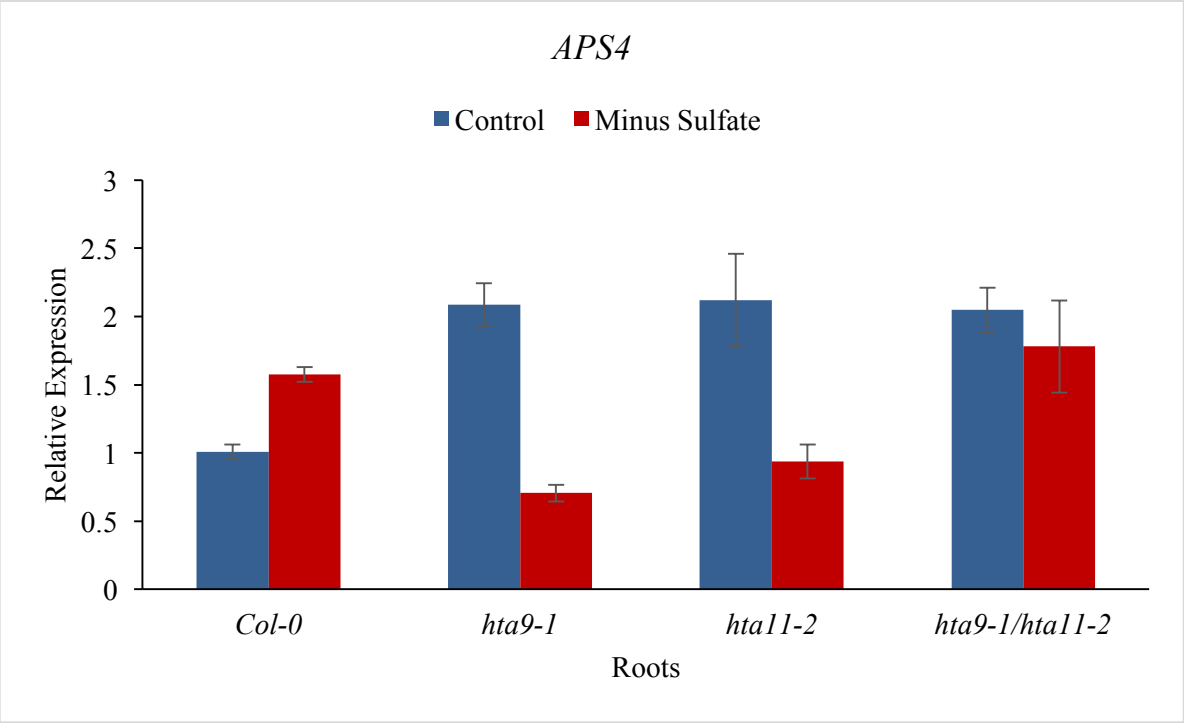

Figure 20. Expression profiles of genes targeted by miR395 in roots of WT and *hta* mutants.

A - D. The qRT-PCR for expression levels of miR395 target genes in root tissues under control and sulfate stress conditions. The *PP2A* transcript levels were used to normalize the expression levels. Error bars denotes the standard deviation. Results shown are the average of three technical replicates.

CHAPTER V

DISCUSSION

5.1 Histone Methylation and H2A.Z Variants Are Involved in The Regulation of MicroRNA395 at Varying Levels

The transcriptional regulation of *MIR* genes is thought to be similar to the protein coding genes involving diverse factors including the transcription factor binding to the *cis*-elements in the promoter region and driving the transcription by recruiting RNA polymerase II. Diverse epigenetic processes such as the DNA methylation and histone modifications facilitate transcriptional regulation. For controlling gene regulation, among the many histone modifications, histone methylation and acetylation are widely known for their profound effects. Here, the role of H3K4me3 (mark that generally positively regulate gene expression) and H3K27me3 (mark that largely negatively regulate gene expression) are investigated in regulating miR395 induction under S deprivation. The histone variants, more specifically the H2A variants such as H2A.Z (known to affect gene expression) are also known to influence gene expression. Therefore, the role of H2A.Z variants in regulating miR395 induction under S deprivation was also examined. Overall, the importance of H3K4me3, H3K27me3 and H2A.Z in regulating miR395 expression was assessed in mutants that lack the capacity to deposit these epigenetic marks.

MiR395 is induced both in shoots and roots of *Arabidopsis* under S deprivation. In Col-0 (WT) plants, the quantitative analysis of all six pri-*MIR395* transcripts (*MIR395a, b, c, d, e* and *f*) in shoots revealed a strong up-regulation, however in roots, at least four (*MIR395a, b, c* and *f*) of the six loci exhibited up-regulation under S deprivation. In general, the degree of up-regulation was much stronger in shoots compared to roots. However, in mutants lacking H3K4me3 and H3K4me2 and their combination (*atx1-2*, *atx2-1* and *atx1*/*atx2*), the expression levels from these loci were significantly different; 5 and 4 loci in shoots and roots, respectively, were more strongly up-regulated in mutants compared to the WT plants. Similarly, in mutants lacking H3K27me3, i.e., *swn3* mutant, 3 (shoots) and 4 (roots) loci in shoots and roots, respectively, showed more up-regulation compared to Col-0.

Compared to the Col-0 responses, the pri-*MIR395* levels in *hta* mutants also showed differences both in shoots and roots. Differences in regulation was evident between *hta9-1* and *hta11-2* mutants compared to the Col-0, but the differences were more pronounced in case of *hta9-1*/*hta11-2* double mutants. In shoots, with the exception of *MIR395c*, the remaining 5 loci and in roots, at least two loci (*MIR395a* and *MIR395c*) showed decreased up-regulation of pri-*MIR395* levels in the mutants relative to the Col-0.

H3K4me3 are known to activate gene expression. Because of its positive role, mutants that lack H3K4me3 are likely to show decreased expression. On this basis, the predicted results from the *atx1-2* mutant analysis are that, if H3K4me3 play an activating role in miR395 regulation at least in some of the miR395 loci, mutants are expected to show decreased expression levels from those loci. Accordingly, when compared WT with the *atx1-2* mutant, the pri-*MIR395e* levels in shoots and pri-*MIR395d* and *e* levels in roots showed decreased expression both under control and under S deprivation.

On the other hand, H3K27me3 is known to silence gene expression. Because of its repressive role, mutants that lack H3K27me3 are likely to show enhanced expression. On this basis, the predicted results from the *swn3* mutant analysis are that, if H3K27me3 play a silencing role in miR395 regulation at least in some of the miR395 loci, mutants are expected to show enhanced expression levels from those loci. Accordingly, when compared WT with the *swn3* mutant under S deprivation, the pri-*MIR395b, c* and *e* levels in shoots and pri-*MIR395a, b, c* and *e* levels in roots were more strongly up-regulated.

Along the same lines, the predicted results from the *hta* double mutant analysis are that if HTA9 or HTA11 plays a role in miR395 regulation at least in some of the miR395 loci, mutants are expected to show decreased levels from those loci. Accordingly, when compared WT with the *hta* double mutant, the pri-*MIR395a, b, d* and *e* levels in shoots and pri-*MIR395a* and *c* levels in roots were more strongly decreased both in control and S deprived samples of mutant. Although previous reports suggested an ambiguous role for H2A.Z, but the observed response is consistent with some of the earlier reports i.e., in *Arabidopsis*, H2A.Z was implicated in positive regulation of gene regulation at the FLC locus (Deal et al., 2007) and *MIR156A* and *MIR156C* loci in *Arabidopsis* (Xu et al., 2018). These observations are significant because these results suggest that these epigenetic modifications have significant effects in regulating miR395 expression both under control and under S deprivation in *Arabidopsis*.

Overall, some of the observations are consistent with the expectations and suggests that these epigenetic marks are important for regulating some *MIR395* loci in *Arabidopsis*. Contrastingly, some other *MIR395* loci showed contradictory results to the expectations in *atx*, *swn3* and *hta* mutants. Consistent with these unexpected results, previous analysis of miRNA accumulation in a histone acetyltransferase mutant (*gcn5* mutant – general control non-repressed protein 5) mutant revealed both expected and unexpected results (Kim et al., 2009). Generally, histone acetylation at H3K9, K14 and K27 was recognized as a positive epigenetic mark and

contributes to activation of gene expression. However, *gcn5* mutant analysis revealed both up- and down-regulation of a large number of genes in yeast (Lee et al., 2000). Similarly, *gcn5* mutant also displayed a large number of miRNAs that were up- or down-regulated in *Arabidopsis* (Kim et al., 2009). It is possible that the *ATX1*, *ATX2*, *SWN3*, *HTA9* and *HTA11* genes that are analyzed in the present study is only targeting sub-set of miR395 loci in *Arabidopsis*.

The up-regulation of miR395 under S deprivation causing down-regulation of *AST68*, *APS1*, *APS3* and *APS4* transcript levels in Col-0. Accordingly, in case of mutants in which pri-*MIR395* levels were even more strongly up-regulated and this was correlated with a stronger suppression of *AST68* levels and to certain extent in case of *APS4* levels, especially in roots under S deprivation. The lack of expected correlations between miR395 levels and target genes in mutants can be attributed to other factors such as differential transcriptional regulation of target genes in the mutants compared to WT.

REFERENCES

Agarwal, G., Kudapa, H., Ramalingam, A., Choudhary, D., Sinha, P., Garg, V., Singh, V., Patil, G., Pandey, M., Nguyen, H., Guo, B., Sunkar, R., Niederhuth, C. and Varshney, R*. (2020). Epigenetics and Epigenomics: Underlying mechanisms, relevance and implications in crop improvement. *Functional & Integrative Genomics, 20*, 739-761

Alvarez-Venegas, R., Pien, S., Sadder, M., Witmer, X., Grossniklaus, U., & Avramova, Z. (2003). ATX-1, an Arabidopsis Homolog of Trithorax, Activates Flower Homeotic Genes. *Current Biology, 13*(8), 627–637.

Ashapkin, V. V., Kutueva, L. I., Aleksandrushkina, N. I., & Vanyushin, B. F. (2020). Epigenetic Mechanisms of Plant Adaptation to Biotic and Abiotic Stresses. *International journal of molecular sciences*, *21*(20), 7457.

Aslam, M., Fakher, B., Jakada, B. H., Cao, S., & Qin, Y. (2019). SWR1 Chromatin Remodeling Complex: A Key Transcriptional Regulator in Plants. *Cells*, *8*(12), 1621.

Awazuhara, M., Fujiwara, T., Hayashi, H., Watanabe-Takahashi, A., Takahashi, H., and Saito, K. (2005). The function of SULTR2;1 sulfate transporter during seed development in Arabidopsis thaliana. *Plant Physiol, 125*, 95–105.

Baramidze, V., Khetereli, A., and Kushad, M. (2015). Identification and control of major diseases and insect pests of vegetables and melons in Georgia. Agricultural University of Georgia 2015, 27.

Bernstein, E. and Hake, S. B. (2006). The nucleosome: a little variation goes a long way. *Biochemistry and Cell Biology, 84*(4), 505-507.

Berriri, S., Gangappa, S. N., & Kumar, S. V. (2016). SWR1 Chromatin-Remodeling Complex Subunits and H2A.Z Have Non-overlapping Functions in Immunity and Gene Regulation in Arabidopsis. *Molecular plant*, *9*(7), 1051–1065.

Binda, O., LeRoy, G., Bua, D., Garcia, B., Gozani, O., & Richard, S. (2010). Trimethylation of histone H3 lysine 4 impairs methylation of histone H3 lysine 9: Regulation of lysine methyltransferases by physical interaction with their substrates. *Epigenetics, 5*(8), 767–775.

Blum, R., Beck, A., Korte, A., Stengel, A., Letzel, T., Lendzian, K., & Grill, E. (2007). Function of phytochelatin synthase in catabolism of glutathione-conjugates. *The Plant Journal: for Cell and Molecular Biology*, *49*(4), 740–749.

Bönisch, C., & Hake, S. B. (2012). Histone H2A variants in nucleosomes and chromatin: more or less stable?. *Nucleic acids research*, *40*(21), 10719–10741.

Boros, I. (2012). Histone modification in Drosophila. *Briefings in Functional Genomics, 11*(4), 319–331.

Brader, G., Mikkelsen, M., Halkier, B., & Tapio Palva, E. (2006). Altering glucosinolate profiles modulates disease resistance in plants. *The Plant Journal: for Cell and Molecular Biology*, *46*(5), 758–767.

Carciochi, W.D., Mateos, J., Divito, G.A., Inchauspe, F.M. and Sainz Rozas, H.R. (2019). Sulfur Mineralization: A Key Process for Diagnosing Its Deficiency in Wheat. *Soil Sci. Soc. Am. J., 83,* 1553-1563.

Coleman-Derr, D., & Zilberman, D. (2012). Deposition of histone variant H2A.Z within gene bodies regulates responsive genes. *PLoS Genetics, 8*(10), e1002988–e1002988.

Cortijo S, Charoensawan V, Brestovitsky A, Buning R, Ravarani C, Rhodes D, van Noort J, Jaeger KE, Wigge PA. 2017. Transcriptional regulation of the ambient temperature response by H2A.Z nucleosomes and HSF1 transcription factors in Arabidopsis. *Molecular Plant* 10, 1258–1273.

Couto, N., Malys, N., Gaskell, S., & Barber, J. (2013). Partition and Turnover of Glutathione Reductase from Saccharomyces cerevisiae: A Proteomic Approach. *Journal of Proteome Research*, *12*(6), 2885–2894.

Creissen, G., Broadbent, P., Stevens, R., Wellburn, A. R. and Mullineaux, P. (1996). Manipulation of glutathione metabolism in transgenic plants. *Biochem Soc Trans,. 24*(2), 465-9.

De Kok, LJ., Castro, A., Durenkamp, M., Stuiver, CEE., Westerman, S., Yang, L., Stulen, I. (2002) Sulphur in plant physiology. *In* Proceedings No. 500. The International Fertiliser Society, York, UK, 1–26.

Deal, R. B., Topp, C. N., McKinney, E. C., Meagher, R. B. (2007). Repression of flowering in Arabidopsis requires activation of *FLOWERING LOCUS C* expression by the histone variant H2A.Z. *The Plant Cell, 19*, 74–83.

Ding, Y., Ndamukong, I., Xu, Z., Lapko, H., Fromm, M., & Avramova, Z. (2012). ATX1-generated H3K4me3 is required for efficient elongation of transcription, not initiation, at ATX1-regulated genes. *PLoS genetics*, *8*(12), e1003111.

Dong, H., Liu, D., Han, T., Zhao, Y., Sun, J., Lin, S., Cao, J., Chen, Z., & Huang, L. (2015). Diversification and evolution of the SDG gene family in Brassica rapa after the whole genome triplication. *Scientific Reports*, *5*(1), 16851–16851.

Durán, A., Morris, H., Studdert, G., and Liu, X. (2011). Distribution, Properties, Land Use and Management of Mollisols in South America. *Chinese Geographical Science, 21*(5), 511–530.

Durenkamp, M., & De Kok, L. J. (2004). Impact of pedospheric and atmospheric sulphur nutrition on sulphur metabolism of Allium cepa L., a species with a potential sink capacity for secondary sulphur compounds. *Journal of experimental botany*, *55*(404), 1821–1830.

Falk K. L., Tokuhisa J. G., Gershenzon J. (2007). The effect of sulfur nutrition on plant glucosinolate content: physiology and molecular mechanisms. *Plant Biol.,* 9, 573–581.

Ferrier, P., Pekowska, A., Belhocine, M., Holota, H., Spicuglia, S., Zacarias-Cabeza, J., Koch, F., Benoukraf, T., Andrau, J., & Imbert, J. (2011). H3K4 tri-methylation provides an epigenetic signature of active enhancers. *The EMBO Journal, 30*(20), 4198–4210.

Foroozani, M., Vandal, M., & Smith, A. (2021). H3K4 trimethylation dynamics impact diverse developmental and environmental responses in plants. *Planta*, *253*(1), 4–4.

Freeman, J. L., Persans, M. W., Nieman, K., Albrecht, C., Peer, W., Pickering, I. J., & Salt, D. E. (2004). Increased Glutathione Biosynthesis Plays a Role in Nickel Tolerance in Thlaspi Nickel Hyperaccumulators. *The Plant Cell*, *16*(8), 2176–2191.

Frerigmann, H., Böttcher, C., Baatout, D., & Gigolashvili, T. (2012). Glucosinolates are produced in trichomes of Arabidopsis thaliana. *Frontiers in Plant Science, 3,* 242–242.

Gómez-Zambrano, Á., Merini, W., & Calonje, M. (2019). The repressive role of Arabidopsis H2A.Z in transcriptional regulation depends on AtBMI1 activity. *Nature Communications*, *10*(1), 2828–12.

Grunstein, M. (1997). Histone acetylation in chromatin structure and transcription. *Nature, 389*(6649), 349-352.

Hark, A., Vlachonasios, K., Pavangadkar, K., Rao, S., Gordon, H., Adamakis, I., Kaldis, A., Thomashow, M., & Triezenberg, S. (2009). Two Arabidopsis orthologs of the transcriptional coactivator ADA2 have distinct biological functions. *Biochimica et Biophysica Acta. Gene Regulatory Mechanisms*, *1789*(2), 117–124.

Hoagland, D., & Arnon, D. (1950). *The water-culture method for growing plants without soil* (Rev. ed. / by D.I. Arnon.). College of Agriculture, University of California.

Huang, Y., Nayak, S., Jankowitz, R., Davidson, N. E., & Oesterreich, S. (2011). Epigenetics in breast cancer: what's new?. *Breast cancer research: BCR*, *13*(6), 225.

Hyun, K., Jeon, J., Park, K., & Kim, J. (2017). Writing, erasing and reading histone lysine methylations. *Experimental & Molecular Medicine*, *49*(4), e324–e324.

Iwasaki, S., Kobayashi, M., Yoda, M., Sakaguchi, Y., Katsuma, S., Suzuki, T., & Tomari, Y. (2010). Hsc70/Hsp90 Chaperone Machinery Mediates ATP-Dependent RISC Loading of Small RNA Duplexes. *Molecular Cell, 39*(2), 292–299.

Jagadeeswaran, G., Li, Y., and Sunkar, R. (2014). Redox Signaling Mediates the Expression of a Sulfate-deprivation-inducible MicroRNA 395 in Arabidopsis. *Plant Journal, 77*(1), 85-96.

Jagadeeswaran, G., Zheng, Y., Li, Y., Shukla, L., Matts, J., Hoyt, P., Macmil, S. L., Wiley, G. B., Roe, B. A., Zhang, W. and Sunkar, R. (2009). Cloning and Characterization of Small RNAs from Medicago truncatula Reveals Four Novel Legume-Specific MicroRNA Families. *The New Phytologist, 184*(1), 85-98.

Jiang, D., Borg, M., Lorkovic, Z., Montgomery, S., Osakabe, A., Yelagandula, R., Axelsson, E., Berger, F., Bickmore, W., & Malik, H. (2020). The evolution and functional divergence of the histone H2B family in plants. *PLoS Genetics*, *16*(7), e1008964–e1008964.

Jones-Rhoades, M.W., and Bartel, D.P. (2004). Computational identification of plant microRNAs and their targets, including a stress-induced miRNA. *Mol. Cell 14*, 787–799.

Kawashima, C., Matthewman, C., Huang, S., Lee, B., Yoshimoto, N., Koprivova, A., Rubio-Somoza, I., Todesco, M., Rathjen, T., Saito, K., Takahashi, H., Dalmay, T., & Kopriva, S. (2011). Interplay of SLIM1 and miR395 in the regulation of sulfate assimilation in Arabidopsis. *The Plant Journal: for Cell and Molecular Biology, 66*(5), 863–876.

Kawashima, C., Yoshimoto, N., Maruyama-Nakashita, A., Tsuchiya, Y., Saito, K., Takahashi, H., & Dalmay, T. (2009). Sulphur starvation induces the expression of microRNA-395 and one of its target genes but in different cell types. *The Plant Journal : for Cell and Molecular Biology*, *57*(2), 313–321.

Kim, J.-M., Sasaki, T., Ueda, M., Sako, K. & Seki, M. (2015). Chromatin changes in response to drought, salinity, heat, and cold stresses in plants. *Front. Plant Sci., 6*, 114.

Kim, W., Benhamed, M., Servet, C., Latrasse, D., Zhang, W., Delarue, M., Zhou, D. X. (2009). Histone acetyltransferase GCN5 interferes with the miRNA pathway in Arabidopsis. *Cell Research, 19*(7):899-909.

Klapheck, S., Latus, C., Bergmann, L. (1987). Localization of glutathione synthetase and distribution of glutathione in leaf cells of *Pisum sativum* L. *J Plant Physiol*, *l31*, 123-131.

Kobor, M., Venkatasubrahmanyam, S., Meneghini, M., Gin, J., Jennings, J., Link, A., Madhani, H., & Rine, J. (2004). A protein complex containing the conserved Swi2/Snf2-related ATPase Swr1p deposits histone variant H2A.Z into euchromatin. *PLoS Biology*, *2*(5), E131–E131.

Kopriva, S. (2006). Regulation of sulfate assimilation in Arabidopsis and beyond. *Ann Bot, 97,* 479–495.

Koprivova A., North K.A., & Kopriva S. (2008). Complex signaling network in regulation of adenosine 5′-phosphosulfate reductase by salt stress in Arabidopsis roots. *Plant Physiol, 146*, 1408-1420.

Koprivova, A., & Kopriva, S. (2014). Molecular mechanisms of regulation of sulfate assimilation: first steps on a long road. *Frontiers in Plant Science*, *5,* 589–589.

Kumar, S. V. and Wigge, P.A. (2010). H2A.Z-containing nucleosomes mediate the thermosensory response in Arabidopsis. *Cell, 140*, 136–147.

Lee, T. I., Causton, H. C., Holstege, F. C., Shen, W. C., Hannett, N., Jennings, E. G., Winston, F., Green, M. R., & Young, R. A. (2000). Redundant roles for the TFIID and SAGA complexes in global transcription. *Nature, 405*(6787), 701–704.

Leustek, S. (1999). Sulfate Transport and Assimilation in Plants. *Plant Physiology (Bethesda), 120*(3), 637–643.

Leustek, T. (2002). Sulfate metabolism. The *Arabidopsis* Book, *1*, e0017.

Leustek, T., Martin, M. N., Bick, J. A., & Davies, J. P. (2000). Pathways and regulation of sulfur metabolism revealed through molecular and genetic studies. *Annual review of plant physiology and plant molecular biology*, *51*, 141–165.

Li, Z., Zheng, Y., Jagadeeswaran, G. Li, Y., Gowdu, K and Sunkar, R. (2011). Identification and temporal expression analysis of conserved and novel miRNAs in Sorghum. *Genomics, 98,* 460-468.

Liang, G., & Yu, D. (2010). Reciprocal regulation among miR395, APS and SULTR2;1 in Arabidopsis thaliana. *Plant signaling & behavior*, *5*(10), 1257–1259.

Liang, G., Yang, F., & Yu, D. (2010). MicroRNA395 mediates regulation of sulfate accumulation and allocation in Arabidopsis thaliana. *The Plant Journal : for Cell and Molecular Biology*, *62*(6), 1046–1057.

Liu, S., Zhou, J., Hu, C., Wei, C., & Zhang, J. (2017). MicroRNA-Mediated Gene Silencing in Plant Defense and Viral Counter-Defense. *Frontiers in Microbiology, 8*, 1801–1801.

Liu, Y., Liu, K., Yin, L., Yu, Y., Qi, J., Shen, W., Zhu, J., Zhang, Y., & Dong, A. (2019). H3K4me2 functions as a repressive epigenetic mark in plants. *Epigenetics & Chromatin, 12*(1), 40–40.

Liu, Y., Zhang, A., Yin, H., Meng, Q., Yu, X., Huang, S., Wang, J., Ahmad, R., Liu, B., & Xu, Z. (2018). Trithorax-group proteins ARABIDOPSIS TRITHORAX4 (ATX4) and ATX5 function in abscisic acid and dehydration stress responses. *The New Phytologist, 217*(4), 1582–1597.

Luger, K., Dechassa, M. L., & Tremethick, D. J. (2012). New insights into nucleosome and chromatin structure: an ordered state or a disordered affair?. *Nature reviews. Molecular cell biology*, *13*(7), 436–447.

March-Díaz, R., & Reyes, J. (2009). The Beauty of Being a Variant: H2A.Z and the SWR1 Complex in Plants. *Molecular Plant, 2*(4), 565–577.

Maruyama-Nakashita, A., Nakamura, Y., Tohge, T., Saito, K., & Takahashi, H. (2006). Arabidopsis SLIM1 is a central transcriptional regulator of plant sulfur response and metabolism. *The Plant cell*, *18*(11), 3235–3251.

Mizuguchi, G., Shen, X., Landry, J., Wu, W., Sen, S., & Wu, C. (2004). ATP-Driven Exchange of Histone H2AZ Variant Catalyzed by SWR1 Chromatin Remodeling Complex. *Science (American Association for the Advancement of Science)*, *303*(5656), 343–348.

Mizuguchi, G., Wu, W., Alami, S., & Luk, E. (2012). Biochemical Assay for Histone H2A.Z Replacement by the Yeast SWR1 Chromatin Remodeling Complex. *Methods in Enzymology, 512*, 275–291.

Mullineaux, P. M., & Rausch, T. (2005). Glutathione, photosynthesis and the redox regulation of stress-responsive gene expression. *Photosynthesis research*, *86*(3), 459–474.

Nakanishi, K. (2016). Anatomy of RISC: how do small RNAs and chaperones activate Argonaute proteins?. *Wiley interdisciplinary reviews. RNA, 7*(5), 637–660.

Osabe, K., Harukawa, Y., Miura, S., & Saze, H. (2017). Epigenetic Regulation of Intronic Transgenes in Arabidopsis. *Scientific Reports*, *7*(1), 45166–45166.

Passardi, F., Dobias, J., Valério, L., Guimil, S., Penel, C., & Dunand, C. (2007). Morphological and physiological traits of three major Arabidopsis thaliana accessions. *Journal of Plant Physiology, 164*(8), 980–992.

Peterson, A., Mallin, D., Francis, N., Ketel, C., Stamm, J., Voeller, R., Kingston, R., & Simon, J. (2004). Requirement for Sex Comb on Midleg Protein Interactions in Drosophila Polycomb Group Repression. *Genetics (Austin)*, *167*(3), 1225–1239.

Pontvianne, F., Blevins, T., & Pikaard, C. S. (2010). Arabidopsis Histone Lysine Methyltransferases. *Advances in botanical research*, *53*, 1–22.

Rausch, T., & Wachter, A. (2005). Sulfur metabolism: a versatile platform for launching defence operations. *Trends in plant science*, *10*(10), 503–509.

Saleh, A., Alvarez-Venegas, R., Yilmaz, M., Oahn-Le, Hou, G., Sadder, M., Al-Abdallat, A., Xia, Y., Lu, G., Ladunga, I., & Avramova, Z. (2008). The Highly Similar Arabidopsis Homologs of Trithorax ATX1 and ATX2 Encode Proteins with Divergent Biochemical Functions. *The Plant Cell, 20*(3), 568–579.

Schachtman, D. P., & Shin, R. (2007). Nutrient sensing and signaling: NPKS. *Annual review of plant biology*, *58*, 47–69.

Shu, J., Chen, C., Thapa, R., Bian, S., Nguyen, V., Yu, K., Yuan, Z., Liu, J., Kohalmi, S., Li, C., & Cui, Y. (2019). Genome-wide occupancy of histone H3K27 methyltransferases CURLY LEAF and SWINGER in Arabidopsis seedlings. *Plant Direct*, *3*(1), e00100.

Smith, A. P., Jain, A., Deal, R. B., Nagarajan, V. K., Poling, M. D., Raghothama, K. G., Meagher, R. B. (2010). Histone H2A.Z regulates the expression of several classes of phosphate starvation response genes but not as a transcriptional activator. *Plant Physiology, 152*, 217–225.

Sun, Z. W., & Allis, C. D. (2002). Ubiquitination of histone H2B regulates H3 methylation and gene silencing in yeast. *Nature*, *418*(6893), 104–108.

Sunkar, R., & Jagadeeswaran, G. (2008). In silico identification of conserved microRNAs in large number of diverse plant species. *BMC plant biology*, *8*, 37.

Sunkar, R., Li, Y., & Jagadeeswaran, G. (2012). Functions of microRNAs in plant stress responses. *Trends in Plant Science, 17*(4), 196–203.

Sura, W., Kabza, M., Karlowski, W. M., Bieluszewski, T., Kus-Slowinska, M., Pawełoszek, Ł., Sadowski, J., Ziolkowski, P. A. (2017). Dual role of the histone variant H2A.Z in transcriptional regulation of stress-response genes. *The Plant Cell, 29*, 791–807.

Takahashi, H. (2019). Sulfate transport systems in plants: functional diversity and molecular mechanisms underlying regulatory coordination. *Journal of experimental botany*, *70*(16), 4075–4087.

Takahashi, H., Watanabe-Takahashi, A., Smith, F., Blake-Kalff, M., Hawkesford, M., & Saito, K. (2000). The roles of three functional sulphate transporters involved in uptake and translocation of sulphate in Arabidopsis thaliana. *The Plant Journal: for Cell and Molecular Biology*, *23*(2), 171–182.

Takahashi, H., Yamazaki, M., Sasakura, N., Watanabe, A., Leustek, T., De Almeida Engler, J., Engler, G., Van Montagu, M., & Saito, K. (1997). Regulation of sulfur assimilation in higher

plants: a sulfate transporter induced in sulfate starved roots plays a central role in Arabidopsis thaliana. *Proc. Natl Acad. Sci. USA, 94*, 11102-11107.

Tamada, Y., Yun, J., Woo, S., & Amasino, R. (2009). ARABIDOPSIS TRITHORAX-RELATED7 is required for methylation of lysine 4 of histone H3 and for transcriptional activation of FLOWERING LOCUS C. *The Plant Cell, 21*(10), 3257–3269.

To, T., & Kim, J. (2014). Epigenetic regulation of gene responsiveness in Arabidopsis. *Frontiers in Plant Science, 4*, 548–548.

Tomasz J. Sarnowski, Gabino Ríos, Jan Jásik, Szymon Świeżewski, Szymon Kaczanowski, Yong Li, Aleksandra Kwiatkowska, Katarzyna Pawlikowska, Marta Koźbiał, Piotr Koźbiał, Csaba Koncz, & Andrzej Jerzmanowski. (2005). SWI3 Subunits of Putative SWI/SNF Chromatin-Remodeling Complexes Play Distinct Roles during Arabidopsis Development. *The Plant Cell*, *17*(9), 2454–2472.

Wiles, E. T., & Selker, E. U. (2017). H3K27 methylation: a promiscuous repressive chromatin mark. *Current opinion in genetics & development, 43,* 31–37.

Xu, M., Leichty, A. R., Hu, T., & Poethig, R. S. (2018). H2A.Z promotes the transcription of MIR156A and MIR156C in Arabidopsis by facilitating the deposition of H3K4me3. Development (Cambridge, England), 145(2), dev152868.

Yan, B., Lv, Y., Zhao, C., & Wang, X. (2020). Knowing When to Silence: Roles of Polycomb-Group Proteins in SAM Maintenance, Root Development, and Developmental Phase Transition. *International Journal of Molecular Sciences, 21*(16), 5871.

Yoshida, S., Forno, D. A., Cock, J. A. and Gomez, K. A. (1976). Laboratory Manual for Plant Physiological Studies of Rice, Ed 3. International Rice Research Institute, Manila, Philippines.

Zahraeifard, S., Foroozani, M., Sepehri, A., Oh, D. H., Wang, G., Mangu, V., Chen, B., Baisakh, N., Dassanayake, M., & Smith, A. P. (2018). Rice H2A.Z negatively regulates genes responsive to nutrient starvation but promotes expression of key housekeeping genes. *Journal of experimental botany*, *69*(20), 4907–4919.

Zhang, X., Bernatavichute, Y., Cokus, S., Pellegrini, M., & Jacobsen, S. (2009). Genome-wide analysis of mono-, di- and trimethylation of histone H3 lysine 4 in Arabidopsis thaliana. *Genome Biology*, *10*(6), R62–R62.

Zhang, Y., Li, X., Goodrich, J., Wu, C., Wei, H., Yang, S., & Feng, X. (2016). Reduced function of the RNA-binding protein FPA rescues a T-DNA insertion mutant in the Arabidopsis ZHOUPI gene by promoting transcriptional read-through. *Plant Molecular Biology*, *91*(4), 549–561.

Zlatanova, J., Leuba, S., & van Holde, K. (1998). Chromatin Fiber Structure: Morphology, Molecular Determinants, Structural Transitions. *Biophysical Journal, 74*(5), 2554–2566.

APPENDICES

Table 1. Primer sequences used for the tissue-specific profiles of *ATX1, ATX2, SWN3, HTA9* and *HTA11* in wild type Col-0.

NAME	Description	Sequence
ATX1	FOR	GCACCATCTGCGGGGTATCT
	REV	TCTGCTTCTTCACCCTCCACT
ATX2	FOR	AGGACAGGAAGCATTGCTCACCT
	REV	CGGCATCTTGGGAAACCACAG
SWN3	FOR	ATGGACCAGACCAAGCACCAG
	REV	TGAGATTGGTGCTTTCTGGCTCT
HTA9	FOR	GCTATTGTTCGTTCGATCAGCGT
	REV	TGCTTTCAAGCTTCTCCAGCGA
HTA11	FOR	ACCACCAAGGAGTGATGTGTAGC
	REV	ACCTGAGGATGTCCAGAAGAGGT

Table 2. Primer sequences used for the expression profiles of pri-*MIR395* in *atx, swn and hta* mutants.

NAME	Description	Sequence
PP2A	FOR	ACCCAGATGTTGATGTTCGGTATTTC
	REV	ACCAAACACAATTCGTTGCTGTCTTC
miR395a	FOR	ATGTCTCCTAGAGTTCCTCTG
	REV	ATGGGTCCGGGAGTTCCCCCA
miR395b	FOR	GTCCCCATGAGTTCCCTTTAA
	REV	ATGACACCAAGAGTCCCCCCAA
miR395c	FOR	ATCATGACAGAGCAAGAAGAAG
	REV	GTGGCCACTTCAACGCCAGA
miR395d	FOR	TCATGGTGGTAACTAGCAAC
	REV	ATACATGGCTTGGCATCACCA
miR395e	FOR	TCAAACAATCGTCGTGTTGGTC
	REV	CAAACTCAGCTAGCTAGTCTACTG
miR395f	FOR	CTTGAGTTCCCTTAAACGCTTCA
	REV	CTCACCTCAACCGTTGACTACAC

Table 3. Primer sequences used for the expression profiles of miR395 target genes in shoot and root tissues.

NAME	Description	Sequence
AST68 Target FOR	Target region	CAGCATCCACACACACTTTGAATG
AST68 Target REV	Target region	CGGCTGCAGATGAACCTGAG
APS1 Target FOR	Target region	GCTGACGGCGATTGACTTGC
APS1 Target REV	Target region	CGTGTAGACTCGCCGATACGTG
APS3 Target FOR	Target region	GACGGCGATTGATTTGCAATGGA
APS3 Target REV	Target region	CATCAGAATCAACAAGGGAGACACG
APS4 Target FOR	Target region	GAGTGGGTACATGTGCTTAGCG
APS4 Target REV	Target region	GAGTCAACGAGTGTGACTTGGTTG

VITA

Pei Jia Ng

Candidate for the Degree of

Master of Science

Thesis: THE EPIGENETIC REGULATION OF MICRORNA395 EXPRESSION UNDER SULFATE DEPRIVATION IN ARABIDOPSIS THALIANA

Major Field: Biochemistry and Molecular Biology

Biographical:

Education:

Completed the requirements for the Master of Science in Biochemistry and Molecular Biology at Oklahoma State University, Stillwater, Oklahoma in May, 2021.

Completed the requirements for the Bachelor of Science in Biochemistry at Oklahoma State University, Stillwater, Oklahoma in 2018.

Experience:

Graduate Research Assistant, Department of Biochemistry and Molecular Biology at Oklahoma State University, Stillwater, Oklahoma. August 2018 – present.

Undergraduate Research Assistant, Department of Biochemistry and Molecular Biology at Oklahoma State University, Stillwater, Oklahoma. August 2017 – August 2018.

Honors and Awards:

The Gregory and Ruth Schultz Endowed Scholarship and Grant 2021

Professional Memberships:

Vice President, Oklahoma State University Biochemistry and Molecular Biology Graduate Student Association. February 2021 – present.

American Association for the Advancement of Science (AAAS). June 2019 – June 2020.